

THESIS ON CHEMISTRY AND CHEMICAL ENGINEERING G26

**Aqueous Photocatalytic Oxidation of
Non-Biodegradable Pollutants**

DENISS KLAUSON

TUT
PRESS

TALLINN UNIVERSITY OF TECHNOLOGY
Faculty of Chemical and Materials Technology
Department of Chemical Engineering

Dissertation was accepted for the defence of the degree of Doctor of Philosophy in Engineering on March 22, 2010

Supervisor: Senior Researcher Sergei Preis, Department of Chemical Engineering,
Tallinn University of Technology

Opponents: Prof. Mika Sillanpää, University of Kuopio, Finland
Prof. Jean Victor Weber, Paul Verlaine University, Metz, France

Defence of the thesis: June 11, 2010, 12.00
Lecture hall VII-131
Tallinn University of Technology, Ehitajate tee 5, Tallinn

Declaration

Hereby I declare that this doctoral thesis, my original investigation and achievement, submitted for the doctoral degree at Tallinn University of Technology has not been submitted for any academic degree.

Deniss Klauson

Copyright: Deniss Klauson, 2010
ISSN 1406-4774
ISBN 978-9985-59-984-6

KEEMIA JA KEEMIASTEHNKA G26

**Bioloogiliselt mittelagunevate saasteainete
fotokatalüütiline oksüdatsioon vesifaasis**

DENISS KLAUSON

TABLE OF CONTENTS

List of publications	6
Supplementary materials.....	7
The author's contribution to the publications	8
List of abbreviations and symbols in alphabetical order.....	9
Chemical formulae substances in alphabetical order	10
INTRODUCTION	12
Acknowledgements.....	13
1. LITERATURE REVIEW	14
1.1. Aqueous photocatalytic oxidation – state of the art	14
1.2. Aqueous pollutants under consideration: an overview	16
Ethylene glycol and its derivatives	16
Methyl- <i>tert</i> -butyl ether and <i>tert</i> -butyl alcohol.....	17
Aromatic compounds.....	17
Antibiotics.....	18
2. MATERIALS AND METHODS	19
3. OBJECTIVES	22
4. RESULTS AND DISCUSSION	22
4.1. Degussa P25 titanium dioxide.....	23
PCO performance	23
The influence of iron ions.....	23
Catalyst application mode.....	24
Solar experiments	24
Reaction pathways	24
4.2. Modified titania catalysts	25
Carbon-containing titania	25
Nitrogen and nitrogen-cerium-containing titania.....	26
Sulphur-containing titania.....	27
Boron-containing titania	28
Iron-containing titania	29
5. CONCLUSIONS	29
6. REFERENCES	33
KOKKUVÖTE	39
ABSTRACT	41
APPENDIX I: PUBLICATIONS	43
APPENDIX II: SUPPLEMENTARY MATERIALS	127
APPENDIX III: CURRICULUM VITAE	147

LIST OF PUBLICATIONS

Article I:

Klauson, D., Portjanskaja, E., Kachina, A., Krichevskaya, M., Preis, S. and Kallas, J., The influence of ferrous/ferric ions on the efficiency of photocatalytic oxidation of pollutants in groundwater. *Environmental Technology*, 2005, 26 (6), pp. 653-662

Article II:

Klauson, D., Preis, S. The influence of ferrous ions on the efficiency of aqueous photocatalytic oxidation of 2-ethoxy ethanol. *International Journal of Photoenergy*, 2005, 7 (4), pp. 175-180

Article III:

Klauson, D., Preis, S., The influence of iron ions on the aqueous photocatalytic oxidation of de-icing agents. *International Journal of Photoenergy*, 2007, 2007, Article ID 89359, pp. 1-7.

Article IV:

Klauson, D., Portjanskaja, E., Preis, S., Visible light-assisted photocatalytic oxidation of organic pollutants using nitrogen-doped titania. *Environmental Chemistry Letters*, 2008, 6 (1), pp. 35-39.

Article V:

Klauson D, Babkina J., Stepanova K., Krichevskaya M., Preis S., Aqueous photocatalytic oxidation of amoxicillin. *Catalysis Today*, 2010, in press, doi: 10.1016/j.cattod.2010.01.015

Article VI:

Klauson D., Portjanskaja E., Budarnaja O., Krichevskaya M., Preis S., The synthesis of sulphur and boron-containing titania photocatalysts and the evaluation of their photocatalytic activity. *Catalysis Communications*, 2010, 11 (8), pp. 715-720, doi: 10.1016/j.catcom.2010.02.001

Article VII:

Klauson D., Krichevskaya M., Borissova M., Preis S., Aqueous photocatalytic oxidation of sulphamethizole, *Environmental Technology*, 2010, in press

SUPPLEMENTARY MATERIALS

Article VIII:

Klauson D., Poljakova A., Krichevskaya M., Preis S., Aqueous photocatalytic oxidation of doxycycline, submitted to Journal of Photochemistry and Photobiology A (as of 14.04.2010)

Article IX:

Klauson D., Budarnaja O., Stepanova K., Krichevskaya M., Preis S., Aqueous photocatalytic oxidation of selected organic pollutants using carbon-containing titania, submitted to Environmental Technology (as of 14.04.2010)

THE AUTHOR'S CONTRIBUTION TO THE PUBLICATIONS

Article I: The author fulfilled a major part of the experiments and analyses in co-operation with colleagues, analysed the results and wrote the paper. The results were also presented by the author at EcoBalt 2004 conference in Riga, Latvia.

Article II: The author fulfilled the experiments and analyses, analysed the results and wrote the paper.

Article III: The author fulfilled the experiments and analyses, analysed the obtained results and wrote the paper. The results were also presented by the author at the 1st European Conference on Environmental Applications of Advanced Oxidation Processes (EAAOP-1) conference in Chania, Greece, in 2006.

Article IV: The author fulfilled the experiments and analyses in co-operation with his colleagues, analysed the results and wrote the paper.

Article V: The author obtained the experimental data in co-operation with the supervised MSc-student, analysed the results and wrote the article. The results were also presented by the author at EAAOP-2 conference in Nicosia, Cyprus, in 2009.

Article VI: The author obtained the experimental results in co-operation with his colleagues, analysed them and wrote the article. Results were also presented by the author at 8th European Meeting on Environmental Chemistry (EMEC8) conference in Inverness, United Kingdom, in 2007.

Article VII: The author fulfilled the experiments and analyses, analysed the obtained results and wrote the paper. The results were presented by the author at SPEA5 conference in Palermo, Italy, in 2008.

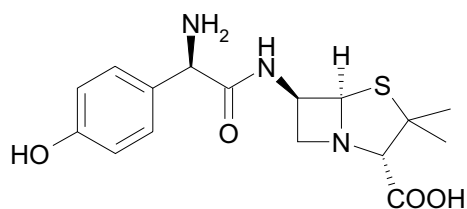
Article VIII: The author obtained the experimental data in co-operation with the supervised MSc-student, analysed the results and wrote the article.

Article IX: The author obtained the experimental data in co-operation with the supervised MSc-student and colleagues, analysed the results and wrote the article.

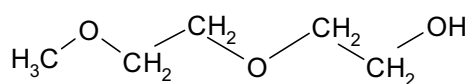
LIST OF ABBREVIATIONS AND SYMBOLS IN ALPHABETICAL ORDER

2-EE – 2-Ethoxy ethanol
AMO – Amoxicillin
AOP – Advanced Oxidation Process
COD – Chemical Oxygen Demand
DEGMME – Diethylene glycol monomethyl ether
DC – Doxycycline
 e^- – Electron
EG – Ethylene glycol
 h^+ – Positively charged hole
 k – Reaction rate constant
 K – Adsorption constant
L-H – Langmuir-Hinshelwood
MTBE – Methyl-*tert*-butyl ether
PCO – Photocatalytic oxidation
SMZ – Sulphamethizole
TBA – *tert*-Butyl alcohol

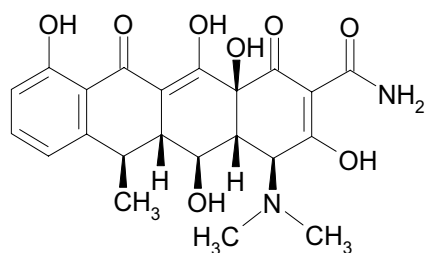
CHEMICAL FORMULAE OF SUBSTANCES IN ALPHABETICAL ORDER



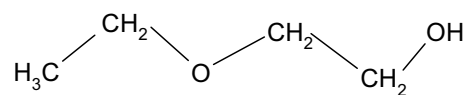
AMO



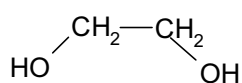
DEGMME



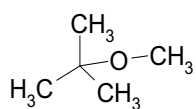
DC



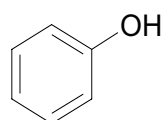
2-EE



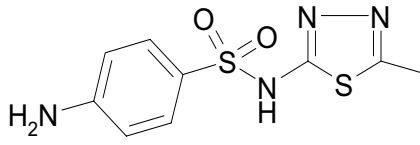
EG



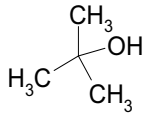
MTBE



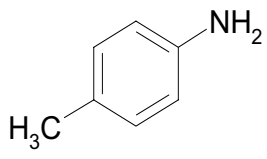
Phenol



SMZ



TBA



p-Toluidine

INTRODUCTION

Presently, aqueous pollutants are largely emitted worldwide in a wide range. These include substances targeted in the present research often appearing simultaneously in polluted waters: jet and motor fuel additives, de-icing agents, aromatic substances and antibiotics. The latter are considered to be emerging pollutants, as the interest to their environmental fate has intensively risen within the last decade. The non-biodegradable substances under scope are generally problematic and/or costly to remove using conventional and even some advanced water treatment methods. Photocatalytic oxidation (PCO) thus poses a very competitive alternative treatment method of the highest oxidation potential available at the ambient conditions, and able of using direct solar light.

PCO consists of the creation of positively charged holes on the surface of irradiated semiconductor, mostly titanium dioxide. Upon holes, which are known to be the most powerful oxidants, water molecules decompose to form hydroxyl radicals reacting with pollutants; also, the latter can decompose by direct subtraction of their electrons by the holes. Although PCO with TiO_2 needs UV-irradiation to perform, the photocatalyst can be modified by introduction of various elements to its crystal lattice or surface in order to make it sensitive to the visible light thus increasing the PCO energy efficiency.

The main objectives of the present research include:

1. Determining the limits of PCO applicability to substances of various structure and properties;
2. Acceleration of PCO through additives to the solution to be treated and to the structure of the photocatalysts;
3. Engineering solutions for catalyst applications.

The following questions were studied:

1. The efficiency of PCO in degradation of pollutants;
2. The PCO mechanism (radical *vs.* hole reactions, role of adsorption, reaction by-products, the description of reaction kinetics);
3. The impact of external factors (concentration of pollutants, pH, dissolved admixtures);
4. Synthesis and examination of modified catalysts with wider radiation absorbance spectrum: non-metal dopants - sulphur, boron, nitrogen and carbon; metal dopants - iron.

Acknowledgements

The author would like to express his deepest gratitude to his supervisor, Dr. Sergei Preis, for their cooperation lasting for almost nine years, which allowed the author to obtain his previous scientific degrees and submit the PhD thesis. The author is very much grateful to Dr. Marina Krichevskaya for sharing practical knowledge on scientific work and fruitful discussions. Special gratitude goes to the author's MSc students, Julia Babkina, Kristina Stepanova and Alissa Poljakova, co-authors of the manuscripts, for their practical input into the work. Advice and help from colleagues, Dr. Elina Portjanskaja and Dr. Anna Kachina, is also appreciated. The author would also like to thank Dr. Mai Uibu, Dr. Rein Kuusik, Dr. Anna Goi, Mrs. Jelena Veressinina, Ms. Kristi L. Pelz, Mr. Andrew S. Cavanaugh, Dr. Anna Moiseev, Mr. Petri-Jaan Lahtvee and Ms. Liisa Arike for helping with or providing some of the measurements used in this work. The last but definitely not the least personal thanks goes to the author's spouse, relatives and closest friends who have supported him all these years and thus have also contributed to this work, directly or indirectly.

Financial support of the research from Estonian Scientific Foundation, United States Civilian Research and Development Foundation, Doctoral School of New Production Technologies and Processes and Doctoral School of Functional Materials and Technologies is also very much appreciated.

1. LITERATURE REVIEW

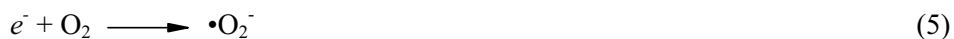
1.1. Aqueous photocatalytic oxidation – state of the art

Photocatalytic oxidation (PCO) is an advanced oxidation process (AOP), based on the action of positively charged holes on the surface of irradiated semiconductor material (Blake et al., 1991), mostly titanium dioxide. Quanta of electromagnetic radiation, having sufficient energy to cross the band gap, displace valence band electrons to the conduction band. This way, positively charged holes are created. The holes are extremely powerful oxidants (Sun et al., 1997, Bahnemann, 2004, see Table I): water molecules decompose on them, forming hydroxyl radicals that subsequently react with the pollutant molecule. Also, pollutant molecule, adsorbed on the photocatalyst surface, can react with the hole directly, with hole subtracting an electron from the pollutant molecule, turning it into a radical. The predominance of these pathways depends on the adsorption and oxidation properties of the substances to be degraded. Also, there are a number of substances that can be degraded by both pathways simultaneously (Matthews, 1986, Brezova et al., 1991, Chen et al., 1999). Reaction Equations 1-12 give a short overview of reactions taking place during PCO including Haber-Weiss reaction cycle (Equations 11 and 12).

Table 1. Oxidation potentials of oxidants

Oxidant	Oxidation potential, V
h^+ (TiO ₂)	3.50
F ₂	3.03
•OH	2.80
•O	2.42
O ₃	2.07
H ₂ O ₂	1.78
HO ₂ •	1.70
KMnO ₄	1.68
ClO ₂	1.57
HClO	1.49
Cl ₂	1.36





The main advantages of PCO as a treatment method is its high oxidation potential and the ability of using direct solar radiation for the catalyst performance, which may considerably lower the treatment cost. Relatively low reaction rate and quantum yield are considered to be the main disadvantages of PCO. The most challenging issue of PCO appears to be its often unpredictable performance under various process conditions, which makes the investigations aimed at enlarging the spectrum of pollutants degradable by PCO interesting from the point of view of future applications of this technology.

The effective performance of PCO is limited by recombination, which is the return of the electrons to the valence band and their reaction with the holes before water or pollutant molecule decomposition on them. Thus, recombination neutralises the holes; according to the available knowledge (Kolen'ko et al., 2004) the recombination time is around 40 ns.

In order to extend the electron-hole recombination time, as one of the methods to improve quantum yield, multivalent metal ions may be added to the treated solution (Brezova et al., 1995, Chen et al., 1999, Hameed and Gondal, 2004). The mechanism of their influence to PCO consists of the metal ions reduced by the electrons of the conductance band. When adsorbed to the catalyst surface, metal ion can further be returned to its oxidized state by the positively charged holes. However, the time taken by the electron to return through the metal ion is longer than the direct recombination time, which increases the probability of dissolved organic substances to be oxidised (Krichevskaya et al., 2003). From the sources published by the time this research was undertaken, there was neither enough evidence the multivalent ions may improve PCO, nor unequivocal clarity about the concentrations of iron ions appropriate for the purpose. The author undertook the experimental research to find out the answers.

Another approach currently widely applied by the various research groups is the reduction of the semiconductor's band gap. Commercially available titanium

dioxide photocatalysts, including the renowned Degussa P25, can utilize for their action only a small fraction, about 4 %, of the solar radiation reaching the Earth's surface, i.e. UV-radiation (300-387.5 nm), due to the band gap of 3.2 eV (Zhang et al., 1994). However, titanium dioxide can be modified with the addition of various elements in order to make it visible light-sensitive (Lettmann et al., 2001, Ihara et al., 2003, Bessekhoud et al., 2004, Ohno et al., 2004, Wang et al., 2005, Sharma et al., 2006, Arpac et al., 2007). Titanium dioxide sensitization takes place through the formation of structure with charge carrier disbalance; this can occur via two mechanisms. In case if electrons in the new structure are in excess, they form a new energetic level inside the band gap, named donor level. This situation is generally described as *n*-type conductivity. Electromagnetic irradiation excites and displaces electrons from donor level. If, on the other hand, holes are in excess, the semiconductor is of *p*-type. The holes form so-called acceptor level inside the band gap; at room temperature, valence band electrons have enough energy to transfer to the acceptor level, from which they are subsequently displaced by the electromagnetic radiation. Both ways, the electrons are displaced from an energetic level inside the band gap, this way the latter is effectively decreased. As a result, a larger portion of solar radiation reaching the Earth's surface can be utilised, and larger amount of photons can create more holes thus accelerating the PCO. However, as the preliminary knowledge suggests, the decreased band gap comes at the price of photocatalyst oxidation potential reduction (Liu et al., 2007). There is, however, no clarity in understanding of the role of so-called "red shift" in the band gap. Some researchers find this phenomenon to be non-existent (Xekoukoulotakis et al., 2010), some blame the residual UV in the visible light, some, however, bring serious proof for the catalysts doping.

The latter made the author to undertake the experimental research into modifying the titania photocatalysts with various dopants. The author shares the findings indicating pronounced selectivity of doped catalysts in oxidation of various organic compounds (Articles IV-IX).

1.2. Aqueous pollutants under consideration: an overview

Ethylene glycol and its derivatives

Ethylene glycol is mainly used as antifreeze, although substantial amounts of EG are consumed in polymer synthesis. 2-Ethoxyethanol is used as a solvent, a de-icing agent for runways and aircrafts, and a de-icing additive in the jet fuel. The usage of DEGMME is similar to that of 2-EE; it is also used as a diluent for hydraulic brake fluids. Massive use of the de-icing substances, their leakage, accidental spillages and uncontrolled disposal of fuels, de-icing and brake liquids and antifreezes result in their occurrence in groundwater. All these substances act as central nervous system depressants and may inflict substantial kidney damage which can be fatal; they have also negative effects on respiratory and reproductive systems (Verschueren, 1983, Sax, 1984). Glycol-based de-icing agents have been

proven by earlier studies to be refractory against biodegradation and thus they accumulate and remain intact in groundwater for long times (Nitschke et al., 1996). Chemical oxidation methods, such as ozonation and treatment with Fenton's reagent, have been proven inadequate in dealing with glycolic pollution (Andreozzi et al., 1996, Beschkov et al. 1997, McGinns et al., 2001, Turan-Ertas et al., 2002), resulting in insufficient pollutant removal and poor mineralization, not to mention high treatment cost.

PCO, known to be the AOP with the highest oxidation potential, showed much better results than the other AOPs in the removal of glycolic substances, although the reaction rate was somewhat slow (Yamagata et al., 1989, Brezova et al., 1991). The impact of glycol molecule structure and especially the ways to accelerate the PCO of glycols were, therefore, the topics of major interest in this research.

Methyl-tert-butyl ether and tert-butyl alcohol

Methyl *tert*-butyl ether, banned for its use in the USA, is still widely used as an oxygenated component of motor fuels by the rest of the world. This substance is of particular concern because of its accumulation in groundwater due to its low biodegradability (Yeh and Novak, 1994). Physical removal and chemical oxidation methods, such as air stripping, activated carbon adsorption, non-assisted ozonation and treatment with Fenton's reagent have been proven to be ineffective against MTBE (Johnson, 1998, Xu et al., 2004; Safarzadeh-Amiri, 2001).

TBA was primarily found as a result of MTBE hydrolysis and thus also enters groundwater as an impurity of MTBE-blended motor fuels (Church et al., 1999). TBA shows behaviour similar to that of MTBE towards conventional treatment methods being even more resistant towards oxidation.

Primary research into MTBE PCO seems to be focused mainly onto gaseous phase, although aqueous PCO of MTBE deserves also a more systematic approach. Although MTBE is degraded well by PCO (Rodriguez-Gonzales et al., 2008), the process can be accelerated in order to reduce the treatment cost. Expanding the light spectrum utilized by the catalysts received attention in the present research.

Aromatic compounds

p-Toluidine is a widely used industrial chemical, with its use ranging from a component of several jet and rocket fuels to applications in paint and pharmaceutical industries (Papok and Semenido, 1962). Also, at former munitions sites *p*-toluidine is a degradation intermediate of *p*-nitrotoluene (Schmeltz et al., 1977). Non-biodegradable *p*-toluidine may accumulate in groundwater aquifers in toxic amounts. Biological water treatment methods have been shown to be inadequate against aromatic amino compounds pollution (Rozkov et al., 1999).

Phenol, being a substantial environment pollutant of, for example, oil shale industry (Kahru et al., 2002), has a reputation of a standard model contaminant used to test the activity of various oxidation methods and catalysts.

Along with the application of phenol to testing the catalysts, the author showed the approach with the single standard compound to be compromised with the selective oxidation performance of doped photocatalysts: showing low performance in PCO of phenol and glycols, the N-, S, B- and C-doped catalysts appeared to be effective against *p*-toluidine, MTBE and antibiotics (see Articles IV-IX).

Antibiotics

For the last years the interest towards the environmental fate of medicines, especially antibiotics, has been arising. Being refractory substances (Al-Ahmad et al., 1999, Kümmerer et al., 2000, Alexy et al., 2004), antibiotics pass the biological treatment plants intact (Herberer, 2002), either remaining in the liquid phase or, dependent on their hydrophilicity, adsorbing to the active sludge with subsequent desorption to the environment (Abellan et al., 2007). These substances in the environment are potent in damage of micro-flora and fauna, accumulate in food chains (Halling-Sørensen et al., 1998, Hartig et al., 1999), and accelerate the development of resistant micro-organisms, including pathogens (Kim et al., 2005, Baran et al., 2006, Sørum, 2006, Chatzikakis et al., 2008). The accumulation of antibiotics in organisms may cause arthropathy, nephropathy, damages in central nervous system and spermatogenesis, mutagenic effects and light sensitivity (Kümmerer et al., 2000). Three widely used antibiotics have been chosen for this research.

Amoxicillin (AMO, (2*S*, 5*R*, 6*R*)-6-[[*(2R)*-2-amino-2-(4-hydroxyphenyl)acetyl]amino]-3,3-dimethyl-7-oxo-4-thia-1-azabicyclo[3.2.0] heptane-2-carboxylic acid), is a moderate-spectrum bacteriolytic β -lactam antibiotic.

Doxycycline (DC, (4*S*,4*aR*,5*S*,5*aR*,6*R*,12*aS*)-4-(dimethylamino)-3,5,10,12,12a-pentahydroxy-6-methyl-1,11-dioxo-1,4,4*a*,5,5*a*,6,11,12*a*-octahydrotetracene-2-carboxamide) is a tetracycline antibiotic widely used against bacteria, protozoa and helminths. Since DC is used as a treatment or prophylactic of some of the most hazardous diseases known to mankind, such as bubonic plague and anthrax (Greenfield et al., 2003, Brook, 2002), its prevention from entering the environment is of great importance.

Sulfamethizole ((4-amino-N-(5-methyl-1,3,4-thiadiazole-2-yl)-benzenesulfonamide, SMZ) is one of the most commonly used sulphonamide antibiotic effective against *Escherichia coli* and many other micro-organisms. Sulphonamides constitute a synthetic antibiotics class widely used as both human and veterinary medicine against a majority of Gram-positive and many Gram-negative micro-organisms and protozoa. In livestock and poultry production, these are used also in growth promoting. The residues of sulphonamides can be found in animal products for human consumption, such as honey, milk, eggs, fish or meat (Wang et al., 2006). Most sulphonamides have a relatively long half-life, generating on accumulation serious unwanted effects on human health, such as allergic or toxic reactions (Sanderson et al., 2006) and there have already been reports of sulphonamides

(Sanderson et al., 2006, Jen et al., 1998, Haller et al., 2002, Hartig et al., 2003) and sulphonamide-resistant micro-organisms being encountered in the environment (Diaz-Cruz and Barcelo, 2005).

Several works have been published concerning the degradation of antibiotics using ozonation (Balcioglu and Ötoker, 2003, Beltran et al., 2008, Dantas et al., 2008) and Fenton reagent treatment (Elmolla and Chaudhuri, 2009, Rozas et al., 2010). Showing rather efficient performance against antibiotics, these methods are quite expensive due to high ozone doses and reagent consumption. Inexpensive and efficient PCO provides a good alternative for these methods.

Generally speaking, most of the works dealing with antibiotics degradation by PCO and other AOPs focus mainly on parent compound destruction and mineralization at best, leaving all the rest, including their degradation pathways and, especially, their by-products largely unexplored. This, however, is quite important, as one needs to be sure that the parent compound destruction does not produce even more hazardous pollution. The author could find only one report (Li et al., 2009) on using visible light-sensitive photocatalysts for the PCO of antibiotics.

2. MATERIALS AND METHODS

Two thermostatted at $20 \pm 1^\circ\text{C}$ 200-mL batch reactors with inner diameter 100 mm (evaporation dishes), irradiated contact surface $40 \text{ m}^2 \text{ m}^{-3}$, agitated with magnetic stirrers, were used in PCO experiments: the one used for the PCO was called “active” and the other containing no photocatalyst was called “reference”. Both reactors were exposed to the identical experimental conditions. The samples from the active reactor were compared to the reference samples to avoid complications caused by water evaporation. An artificial UV–light source, Phillips 365-nm low pressure luminescent mercury UV-lamp (15 W), was positioned horizontally over the reactors, providing the irradiance of about 0.5 mW cm^{-2} (Phillips Sylvania Blacklight, Articles I-VII and IX) or 1.5 mW cm^{-2} (Phillips Actinic, Article VIII) measured at a distance corresponding to the level of the surface of the reactor by the optical radiometer Micropulse MP100 (Micropulse Technology, UK). With artificial daylight fluorescent lamp (Phillips TL-D 15W/33-640), the irradiance could not be directly measured. The illuminance was measured using TES 1332 luxmeter (TES Inc., Taiwan) reaching $3,700 \text{ lx}$ (lm m^{-2}), which corresponds to the irradiance of 0.6 mW cm^{-2} . The irradiance was calculated using lumen to watt ratio of 684, as the response of the human eye to the illuminance of 684 lm equals to that to the irradiance of 1 W (Kirkpatrick, 2005). With AMO PCO experiments were conducted outdoors using natural solar radiation; the irradiance was measured by luxmeter approximating 16 mW cm^{-2} .

Titanium dioxide was used as 1 g L^{-1} slurry. The experiments were carried out with aqueous solutions of AMO supplied by Sigma-Aldrich. In the experiments, the initial concentration of AMO varied between 1 and 100 mg L^{-1} . The influence of the initial pH was studied in the range from 3 to 12 for different substances,

adjusted by 4 N sulphuric acid or 15 % sodium hydroxide. Generally, the pH was monitored throughout the experiments without adjustment. The treatment time under artificial light sources, i.e. lamps, was chosen to be 2 h for MTBE, 4 h for TBA, 6 h for AMO and SMZ, 2-6 h for DC (depending on the initial concentration), and 24 h for glycols (EG, 2-EE and DEGMME) and aromatic substances (phenol and *p*-toluidine). Under natural solar irradiation, the treatment time was reduced to 0.5 h for MTBE, and 2 h for AMO and SMZ.

All the experiments were carried out for at least three times under identical experimental conditions. The average deviation of data in parallel experiments did not exceed 5 %.

The decrease of MTBE, TBA, and glycolic substances concentrations was determined from the decrease in chemical oxygen demand (COD), measured by a standard method. This parameter, unlike TOC, was proven to be universal, decreasing with the increased conversion degree in oxidation reactions. Concentrations of *p*-toluidine were measured photometrically after diazotation and reaction with phenol at 490 nm, and those of phenol were determined photometrically after reaction with *p*-nitroaniline at 570 nm using Helios β spectrophotometer together with the COD. In case of *p*-toluidine, the evolution of nitrite and nitrate ions was also determined using Metrohm 761 Compact IC ion chromatograph.

Antibiotics concentration was determined photometrically, using the light absorbance at 230 nm, using Helios β spectrophotometer. Nitrate and sulphate anions were determined using Metrohm 761 Compact IC ionic chromatograph, whereas ammonium ion was determined photometrically using a modified version of a standard phenate method. A Waters Aquity UPLC combined with MS and quadrupole-time of flight (Q-TOF) mass-analyzer (Competence Centre for Food and Fermentation Technology) was used for the determination of organic AMO PCO by-products. An Aquity UPLC BEH C₁₈ 1.7 μ m 2.1 \times 100 mm column was used, with water and 0.1 % formic acid as eluent A (initial eluent) and acetonitrile with 0.1 % formic acid as eluent B. The complete change from eluent A to B was achieved in 15 min out of 20 min run with linear gradient used. Mass spectra were acquired in a full scan mode (50-500 amu). The instrument was operated in positive ion mode, with capillary voltage of 2400 V. The mass spectrometry data was handled using MassLynx software. With SMZ, PCO by-products were determined using a Q-Star Elite mass-spectrometer (MS) (Applied Biosystems, Germany) equipped with an electrospray ionization (ESI) source and a quadrupole-time of flight (Q-TOF) mass-analyzer (TUT Department of Chemistry). Samples were diluted with 50 % MeOH containing 0.1 % CH₃COOH and injected directly into the MS using a syringe pump with a flow rate of 7.0 μ L min⁻¹. Mass spectra were acquired in a full scan mode (30-500 amu). The instrument was operated in positive ion mode under the following conditions: ionspray voltage 4500 V; curtain gas, 20 arbitrary units; nebulizer gas, 23 arbitrary units. The MS data were treated using Analyst QS 2.0 software.

The accuracy of UV-absorbance in antibiotics concentration measurements was checked by the parallel determination of AMO in MS analysis of the PCO-treated samples with the AMO pre-constructed calibration curves for both methods: the difference observed between AMO concentrations determined by UV-absorbance and MS did not exceed 2 % at highest, suggesting negligible amounts of UV-absorbance by PCO by-products. For this reason, the UV-absorbance was used as a simpler and less time- and resource-consuming approach than MS. It was noted that the UV-absorbance spectra of PCO-treated solutions did not exhibit a change in shape, showing no new peaks or a wave-length shift in maximum absorbance. Poor accumulation of UV-absorbing PCO by-products may be explained by their oxidation rates being comparable to or exceeding those of AMO. A similar analytical approach has been used in oxidation studies with other antibiotics of aromatic structure, such as sulphamethazine (Kaniou et al., 2005), chloramphenicol (Chatzikakis et al., 2008), and flumequine (Palominos et al., 2008).

Adsorption experiments were carried out in closed thermostatted flasks equipped with magnetic stirrers at 20 ± 1 °C. The amount of adsorbed substance was derived from the batch mass balance: the concentration of the dissolved substance was determined before and after adsorption

Carbon-doped titania photocatalysts were obtained by the hydrolysis of tetrabutyl orthotitanate at room temperature without adjustment of pH being around 5.5 to 6.0, followed by drying and calcination at different temperatures (200 to 700 °C). After this, the catalyst was washed with hot distilled water applied in a sequence of 10 to 15 rinsing rounds (ca. 1 L per 1 g of catalyst) in order to clean the catalyst surface from water-soluble compounds.

Two nitrogen-doped catalysts were produced by the addition of 25 mL of aqueous solution containing 11.65 g of carbamide to 33 mL of tetrabutyl orthotitanate under constant stirring. The acquired product of hydrolysis was then dried and heated in a furnace at 400 °C. The N-Ce-containing catalyst was synthesised in a similar way, except the addition of 5 mL of ammonium cerium nitrate solution containing 200 g L^{-1} in 4-N nitric acid. Another two nitrogen-doped catalysts were synthesised by the methods described by Wang et al. (2005) and Gandhe and Fernandes (2005).

Sulphur-containing photocatalysts were prepared by the hydrolysis of titanium tetrabutoxide with addition of a pre-calculated amount of 0.1 N sodium thiosulphate as sulphur source, followed by calcination at 400 °C for 4 h, and, subsequently, washing, as described. In case of boron-containing photocatalysts, sodium tetraborate was used as boron source. An additional catalyst was synthesised using the same pattern, although without the addition of sulphur or boron sources. The experiments were performed in photocatalyst suspensions of 1 g L^{-1} .

Iron-doped titania catalysts with calculated iron content from 0.42 to 3 at. % were prepared by the pulverisation of 75 mL of tetrabutyl orthotitanate into 1 l pre-sonicated Fe_2O_3 suspensions of various concentration (0.1 to 0.7 g L^{-1}); the

hydrolysis was followed by sonication, drying and calcination at 200 °C. After calcinations, all the catalysts were washed with hot (70-80 °C) distilled water applied in a sequence of 10 to 15 rinsing rounds (ca. 1 L per 1 g of catalyst) in order to clean the catalyst surface from water-soluble compounds.

The crystallinity of doped titania was analysed using D5000 Kristalloflex, Siemens (Cu-K α irradiation source) X-ray diffraction spectroscopy (XRD, TU Clausthal). Doped photocatalysts composition was measured with PHI 5600 X-ray photoelectron spectroscopy (University of Colorado, Boulder). The specific area (BET and Langmuir adsorption) and the pore volume of the catalysts were measured by the adsorption of nitrogen using KELVIN 1042 sorptometer.

3. OBJECTIVES

Based on its strong oxidative action and relatively low treatment cost, especially when using natural solar irradiation, PCO can be regarded as a prospective alternative to the existing treatment methods. One of the major goals of the present research was the alleviation of its shortcomings by different approaches, enlarging the spectrum of known PCO-degradable pollutants and the accumulation of knowledge on PCO mechanism of various substances. These points present the main novelty, theoretical and practical value of the present research.

The immediate main objectives of the present research were as follows:

1. To determine the limits of PCO applicability by using a relatively wide range of model pollutants;
2. Oxidation acceleration by the means of additives to the treated solution and the catalysts;
3. Engineering solutions, i.e. the use of photocatalysts in various forms: slurry, attached to hollow glass microspheres, and the flat glass plates with the photocatalyst attached to them by two different modes.

In order to fulfil the objectives, the following questions were studied:

1. The efficiency of PCO in degradation of pollutants;
2. The study of PCO mechanism (radical vs. hole reactions, role of adsorption, reaction by-products, the description of reaction kinetics);
3. The impact of external factors (concentration of pollutants, pH, dissolved admixtures);
4. Synthesis and examination of modified catalysts with wider electromagnetic radiation absorbance spectrum: non-metal dopants - sulphur, boron, nitrogen and carbon; metal dopants - iron and cerium.

4. RESULTS AND DISCUSSION

The results obtained during the conducted research show that PCO is an effective means against a wide range of pollutants. The efficiency of PCO in removal the pollutants was studied throughout all the articles in this dissertation. Mechanisms of various substances' PCO were studied in Articles II-IX; PCO reaction pathways

for individual substances were established in Articles II, III, V, VII and VIII. PCO acceleration in presence of iron ions was studied in Articles I-III. PCO acceleration through using various visible light-sensitive titania photocatalysts was considered in Articles IV-IX. Engineering solutions for more efficient use of the catalyst were presented in Articles I and II.

4.1. Degussa P25 titanium dioxide

PCO performance

The PCO of glycols was proceeding rather slow (Articles I-III), with the PCO efficiency values of 10 to 40 mg O W⁻¹ h⁻¹ (Article III) with EG, 2-EE and DEGMME. Earlier research (Krichevskaya et al., 2001) has shown that the influence of pH to the efficiency of glycols' PCO is not very pronounced, using 2-EE as an example. This is due to the fact that the PCO of glycols proceeds mainly through positively charged holes on the photocatalyst surface (Brezova et al., 1991). In case of MTBE and TBA, PCO proceeds well (Article IV and IX) with both PCO mechanisms, radical and hole oxidation, taking place simultaneously (Liang et al., 1999). Degussa P25 titanium dioxide showed moderate results for aromatic compounds, i.e. phenol and *p*-toluidine (Preis et al., 2002): the PCO efficiency values were mostly under 10 mg W⁻¹ h⁻¹ and decreased with increasing pH.

The PCO of antibiotics, AMO, DC and SMZ, proceeded well, giving substantial pollutant and COD degradation (Articles V, VIII and IX). At smaller concentrations (up to 10 mg L⁻¹) total antibiotic degradation was achieved. The PCO of SMZ (Article VII, Fig. 2, 3, Table 1) and DC (Article IX, Fig. 1, Eq. 2, 3) tended to follow L-H monomolecular reaction model with substrate molecule adsorption and by-products desorption quite well, whereas in case of AMO the reaction mechanism appears to be changing with the initial concentration growth from first to zero order (Article V, Fig. 2). The addition of TBA as a radical scavenger to the solutions of all the substances resulted in almost no effect on their PCO rate, allowing suggesting that their PCO proceeds mainly through the reactions with positively charged holes on the catalyst surface. In case of AMO, a certain increase in PCO efficiency was observed with the increase in pH (Article V, Fig. 3), whereas with DC and SMZ the pH-dependence was not established.

The influence of iron ions

The experiments establishing the influence of iron ions to the aqueous PCO were undertaken with glycols, EG, 2-EE and DEGMME, and MTBE (Articles I-III). An interesting trend was observed: at small concentrations (mostly under 0.1 mM), iron ions were able to significantly accelerate PCO of glycols, from 1.5 to 3 times, dependent on the substance (Article I, Fig. 4, Article III, Fig. 1-3). However, further increase of iron ions' concentration inhibited the PCO of the substances

under scope. With EG, a more complicated pattern was observed (Article III, Fig. I): an initial increase in the PCO efficiency of EG at smaller iron ion concentrations was followed by a minor decrease. The former PCO efficiency decrease was followed by yet another increase and remained stable, followed by a drastic decrease above with yet further iron ions concentration increase. The MTBE PCO efficiency (Article I, Fig. 4) increased with the initial increase of iron, then decreased, and afterwards exhibited another limited increase. The observations can be explained by the competitive adsorption of the pollutant and iron ions on the surface of Degussa P25 titanium dioxide, and also by the adsorption phenomena of the pollutants on the surface of TiO_2 (Article III). Also, radical reactions of MTBE PCO are to be affected by different iron ions concentration.

Catalyst application mode

Although titanium dioxide was used as slurry in the majority of the experiments, in case of 2-EE the experiments were also performed using the catalyst attached to hollow glass microspheres and flat glass plates: TiO_2 was either precipitated from the slurry or the slurry was sprayed upon the glass plate. Even though the slurry proved to provide the highest PCO efficiency, the plate with sprayed titanium dioxide showed the efficiency of about 60 % of the one attained in slurry, with much smaller catalyst amount being used (Article I, Fig. 3).

Solar experiments

A great interest towards PCO is due to the possibility of using solar radiation having wider UV spectrum and much higher irradiance than UV-lamps can sensibly give. When natural solar radiation was used, the PCO of antibiotics accelerated for several times (Article V, Fig. 5, 6, Article VII, Fig. 4, 5, Table 2), providing results similar to or better than the ones observed with UV-lamp in a much shorter time.

Reaction pathways

With glycols and antibiotics, a number PCO by-products were determined, which allowed the construction of respective PCO pathways (Article III, Fig. 6-8, Article V, Fig. 6, Article VIII, Fig. 3, Article IX, Fig. 6). Since with these substances radical reactions play little role in their PCO, the oxidation pathways are strongly related to the adsorption, which, in turn, depends on the nature of molecules. Several PCO reaction pathways for the same substance were identified, dependent either on their adsorption geometry, as with 2-EE and DC (Article III, Fig. 6, Article VIII, Fig. 3), or on their concentration, as with AMO (Article V, Fig. 7-9).

4.2. Modified titania catalysts

Modified titania samples were synthesised by sol-gel method, using tetrabutyl orthotitanate as titanium source, with the exception, where titanium (III) chloride was used instead. In order to modify the catalyst with certain elements, their source had to be added during the synthesis. The only element that did not require external source was carbon.

Modified titania catalysts showed selective performance towards the pollutants under the scope. With glycols, doped catalysts showed inefficient performance (Article IV, VI). The performance of modified catalysts against aromatic substances was comparable to or under the ones obtained with P25. The least efficient results with aromatics were obtained with carbon-containing titania (Article IX), whereas the results obtained with S- and B-TiO₂ were comparable to or surpassing the ones of Degussa P25 (Article VI). With MTBE and TBA, visible light PCO proceeded far better than with UV-irradiated Degussa P25 (Articles IV, VI, IX), with S-TiO₂ showing the best results, followed by B-, N- and C-containing photocatalysts. The performance of modified titania was moderate to high when compared to Degussa P25 oxidising AMO (Article V) and SMZ (Article VII), and was surpassing the performance of commercial photocatalyst with DC (Article VIII). Under natural solar light, the performance of all the photocatalysts was accelerated, however, for the modified titania the acceleration was generally more pronounced than for Degussa P25.

Carbon-containing titania

When synthesising the catalysts by sol-gel method, carbon-containing titania is obtained spontaneously; in practice it is not possible to get rid of carbon even at high calcinations temperatures (Article IX). Carbon content and thus the catalyst properties can be varied by varying the catalysts' calcination temperature: it decreases with the increased temperature. With the increased carbon content, the catalysts' band-gap is decreasing. The composition and surface properties of the carbon-containing titania are shown in Article IX, Table 1.

With MTBE, the catalysts' calcinations temperature, and thus carbon content, did not influence significantly their PCO performance under artificial visible light. The PCO efficiency results obtained with all the catalysts were oscillating at a level significantly surpassing the one obtained with Degussa P25 catalyst under UV-radiation (Article IX, Fig. 1).

With phenol and *p*-toluidine C-TiO₂ showed a declining trend with the growth of the catalysts' calcinations temperature, i.e. the decrease of their carbon content and surface. The catalyst calcinated at the lowest temperature showed performance comparable to or slightly surpassing the one of UV-irradiated Degussa P25 (Article IX, Fig. 2, 3).

In the experiments with AMO, PCO results obtained with C-TiO₂ and luminescent lamp were significantly lower than the performance of Degussa P25

(Article V, Fig. 4), and showed a declining trend with the increase of the catalysts' calcinations temperature. However, when subjected to natural solar radiation, the performance of C-TiO₂ sample with the highest carbon content showed PCO efficiency only somewhat lower than the one obtained with Degussa under similar conditions (Article V, Fig. 6). The improvement of modified catalyst performance under solar radiation may be explained by the wider light spectrum when compared to luminescent lamp, and also by disproportional growth of solar radiation intensity in visible range: the larger the wavelength the higher radiation of solar spectrum.

With DC, PCO efficiency also decreased with the increase of catalyst calcinations temperature. However, the performance of VIS-irradiated C-TiO₂ of several carbon-containing catalysts was up to four times higher than that of UV-irradiated Degussa P25 (Article VIII, Fig. 1, 2).

PCO of SMZ with C-doped photocatalysts proceeded slower than with Degussa P25 (Article VII, Fig. 4, 5).

Generally speaking, the performance of carbon-containing titania under visible light is in most cases less efficient or comparable to UV-irradiated Degussa P25. However, this can be accelerated considerably by using solar light, surpassing the performance of Degussa P25 (Article VIII, Fig. 2, 3). C-TiO₂ PCO efficiency increases with the increased carbon content and the catalyst surface. The selectivity in the C-TiO₂ performance was observed.

Nitrogen and nitrogen-cerium-containing titania

The performance of several nitrogen-containing and one nitrogen and cerium-containing photocatalysts was tested with MTBE, TBA, phenol, 2-EE and EG. MTBE and TBA were oxidised with the performance similar to or superior than that of Degussa P25 (Article IV, Table 2). With phenol and glycols, the performance of these catalysts was inefficient. The surface properties of these photocatalysts can be seen in Article IV, Table 1.

Nitrogen-containing titania shows selective efficiency towards the substances under scope. The difference in the behaviour of the substances in PCO with these catalysts can be explained by the difference in oxidation mechanism and adsorption properties of the substances. 2-EE and EG have been proven by earlier studies to be oxidised only on positively charged TiO₂-holes being rather immune towards radical oxidation, thus making adsorption a crucial factor in the PCO (Krichevskaya et al., 2003). No adsorption of any of the studied substances was, however, determined on N-TiO₂ within the limits of analytical precision. On the other hand, MTBE and phenol can be oxidised by both holes and radicals, although these substances behave differently in PCO: MTBE is readily oxidised, whereas phenol yields poorly to PCO on N-TiO₂.

The author suggests that the selective PCO of MTBE and TBA could be explained by the *tert*-butyl radical in the molecular structure of these substances. Under conditions of protonated media, the surface of the catalysts is protonated, so are the molecules of phenol being electrostatically repelled from the surface,

similarly to the effect proposed by Vilhunen and Sillanpää (2009) for salicylic acid. The MTBE molecule may remain, however, electrically neutral and the TBA molecule protonation may have a smaller repelling effect due to the large neutral *tert*-butyl radical. Therefore, these molecules, although not adsorbed, may approach the N-doped photocatalyst's surface close enough to react with OH-radicals more actively than phenol.

Sulphur-containing titania

Sulphur-containing titania photocatalysts were tested in PCO of MTBE, TBA, phenol, *p*-toluidine and 2-EE. *i*-Propanol was added to the list to study the role of molecular geometry on the PCO of these substances (primary C atom in 2-EE, secondary in *i*-propanol, tertiary in MTBE and TBA). The composition and surface properties of sulphur-containing photocatalysts can be seen in Article VI, Table 1.

In the PCO of MTBE, sulphur-containing titania photocatalysts have shown results surpassing the ones obtained with UV-irradiated Degussa P25 up to two times. With MTBE, the influence of sulphur content on the PCO efficiency was increasing at smaller sulphur concentrations, followed by a gradual decrease. Optimal S content in the catalysts was around 1.5 at. % (Article VI, Fig. 3). Under natural solar radiation, MTBE PCO with Degussa P25 and S-TiO₂ proceeded fairly similarly.

With TBA, the increase of sulphur content resulted in gradual increase of TBA PCO efficiency (Article VI, Fig. 3). The absence of optimum S concentration, observed with MTBE, having similar structure, may be explained by the turning point for TBA laying at higher concentrations.

The best performance in PCO of MTBE and TBA was observed in acidic media, followed by alkaline and neutral media (Article VI, Fig. 2).

With *p*-toluidine, the best performance was observed in alkaline media, with acidic and neutral ones giving no observable oxidation. The performance of *p*-toluidine PCO with sulphur-containing photocatalysts under VIS was comparable to that of UV-irradiated Degussa P25 (Article VI, Fig. 4a).

With phenol and 2-EE, PCO with S-TiO₂ was inefficient.

With aliphatic substances, the modified catalysts showed the best performance with MTBE and TBA, followed by *i*-propanol and 2-EE. Since the adsorption of substances under scope on the surface of the catalysts was found to be negligible, the PCO is assumed to proceed here mainly as a nucleophilic attacks of hydroxyl radicals. Nucleophilic attack proceeds upon the carbon atom having the highest partial positive charge. In ethers and alcohols this is a carbon atom located next to oxygen due to oxygen being more electronegative: with 2-EE, the nucleophilic attack proceeds on both C1 and C2 atoms (Articles II and III). With *i*-propanol, a secondary carbon atom connected to the hydroxyl group is under attack, in TBA and MTBE molecules hydroxyl radical attacks tertiary carbon atom, connected to the hydroxyl and methoxy groups, respectively, although an attack on the methyl group in MTBE may also take place. Despite obvious geometric obstruction, the

nucleophilic attack on tertiary carbon atom is the most effective, followed by secondary and finally by the primary atom, as one can see from the present results. This is to be explained by greater charge localisation on tertiary and secondary carbon atoms: tertiary carbon's electron cloud is pulled to oxygen atom on one hand and to three comparatively electronegative methyl groups on the other hand. The secondary carbon atom is less affected by methyl groups, and the C-atoms in 2-EE are least affected.

Sulphur-containing titania photocatalysts were shown to be the efficient photocatalysts synthesised on course of the research. Even though the catalysts contain larger amounts of carbon than these of sulphur, the positive effect of sulphur addition can be well observed, when comparing the results observed with S-TiO₂ to the catalysts doped only with carbon, obtained under the same conditions, and to the general performance of carbon-containing photocatalysts. However, selective performance can also be seen here. As no substances of the studied ones were shown to adsorb on the surface of S-TiO₂, the differences observed in their PCO patterns can be explained by their chemical structure and different partial charge localisation, leading to different affinity towards hydroxyl radicals at the catalysts' surface.

The increase of the PCO efficiency of sulphur-containing photocatalysts with the growth of sulphur content, and the following decrease may be explained by the overpowering of the positive effect obtained from the band-gap decrease by the decrease of the catalysts' redox potential.

Boron-containing titania

The experiments with boron-containing titania photocatalysts were undertaken with MTBE, TBA, and *p*-toluidine. The properties of B-TiO₂ photocatalysts can be seen in Article VI, Table I.

With B-TiO₂, the dependence of the efficiency of MTBE and TBA PCO on pH was similar to that of S-TiO₂ (see Article VI, Fig. 2b). Under visible radiation at pH 3.0 an increasing trend in PCO efficiency was observed with the boron content increasing to 2 at. %; above that content, the efficiency remained at a constant level (Article VI, Fig. 3b). Under visible light with B-TiO₂ the efficiency of PCO of both MTBE and TBA exceeded the one achieved with Degussa P25 under UV for about two times (Article VI, Fig. 3).

Contrary to the S-TiO₂ catalysts, the boron-containing titania exhibited the fastest *p*-toluidine PCO in acidic media followed by neutral and basic ones (Article VI, Fig. 4b). The PCO efficiency with B-TiO₂ in acidic media under visible light exceeded the one of Degussa's under UV by a factor 1.5 for *p*-toluidine and 2.0 for COD degradation. It is noticeable that in neutral and alkaline media the PCO efficiency decreases slightly with the increase in the boron content in the catalysts (rather similar to the effect observed with S-TiO₂), however, the trend is quite contrary in case of acidic media, where certain growth can be observed. The reason

behind this observation is the different behaviour in acidic media of the catalyst containing only carbon as opposed to those containing boron and carbon.

Among the modified catalysts, the performance of B-TiO₂ was yielding only to S-TiO₂, with the exception of *p*-toluidine. Compared to C-TiO₂ it can be seen that the addition of boron even in negligible amount accelerates the catalysts' performance significantly.

Iron-containing titania

The experiments with iron-containing photocatalysts were undertaken with AMO. The AMO conversion degree with iron-doped titania increased from 12 to 25 % with iron content growing from 0.42 to 0.89 at. % (Article V, Fig. 4), remaining more or less unchanged with further increasing iron content. Iron-doped photocatalysts were used also in solar PCO experiments, with which the AMO degradation proceeded faster than with artificial light: the performance of doped catalysts was moderately inferior to that of P25 (Article V, Fig. 6). The disproportional improvement of oxidation rates, about three times for Degussa P25 and about seven times for the doped catalysts, may be explained by the difference in the irradiance with UV and visible light in solar spectrum: the intensity of radiation in solar spectrum grows dramatically with increasing wavelength from 300 to 500 nm, whereas the experiments with lamps were carried out under similar irradiance conditions.

5. CONCLUSIONS

Aqueous photocatalytic oxidation (PCO) has been experimentally proven to be an effective means against water pollution originating from a wide spectrum of organic pollutants: methyl-*tert*-butyl ether (MTBE), *tert*-butyl alcohol (TBA), and antibiotics, i.e. amoxicillin (AMO), doxycycline (DC) and sulphamethizole (SMZ). This way, the spectrum of substances known to be degradable by PCO was widened. Different catalyst application modes were investigated, with the main stress on preparation of efficiently working systems with the catalyst bonded to solid surfaces. Titanium dioxide attached to flat glass plate by spraying showed performance somewhat inferior to slurry, but far less catalyst was used in this case (186 mg per 1 L of treated solution when compared to 1 g L⁻¹ in slurry), making the system feasible for further research and applications.

With glycols, i.e. ethylene glycol (EG), 2-ethoxy ethanol (2-EE) and diethylene glycol monomethyl ether (DEGMME), aromatic compounds, i.e. phenol and *p*-toluidine, the results were less efficient, however, especially in case of glycols, still better than those provided by the competitive treatment methods. With glycols and MTBE, the addition of small amounts of iron ions to the treated solution was able to significantly accelerate the PCO of these substances. The peak optimum concentration of dissolved iron controlling the PCO efficiency was observed and reported for the first time for these substances.

A number of visible-light sensitive photocatalysts containing different admixtures (C, N, S, B, Fe) were synthesised and successfully tested for the PCO of the substances under scope. These showed selective performance towards the studied substances, but in most cases they showed performance comparable to or superior of the commercial photocatalyst Degussa P25 (Tables 2, 3). This is also a major novelty when compared to most of the works dealing with PCO by modified titania, where only one or two substances, in most cases dyes, are degraded at a time: no selective performance of doped titania has been performed earlier. The influence of the dopant content was generally similar for the modified titania species: in the studied dopant range, the increase in its content resulted in the increase of PCO efficiency. This was in some cases followed by a gradual PCO efficiency decrease, which may be attributed to the decrease in redox potential overpowering the positive effect of the band-gap decrease. Also, the surface properties and charging of the catalysts and the pollutants should play their role on the overall PCO process. Under natural solar radiation, the performance of the photocatalysts was drastically accelerated.

PCO kinetics of the substances under scope was shown mainly to follow Langmuir-Hinshelwood model. Dominating PCO mechanism was determined for the substances under scope. With glycols and antibiotics, this was hole oxidation, whereas aromatic and aliphatic substances seemed to be degraded largely by hydroxyl radicals. A research into PCO by-products of the substances was undertaken, allowing constructing their reaction pathways. With 2-EE, additional PCO reaction pathways were discovered when compared to the literature, and no degradation pathway studies have ever been undertaken with the antibiotics under scope. With substances degrading by surface reactions, the pathways depended strongly on the adsorption behaviour of these, resulting in several oxidation pathways dependent on the part of molecule being bond to the catalyst.

Table 2. The PCO reaction rates ($\text{mg L}^{-1} \text{h}^{-1} / \text{mg O L}^{-1} \text{h}^{-1}$) compared to the Degussa P25 commercial photocatalyst under artificial light sources

Catalyst	Glycols		MTBE	TBA	Aromatics		Antibiotics**		
	EG	2-EE			DEGMME	Phenol	P-Toluidine	AMO	SMZ
P25*	-/2.5	5/10	-/9	-/8	1.2/2.4	1.9/2	3.5/3.6	3.3/2.6	10.6/9.9
P25+Fe ²⁺ *	-/11.8	11.6/16.5	-/15	-/77					
C-TiO ₂		-/0.8		50/50	0.7/-	2/2	1.3/1.3	3.1/0.8	12.6/17.9
N-TiO ₂	0	0		-/50	0.4/-				
S-TiO ₂		0		-/70	-/0.1	1.8/1.2			
B-TiO ₂		0		-/60	-/10	1.4/3.2			
Fe-TiO ₂							1.3/-		

* Experiments performed under UV

** Experiments with 25 mg L^{-1} pollutant's initial concentration

Table 3. The PCO reaction rates ($\text{mg L}^{-1} \text{h}^{-1}$ / $\text{mg O L}^{-1} \text{h}^{-1}$) compared to the action of Degussa P25 commercial photocatalyst under natural solar radiation

Catalyst	MTBE	TBA	Antibiotics	
			AMO*	SMZ*
P25	200/244	-/56	3.5/-	4/3.6
C-TiO ₂	200/-		3.1/-	3.1/-
S-TiO ₂	-/228	-/41		
Fe-TiO ₂			3.1/-	

* Experiments with 25 mg L^{-1} concentration

6. REFERENCES

1. **Abellan M.N., Bayarri B., Gimenez G., Costa J.** 2007. Photocatalytic degradation of sulfamethoxazole in aqueous suspension of TiO₂. – *Applied Catalysis B*, 74, 233-241.
2. **Al-Ahmad A., Daschner F.D., Kümmerer K.** 1999. Biodegradability of cefotiam, ciprofloxacin, meropenem, penicillin G, and sulfamethoxazole and inhibition of wastewater bacteria. – *Archives of Environmental Contamination and Toxicology*, 37, 158-163.
3. **Alexy R., Kümpel T., Kümmerer K.** 2004. Assessment of degradation of 18 antibiotics in the Closed Bottle Test. – *Chemosphere*, 57, 505-512.
4. **Andreozzi R., Caprio V., Insola A.** 1996. Kinetics and mechanisms of polyethyleneglycol fragmentation by ozone in aqueous solution. – *Water Research*, 30 (12), 2955-2960.
5. **Arpac E., Sayilkan F., Asiltürk M., Tatar P., Kiraz N., Sayilkan H.** 2007. Photocatalytic performance of Sn-doped and undoped TiO₂ nanostructured thin films under UV and vis-lights. – *Journal of Hazardous Materials*, 140, 69–74.
6. **Bahnemann, D.** 2004. Photocatalytic water treatment: solar energy applications. – *Solar Energy*, 77 (5), 445-459.
7. **Balciolu I.A., Ötker M.** 2003. Treatment of pharmaceutical wastewater containing antibiotics by O₃ and O₃/H₂O₂ processes. – *Chemosphere*, 50 (1), 85-95.
8. **Baran W., Sochacka J., Wardas W.** 2006. Toxicity and biodegradability of sulfonamides and products of their photocatalytic degradation in aqueous solutions. – *Chemosphere*, 65, 1295-1299.
9. **Beltrán F.J., Aguinaco A., García-Araya J.F., Oropesa A.** 2008. Ozone and photocatalytic processes to remove the antibiotic sulfamethoxazole from water. – *Water Research*, 42, 3799–3808.
10. **Beschkov V., Bardarska G., Gulyas H., Sekoulov I.** 1997. Degradation of triethylene glycol dimethyl ether by ozonation combined with UV irradiation and hydrogen peroxide addition. – *Water Science and Technology*, 36 (2-3), 131-138.
11. **Bessekhouad Y., Robert D., Weber J.-V., Chaoui N.** 2004. Effect of alkaline-doped TiO₂ on photocatalytic efficiency. – *Journal of Photochemistry and Photobiology A*, 167 (1), 49-57.
12. **Blake D.M., Webb J., Turchi C., Magrini K.** 1991. Kinetics and mechanistic overview of TiO₂-photocatalyzed oxidation reactions in aqueous solution. – *Solar Energy Materials*, 1-4 (24), 584-593.
13. **Brezova V., Blažkova A., Borošová E., Ceppan M., Fiala R.** 1995. The influence of dissolved metal ions on the photocatalytic degradation of

- phenol in aqueous TiO₂ suspensions. – *Journal of Molecular Catalysis, A*, 98 (2), 109-116.
14. **Brezova V., Vodny S., Vesely M., Ceppan M., Lapcik L.** 1991. Photocatalytic oxidation of 2-ethoxyethanol in a water suspension of titanium dioxide. – *Journal of Photochemistry and Photobiology A*, 56, 125-134.
 15. **Brook I.** 2002. The prophylaxis and treatment of anthrax. – *International Journal of Antimicrobial Agents*, 20, 320-325.
 16. **Chatzikakis A., Berberidou C., Paspaltsis I., Kyriakou G., Sklaviadis T., Poulios I.** 2008. Photocatalytic degradation and drug activity reduction of Chloramphenicol. – *Water Research*, 42, 386-394.
 17. **Chen J., Ollis D.F., Rulkens W.H., Bruning H.,** 1999. Photocatalysed oxidation of alcohols and organochlorides in the presence of native TiO₂ and metallized TiO₂ suspensions, Part II: photocatalytic mechanisms. – *Water Research*, 33, 669–676.
 18. **Church C.D., Pankow J.F., Tratnyek P.G.** 1999. Hydrolysis of tert-butyl formate: Kinetics, products, and implications for the environmental impact of methyl tert-butyl ether. – *Environmental Toxicology and Chemistry*, 18, 2789-2796.
 19. **Dantas R.F., Contreras S., Sans C., Esplugas S.** 2008. Sulfamethoxazole abatement by means of ozonation. – *Journal of Hazardous Materials*, 150 (3), 790-794.
 20. **Diaz-Cruz M.S., Barcelo D.** 2005. LC-MS² trace analysis of antimicrobials in water, sediment and soil. – *Trends in Analytical Chemistry*, 24, 645-657.
 21. **Elmolla E.S., Chaudhuri M.** 2009. Degradation of the antibiotics amoxicillin, ampicillin and cloxacillin in aqueous solution by the photo-Fenton process. – *Journal of Hazardous Materials*, 172 (2-3), 1476-1481.
 22. **Gandhe A.R., Fernandes J.B.** 2005. A simple method to synthesize N-doped rutyl titania with enhanced photocatalytic activity in sunlight. – *Journal of Solid State Chemistry*, 178, 2953–2957.
 23. **Greenfield R.A., Bronze M.S.** 2003. Prevention and treatment of bacterial diseases caused by bacterial bioterrorism threat agents. – *Drug Discovery Today*, 8, 881-888.
 24. **Haller M.Y., Müller S.R., McArdell C.S., Alder A.C., Suter M.J.-F.** 2002. Quantification of veterinary antibiotics (Sulfonamides and Trimethoprim) in animal manure by liquid chromatography - mass spectrometry. – *Journal of Chromatography A*, 952, 111-120.
 25. **Halling-Sørensen B., Nors Nielsen S., Lanzky P.F., Ingerslev F., F., Holten Lützhof H.C., Jørgensen, S.E.** 1998. Occurrence, fate and effects of pharmaceutical substances in the environment – A review. – *Chemosphere*, 36, 357-393.

26. **Hameed A., Gondal M.A.** 2004. Laser induced photocatalytic generation of hydrogen and oxygen over NiO and TiO₂. – *Journal of Molecular Catalysis A*, 219 (1), 109-119.
27. **Hartig C., Storm T., Jekel M.** 1999. Detection and identification of sulphonamide drugs in municipal waste water by liquid chromatography coupled with electrospray ionisation mass spectrometry. – *Journal of Chromatography A*, 845, 163-173.
28. **Hartig C., Storm T., Jekel M.** 2003. Detection and identification of sulphonamide drugs in municipal waste water by liquid chromatography coupled with electrospray ionisation tandem mass spectrometry. – *Journal of Chromatography A*, 854, 163-173.
29. **Herberer T.** 2002. Occurrence, fate, and removal of pharmaceutical residues in the aquatic environment: a review of recent research data. – *Toxicology Letters*, 131, 5-17.
30. **Ihara T., Miyoshi M., Iriyama Y., Matsumoto O., Sugihara S.** 2003. Visible-light active titanium dioxide realized by an oxygen-deficient structure and by nitrogen doping. – *Applied Catalysis B*, 42, 403–409.
31. **Jen J.F., Lee H.L., Lee B.N.** 1998. Simultaneous determination of seven sulphonamide residues in swine wastewater by high-performance liquid chromatography. – *Journal of Chromatography A*, 793, 378-382.
32. **Johnson P.** 1998. Assessment of the contribution of volatilization and biodegradation to in situ air sparging performance. – *Environmental Science and Technology*, 32 (2), 276-281.
33. **Kahru A., Maloverjan A., Sillak H., Pollumaa L.** 2002. The toxicity and fate of phenolic pollutants in the contaminated soils associated with the oil-shale industry. – *Environmental Science and Pollution Research*, 1, 27-33.
34. **Kaniou S., Pitarakis K., Barlagianni I., Poullos I.** 2005. Photocatalytic oxidation of sulfamethazine. – *Chemosphere*, 60, 372-380.
35. **Kim S., Eichhorn P., Jensen J.N., Weber A.S., Aga D.S.** 2005. Removal of antibiotics in wastewater: effect of hydraulic and solid retention times on the fate of tetracycline in the activated sludge process. – *Environmental Science and Technology*, 39, 5816-5823.
36. **Kirkpatrick S.J.** 2005. A primer on radiometry. – *Dental Materials*, 21, 21-26.
37. **Kolen'ko Yu.V., Churagulov B.R., Kunst M., Mazerolles L., Colbeau-Justin C.** 2004. Photocatalytic properties of titania powders prepared by hydrothermal method. – *Applied Catalysis B*, 54 (1), 51-58.
38. **Krichevskaya M., Kachina A., Malygina T., Preis S., Kallas J.** 2003. Photocatalytic degradation of fuel oxygenated additives in aqueous solutions. – *International Journal of Photoenergy*, 5 (2), 81-86.

39. **Krichevskaya M., Malygina T., Preis S., Kallas J.** 2001. Photocatalytic oxidation of de-icing agents in aqueous solutions and aqueous extract of jet fuel. – *Water Science and Technology*, 44, 1-6.
40. **Kümmerer K., Al-Ahmad A., Mersch-Sundermann V.** 2000. Biodegradability of some antibiotics, elimination of their genotoxicity and affection of wastewater bacteria in a simple test. – *Chemosphere*, 40, 701-710.
41. **Lettmann C., Hildenbrand K., Kisch H., Macyk W., Maier W.H.** 2001. Visible light photodegradation of 4-chlorophenol with a coke-containing titanium dioxide photocatalyst. – *Applied Catalysis B*, 32, 215–227.
42. **Li X., Xiong R., Wei G.** 2009. Preparation and photocatalytic activity of nanoglued Sn-doped TiO₂. – *Journal of Hazardous Materials Volume*, 164 (2-3), 587-591.
43. **Liang S., Palencia L., Yates R., Davis M., Bruno J.-M., Wolfe R.** 1999. Oxidation of MTBE by ozone and peroxone processes. – *Journal of American Water Works Association*, 91, 104-114.
44. **Liu Z., Sun D.D., Guo P., Leckie J.O.** 2007. One-step fabrication and high photocatalytic activity of porous TiO₂ hollow aggregates by using a low-temperature hydrothermal method without templates. – *Chemistry: A European Journal*, 13, 1851-1855.
45. **Matthews R.W.** 1986. Photo-oxidation of organic material in aqueous suspensions of titanium dioxide. – *Water Research*, 20, 569-578.
46. **McGinns D., Adams V.D., Middlebrooks E.J.** 2000. Degradation of ethylene glycol in photo Fenton systems. *Water Research*, 34 (8), 2346-2354.
47. **Nitschke L., Wagner H., Metzner G., Wilk A., Huber L.** 1996. Biological treatment of waste water containing glycols from de-icing agents. – *Water Research*, 30, 644-648.
48. **Ohno T., Akiyoshi M., Umebayashi T., Asai K., Mitsu T., Matsumura M.** 2004. Preparation of S-doped TiO₂ photocatalysts and their photocatalytic activities under visible light. – *Applied Catalysis A*, 265, 115-121.
49. **Palominos R., Freer J., Mondaca M.A., Mansilla H.D.** 2008. Evidence for hole participation during the photocatalytic oxidation of the antibiotic flumequine. – *Journal of Photochemistry and Photobiology A*, 193, 139-145.
50. **Papok K.K., Semenido E.G.** 1962. Motor, jet and rocket fuels (Motornye, reaktivnye i raketnye topliva), Gostoptehizdat, Moscow, (in Russian).
51. **Preis S., Krichevskaya M., Terentyeva Y., Moiseev A., Kallas J.** 2002. Treatment of phenolic and aromatic amino compounds in polluted waters by photocatalytic oxidation. – *Journal of Advanced Oxidation Technologies*, 5 (1), 77-84.
52. **Rodriguez-Gonzalez V., Zanella R., del Angel G., Gomez R.** 2008. MTBE visible-light photocatalytic decomposition over Au/TiO₂ and

- Au/TiO₂-Al₂O₃ sol-gel prepared catalysts. – Journal of Molecular Catalysis A, 281 (1-2), 93-98.
53. **Rozas O., Contreras D., Mondaca M.A., Pérez-Moya M., Mansilla H.D.** 2010. Experimental design of Fenton and photo-Fenton reactions for the treatment of ampicillin solutions. – Journal of Hazardous Materials, 177 (1-3), 1025-1030.
 54. **Rozkov, A., Vassiljeva, I., Kurvet, M., Kahru, A., Preis, S., Kharchenko, A., Krichevskaya, M., Liiv, M., Käär, A., Vilu, R.** 1999. Laboratory study of bioremediation of rocket fuel-polluted groundwater. – Water Research, 33, 1303-1313.
 55. **Safarzadeh-Amiri A.** 2001. O₃/H₂O₂ treatment of methyl-*tert*-butyl ether (MTBE) in contaminated waters. – Water Research, 35 3706-3714.
 56. **Sanderson J.P., Naisbitt D.J., Park B.K.** 2006. Role of bioactivation in drug-induced hypersensitivity reactions. – AAPS Journal, 8, E55-E64.
 57. **Sax N.I.** 1984. Dangerous Properties of Industrial Materials, Van Nostrand Reinhold Co., New York.
 58. **Schmeltz I., Hoffmann D.** 1977. Nitrogen-containing compounds in tobacco and tobacco smoke. – Chemical Reviews, 77, 295-311.
 59. **Sharma S.D., Singh D., Saini K.K., Kant C., Sharma V., Jain S.C., Sharma C.P.** 2006. Sol-gel derived super-hydrophilic nickel doped TiO₂ film as active photo-catalyst. – Applied Catalysis A, 314, 40-46.
 60. **Sorum H.** 2006. Antimicrobial Resistance in Bacteria of Animal Origin/ F.M. Aarestrup, American Society for Microbiology Press, Washington, DC.
 61. **Sun B., Seto M., Clements J.S.** 1997. Optical study of active species produced by a pulsed corona discharge in water. – Journal of Electrostatics, 39 (3), 189-202.
 62. **Turan-Ertas T., Gurol M.D.** 2002. Oxidation of diethylene glycol with ozone and modified Fenton processes. – Chemosphere, 47 (3), 293-301.
 63. **Verschueren K.** 1983. Handbook of Environmental Data of Organic Chemicals. Van Nostrand Reinhold Co. Inc., New York.
 64. **Vilhunen S.H., Sillanpää M.E.T.** 2009. Atomic layer deposited (ALD) TiO₂ and TiO_{2-x}-N_x thin film photocatalysts in salicylic acid decomposition. – Water Science and Technology, 60 (10), 2471-2475.
 65. **Wang Z., Cai W., Hong X., Zhao X., Xu F., Cai C.** 2005. Photocatalytic degradation of phenol in aqueous nitrogen-doped TiO₂ suspensions with various light sources. – Applied Catalysis B, 57, 223–231.
 66. **Wang S., Zhang H.Y., Wang L., Duan Z.J., Kennedy I.** 2006. Analysis of sulfonamide residues in edible animal products: A review. – Food Additives and Contaminants, 23, 362-384.
 67. **Xekoukoulotakis N.P., Mantzavinos D., Dillert R., Bahnemann D.** 2010. Synthesis and photocatalytic activity of boron-doped TiO₂ in

- aqueous suspensions under UV-A irradiation. – *Water Science and Technology*, in press.
68. **Xu X.-R., Zhao Z.-X., Li X.-Y., Gu J.-P.** 2004. Chemical oxidative degradation of methyl-tert-butyl ether in aqueous solution by Fenton's reagent. *Chemosphere*, 55, 73-79.
 69. **Yamagata S., Baba R., Fujishima A.** 1989. Photocatalytic decomposition of 2-ethoxyethanol on titanium dioxide. *Bulletin of the Chemical Society of Japan*, 62 (4), 1004-1010.
 70. **Yeh C.K., Novak J.T.** 1994. Anaerobic biodegradation of gasoline oxygenates in soils. – *Water Environmental Research*, 66 (5), 744-752.
 71. **Zhang Y., Crittenden J.C., Hand D.W., Perram D.L.** 1994. Fixed-bed photocatalysts for solar decontamination of water. – *Environmental Science and Technology*, 28 (3), 435-442.

KOKKUVÕTE

Käesolevas töös läheneti süstemaatiliselt mitme bioloogiliselt mittelaguneva tehnogeense orgaanilise aine poolt reostatud vee puhastamisele fotokatalüütilise oksüdatsiooni (FKO) meetodil. Saasteainete nimekirja kuuluvad:

1. etüleenglükool (EG) ja selle derivaadid, 2-etoksüetanool (2-EE) ja dietüleenglükooli monometüüleeter (DEGMME), mida kasutatakse jäätõrjeks ja jäätumisvastaste kütuselisanditena;
2. metüül-*tert*-butüüleeter (MTBE), laialdaselt kasutatav mootorkütuselisand;
3. *p*-Toluidiin, reaktiivkütuste komponent;
4. erinevatesse klassidesse kuuluvad laialdaselt kasutatavad antibiootikumid, näiteks amoksütsilliin (AMO), doksütsükliin (DC) ja sulfametisool (SMZ).

Peamisteks FKO eeldusteks loetakse selle kõrget oksüdatsioonipotentsiaali ja võimalust kasutada päikesekiirgust. Nõrkadeks külgedeks saab lugeda suhteliselt madalat reaktsioonikiirust ning kvantväljundit.

Käesoleva töö peamisteks eesmärkideks olid:

1. uurida FKO rakendatavuse piire;
2. kiirendada oksüdatsiooniprotsessi;
3. lahendada insenerlikult katalüsaatori kasutusviisi küsimus.

Töös uuriti järgmisi probleeme:

1. FKO võime lagundada eespool mainitud aineid;
2. FKO mehhanism (radikaalsete ja aukreaktsioonide osakaal, adsorptsioon, FKO vaheproduktid, reaktsiooni kirjeldamine Langmuir-Hinshelwoodi mudeliga);
3. väliste tegurite mõju FKO protsessile (saasteainete algkontsentratsioon, pH, rauaioonide kogus lahuses);
4. laiema elektromagnetkiirguse spektriga töötavate fotokatalüsaatorite süntees ja nende töö. Mittemetalletest lisanditest kasutati väävlit, boori, süsinikku ja lämmastikku, metalletest lisanditest kasutati rauda.

Käesoleva töö peamine uudsus seisneb järgmises:

1. laiendati oluliselt FKO poolt lagundatavate ainete spektrit, saadi informatsiooni nende FKO mehhanismist, kineetikast ning reaktsiooniradadest;
2. esmakordselt täheldati rauaioonide optimaalset kontsentratsiooni mõnede ainete FKO-le;
3. saadi informatsiooni FKO reaktsioonimehhanismide domineerimisest erinevate ainete korral;
4. sünteesiti ja katsetati erinevate elementide poolt legeritud titaandioksiidi, mille toime oli osade ainete korral oluliselt kõrgem, kui kommerts-katalüsaatoril Degussa P25. Uuriti ja tehti kindlaks erinevate lisandite koguse mõju;

5. legeritud katalüsaatorite korral täheldati selektiivset toimet;
6. uuritud ainete jaoks tehti kindlaks FKO reaktsioonirajad.

Käesolevas töös sisalduv informatsioon on publitseeritud seitsme artiklina rahvusvahelistes eelretsenseeritavates teadusajakirjades, osa informatsioonist on esitatud publitseerimiseks veel kahe artiklina; töö on aprobeeritud seitsmel rahvusvahelisel teaduskonverentsil.

ABSTRACT

In this research, a systematic approach to the aqueous photocatalytic oxidation (PCO) of non-biodegradable synthetic organic compounds is applied. The list of pollutants includes:

1. Ethylene glycol (EG) and its derivatives: 2-ethoxy ethanol (2-EE) and diethylene glycol monomethyl ether (DEGMME), used as de-icing agents and jet fuel oxygenates;
2. Methyl-*tert*-butyl ether (MTBE), a widely used fuel oxygenate;
3. *p*-Toluidine, a jet and rocket fuel compound;
4. Several widely used antibiotic medicaments of various classes: amoxicillin (AMO), doxycycline (DC) and sulphamethizole (SMZ).

The main advantages of PCO as a treatment method is its high oxidation potential and the ability of using direct solar radiation for the catalyst performance. Relatively low reaction rate and quantum yield are considered to be the main disadvantages of PCO. The most challenging issue of PCO appears to be its often unpredictable performance under various process conditions. Therefore, the main objectives of the present research were:

1. To determine the limits of PCO applicability;
2. Acceleration of PCO;
3. Engineering solutions.

The following points were studied:

1. The efficiency of PCO in degradation of pollutants;
2. The study of PCO mechanism (radical *vs.* hole reactions, role of adsorption, reaction by-products, the description of reaction kinetics);
3. The impact of external factors (concentration of pollutants, pH, dissolved admixtures);
4. Synthesis and examination of modified catalysts with wider electromagnetic radiation absorbance spectrum: non-metal dopants - sulphur, boron, nitrogen and carbon; metal dopants - iron.

The novelty of the present research brought to the discussion includes:

1. The list of the synthetic aqueous pollutants characteristic for groundwater, for which PCO performance is now detailed, was noticeably enlarged;
2. The peak optimum concentration of dissolved iron controlling the PCO efficiency was observed for the first time for a few pollutants;
3. The dominating PCO mechanism for considered pollutants was disclosed;
4. A few modified titania catalysts, active in visible light, were synthesised with the PCO efficiency exceeding the one of the commercial Degussa P25; the role of various dopants was established;
5. The selective performance of the doped catalysts was observed with respect to the pollutants under study;

6. The PCO reaction pathways were established.

The issues of this work were published in seven articles in international peer-reviewed journals and presented at seven international scientific conferences. For the moment the dissertation was submitted, two more article manuscripts are being submitted with their texts attached here for public criticism and discussion.

APPENDIX I
PUBLICATIONS

Article I:

Klauson, D., Portjanskaja, E., Kachina, A., Krichevskaya, M., Preis, S. and Kallas, J., The influence of ferrous/ferric ions on the efficiency of photocatalytic oxidation of pollutants in groundwater. *Environmental Technology*, 2005, 26 (6), pp. 653-661

THE INFLUENCE OF FERROUS/FERRIC IONS ON THE EFFICIENCY OF PHOTOCATALYTIC OXIDATION OF POLLUTANTS IN GROUNDWATER

D. KLAUSON¹, S. PREIS^{2*}, E. PORTJANSKAJA¹, A. KACHINA¹, M. KRICHEVSKAYA¹ AND J. KALLAS²

¹Department of Chemical Engineering, Tallinn University of Technology, Ehitajate tee 5, Tallinn 19086, Estonia

²Department of Chemical Technology, Lappeenranta University of Technology, P. O. Box 20, FIN-53851, Lappeenranta, Finland

(Received 10 December 2004; Accepted 2 February 2005)

ABSTRACT

The complex influence of ferrous/ferric ions on the efficiency of aqueous photocatalytic oxidation (PCO) of 2-ethoxyethanol (2-EE), methyl *tert*-butyl ether (MTBE) and humic substances (HS) was established. A drastic efficiency increase at lower concentration of ferrous/ferric ions was observed to change to a sharp decrease at higher concentrations for 2-EE and MTBE, whereas for HS only an inhibitive effect of Fe^{2+/3+} on the PCO efficiency was noticed. The authors proposed an explanation for the observed phenomena based on the different sensitivities of pollutants towards radical-oxidation reactions and the competitive adsorption of metallic ions and pollutants on the TiO₂ surface.

Keywords: 2-ethoxyethanol (2-EE), methyl *tert*-butyl ether (MTBE), humic substances (HS)

INTRODUCTION

The present research is devoted to analysing the influence of ferrous/ferric ion additives on the photocatalytic oxidation (PCO) of different organic substances in acidic media: humic substances (HS), de-icing agents and motor fuel oxygenates. Humic substances are largely found in natural water as an ultimate decomposition product of living matter. 2-Ethoxyethanol (2-EE, CH₃-CH₂-O-CH₂-CH₂-OH) is used as a solvent, a de-icing agent for runways and aircrafts, and an antifreeze motor and jet fuel additive. Methyl *tert*-butyl ether (MTBE, CH₃-O-C(CH₃)₃) is widely used as an anti-detonating oxygenated component of motor fuels. Despite being different in their chemical nature, these substances are often present simultaneously in groundwater: de-icing agents and motor fuel oxygenates can be found in natural water as a result of leakage, accidental spillages and uncontrolled disposal.

Humic substances may be objectionable due to the colour and turbidity they add to water. More importantly, they represent a health hazard through chelation of heavy metal ions and also bonding with toxics such as pesticides, making the removal of the heavy metals and pesticides problematic. Humic substances also serve as precursors of carcinogenic trihalomethanes in water chlorination [1].

2-Ethoxyethanol has negative effects on the kidneys, respiratory, and reproductive systems, and also acts as a depressant of the central nervous system. The suspected carcinogen MTBE represents a hazard to the environment [2].

These substances have been proven by earlier studies to be refractory against biodegradation and thus they accumulate and remain intact in groundwater for long times [3, 4].

The photocatalytic oxidation of organic pollutants is based on the action of positively charged holes on the semiconductor surface [5]. When subjected to UV-irradiation, the semiconductor's valence band electrons are displaced from the valence band to the conduction band, creating positively charged holes. The positively charged holes oxidise the organic pollutant molecules adsorbed on the photocatalyst surface. The decomposition of water molecules into hydroxyl radicals also takes place on the holes. However, the holes may recombine rapidly with conduction band electrons, decreasing the PCO efficiency. Prolongation of the holes' lifetime should, therefore, increase the efficiency of PCO. For this purpose, multivalent metal ions may be added to the treated solutions, or, more precisely, to the photocatalyst surface, to scavenge electrons at the surface of the titanium dioxide, thus preventing electron-hole recombination and improving the oxidation performance.

Several previous studies [6 - 8] have reported higher PCO rates following the addition of small amounts of ferrous ions. Sucrose, carboxylic acids and textile azo dye were the organic pollutants in these studies. However, higher concentrations of ferrous ion reduced the decomposition rate significantly. A similar trend was observed with other multivalent metals influencing PCO of phenol and sucrose [9, 10]. Our previous studies showed the positive role of ferrous

ions at low concentrations in the efficiency of PCO of MTBE, although the PCO experiments with 2-EE, carried out in the same range of concentrations of $\text{Fe}^{2+/3+}$, indicated only a negative effect of iron ions. The results of more detailed investigation given here broaden the knowledge of the influence of iron ions on pollutants of various types and show the complex character of the dependence of the PCO efficiency on the concentration of iron ions.

EXPERIMENTAL SECTION

Two 200-ml simple batch reactors with inner diameter 100 mm (evaporation dishes), aperture $40 \text{ m}^2 \text{ m}^{-3}$, thermostated at $20 \pm 1^\circ\text{C}$ and mechanically agitated with magnetic stirrers were used in the PCO experiments: the one used for the PCO was called "active" and the other containing no photocatalyst was called "reference". Both reactors were exposed to identical experimental conditions. The samples from the active reactor were compared to the reference samples to avoid complications caused by water evaporation. A UV-light source, Phillips 365-nm low pressure luminescent mercury UV-lamp (15 W), was positioned horizontally over the reactors (see Fig. 1), providing irradiance of about 0.7 mW cm^{-2} measured at a distance corresponding to the level of the free surface of the reactor by the optical radiometer Micropulse MP100 (Micropulse Technology, UK).

The experiments were carried out using aqueous

solutions of 2-EE, MTBE and HS (sodium salt of humic acid) supplied by Aldrich. The experiments were conducted with synthetic solutions at concentrations of 300, 100 and 10 mg l^{-1} , for 2-EE, MTBE and HS respectively. The concentrations of pollutants were chosen to be consistent with their presence in polluted groundwater and experimental conditions applied previously [11]. All experiments were carried out at pH 3.0, adjusted with 4-N solution of sulphuric acid. With 2-EE, the treatment time was 24 h, with MTBE - 1 h and with HS - 6 h. The treatment time was chosen to reduce the concentration of pollutants below 50% of the residual concentration and was used in calculations of the process efficiency E (see eq. i). All the experiments were carried out at least three times under identical experimental conditions to derive the average value of the process efficiency. The average deviation of data in parallel experiments did not exceed 5%.

The experiments were performed using titanium dioxide as Degussa P25 in the following modes. Slurry of TiO_2 at 1 g l^{-1} was used in the PCO experiments with 2-EE and MTBE, since HS formed hard-to-separate stable suspensions with TiO_2 slurry. TiO_2 attached to buoyant hollow glass micro-spheres was used for oxidation of HS to avoid this problem. The buoyant catalyst was also tested for its activity with 2-EE. The hollow glass micro-spheres used in this study had an average diameter of 60 to $70 \mu\text{m}$ and a density 0.27 g cm^{-3} (the product of LP-ImpEx, Estonia). Titanium dioxide was attached to the surface of the micro-beads by the thermal

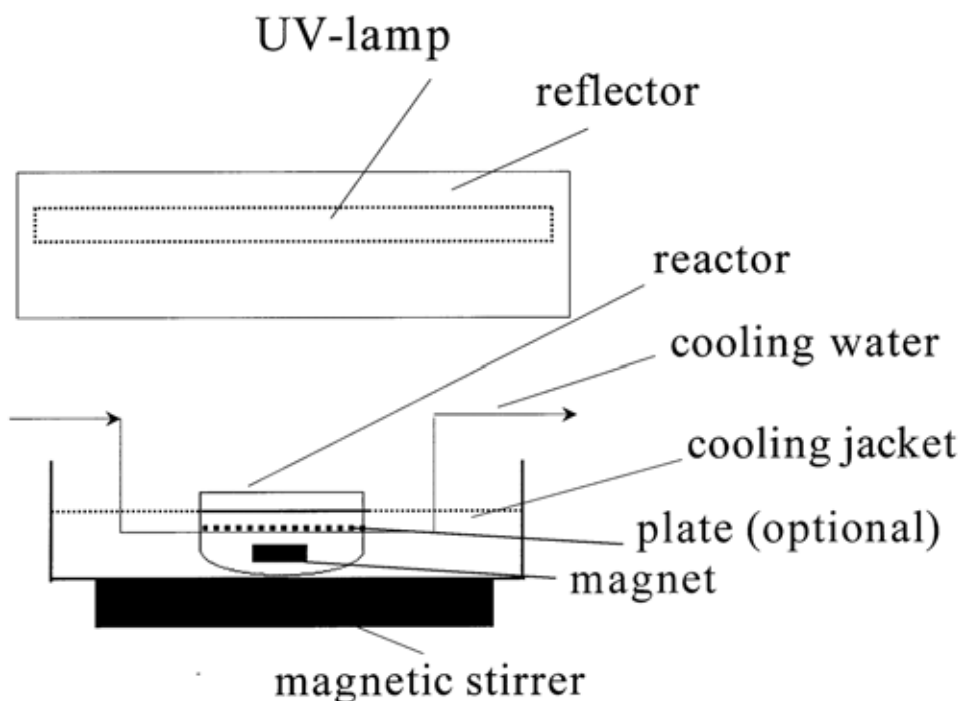


Figure 1. PCO reactor.

method [12]: equal volumes of dry micro-spheres and the aqueous suspension of titanium dioxide with concentration of 1 g l^{-1} were thoroughly mixed by stirring and sonication in an ultrasonic bath for 30 min. The micro-spheres were then separated from the mixture by filtration with a membrane filter, heated to dryness at 120°C and calcinated in air at a temperature of 300°C for 4 h. This procedure was repeated six times, which was found to be the optimum number of the attachment operations for the best performance of the photocatalyst attached to the buoyant glass micro-beads [13]. Analogously, TiO_2 was attached to the surface of the glass plates (one side) in approximately equal amounts either by multiple submerging of the plates in the TiO_2 suspension with subsequent drying after each submersion, or by spraying the TiO_2 suspension over the surface of the plates and drying. TiO_2 attached to glass plates, submerged horizontally in the solution to be treated at a depth from 5 to 10 mm, was used in PCO of 2-EE. Since 2-EE does not absorb UV light at 365 nm, the depth of the submersion was not important within the indicated limits. This was confirmed by specially conducted experiments.

The decrease in the pollutant concentration was determined for 2-EE and MTBE from the decrease in chemical oxygen demand (COD), measured by a standard method [14]. For the HS, colour was determined with the photometer HACH DR/2010 at 455 nm. Absorbance at 254 nm was measured by Spectronic Unicam spectrophotometer (Helios β). Both indices were correlated with the content of HS by preliminary calibration.

Adsorption experiments for ferrous/ferric ion, introduced as sulphates, 2-EE, MTBE and HS on the TiO_2 surface were conducted in closed flasks, equipped with magnetic stirrers, thermostatted at $20 \pm 1^\circ \text{C}$ and adjusted to pH 3.0. The amount of substances adsorbed was derived from the batch mass balance: the concentration of the dissolved substance was determined before and after adsorption. The points of isotherms are the average out of three experimental sets. The concentrations of iron ions were determined by a photometric phenantrolin method described in standard methods [14]. The PCO by-products of 2-EE, mainly carbonic acids, were qualitatively determined by the methods described in Pohloudeck-Fabrini and Beyrich [15]. Oxalic, glycolic and formic acid were determined by their reaction with resorcinol, acetic acid – through the formation of iron (III) acetate.

RESULTS AND DISCUSSION

The performance of PCO with artificial radiation sources was characterised by the process efficiency E . The efficiency E is defined as the decrease in the amount of pollutant divided by the amount of energy reaching the surface of the treated sample (eq. i). The efficiency values were calculated after a period of time equal to the treatment time (24 h for 2-EE, 1 h for MTBE and 6 h for HS).

$$E = \frac{\Delta c \cdot V \cdot 1000}{I \cdot s \cdot t}, \quad (\text{i})$$

where E – PCO efficiency, $\text{mg W}^{-1} \text{h}^{-1}$; Δc – the decrease in the concentration of the pollutant, mg l^{-1} or $\text{mg O}_2 \text{ l}^{-1}$ for COD of 2-EE and MTBE solutions, and mg l^{-1} for HS; V – the volume of the sample to be treated, l; I – irradiance, mW cm^{-2} ; s – irradiated area, cm^2 ; t – treatment time, h.

Both ferrous and ferric ions were tested in the experiments with 2-EE. Sulphate was chosen as the counterion due to its low inhibitive effect on PCO efficiency observed with 2-EE in Krichevskaya *et al* [11]. The results of the experiments are shown in Fig. 2. One can see a similar trend in the dependence of PCO performance on the concentrations of both ionic species. Ferric ions were therefore seen to have the same effect as ferrous ions, which may be explained with an equilibrium established between ferrous and ferric ions in aqueous solutions in the presence of dissolved oxygen at pH 3 in TiO_2 slurry, i.e. a strongly oxidative media, as described in Catastini *et al* [16].

Ferrous ions appeared to play a significant role in PCO of 2-EE. The addition of small amounts of ferrous ion, up to 0.09 mM, resulted in a drastic, up to 60 %, increase in the process efficiency (Fig. 2). With further increase in the concentration of Fe^{2+} , the PCO efficiency decreased dramatically.

A similar dependency pattern, in which the PCO efficiency of 2-EE had its maximum with a $\text{Fe}^{2+/3+}$ concentration of 0.09 mM, was observed for TiO_2 attached to the glass plates, although the absolute values of the PCO efficiency were about 40 to 70% lower than with the TiO_2 slurry. Buoyant micro-beads with attached TiO_2 were the least effective. The maximum PCO efficiency was, however, observed also at 0.09 mM of ferrous/ferric ions (Fig. 3).

Figure 3 shows that the difference in the procedure of TiO_2 attachment to the glass plates makes a difference in the PCO efficiency: attachment by spraying appeared to be more effective. This may not be explained by the difference in the mass of TiO_2 since the attached mass was virtually the same, but is most probably due to uneven relief and porosity of the catalyst surface and, thus, a larger contact surface resulting from non-uniform spray attachment.

Methyl *tert*-butyl ether showed a trend somewhat similar to 2-EE (Fig. 4) the drastic increase in PCO efficiency at smaller concentrations of $\text{Fe}^{2+/3+}$ -ions was followed by a decrease with further addition of ferrous/ferric ions [11]. However, one can see a significant difference in the behaviour between MTBE and 2-EE: the maximum efficiency for MTBE was observed at the $\text{Fe}^{2+/3+}$ concentration of 1 mM, which is about ten times bigger than that for 2-EE. Furthermore, a further increase in the concentration of $\text{Fe}^{2+/3+}$ -ions resulted in a gradual increase of PCO efficiency, which was not observed with 2-EE. This may be explained by the difference in the PCO mechanism of these two substances and their different

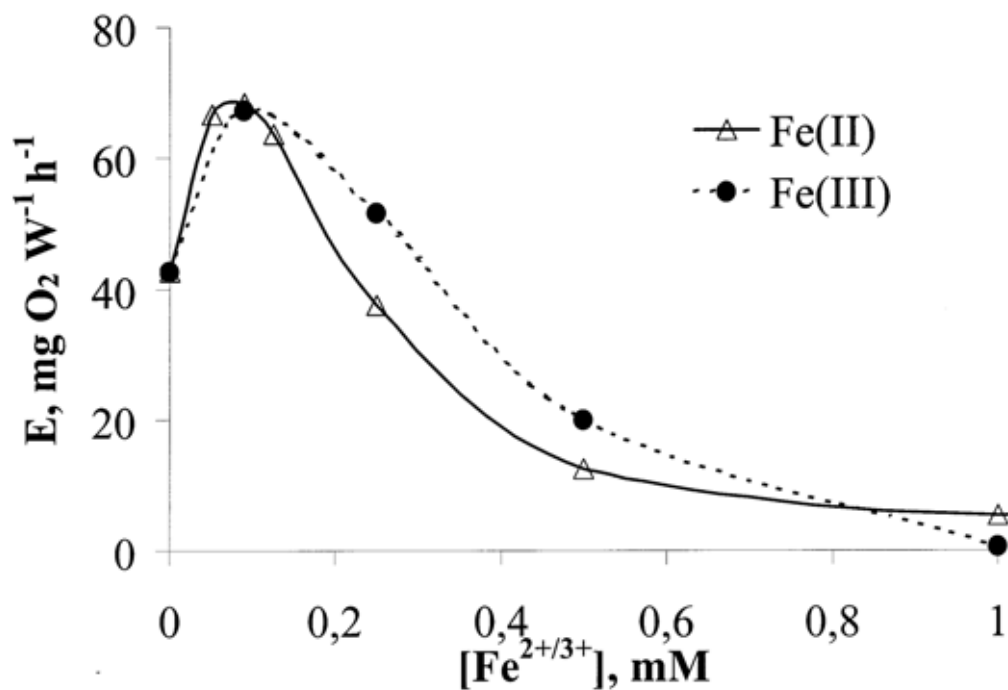


Figure 2. The efficiency of PCO of 2-ethoxyethanol in TiO₂ slurry vs. concentration of Fe²⁺ (Δ) and Fe³⁺ (●) ions at pH 3.0.

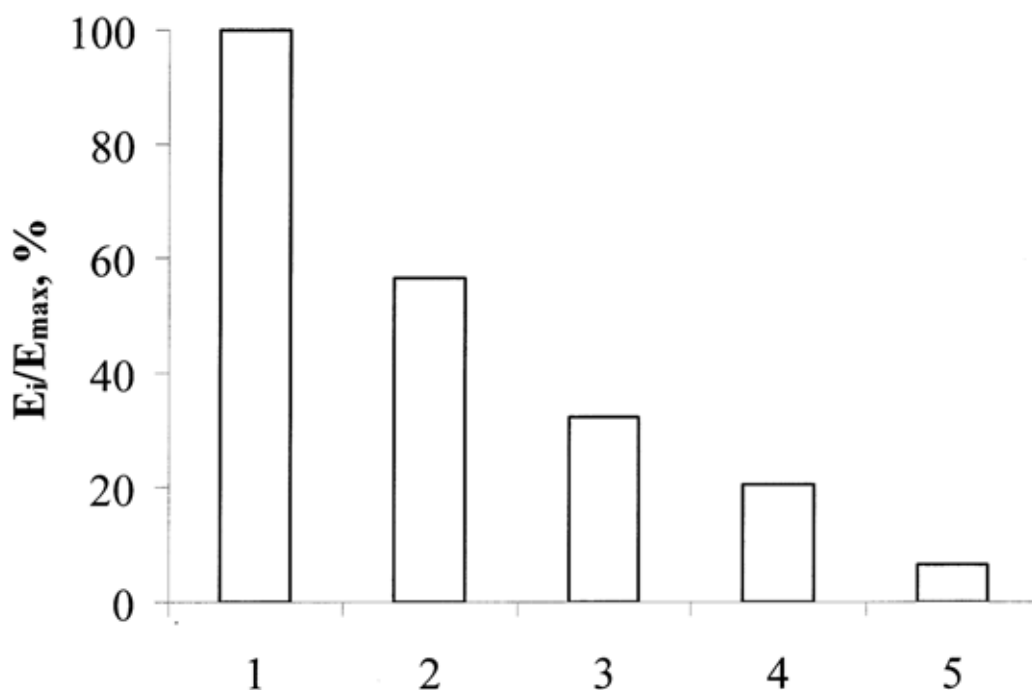


Figure 3. Efficiency of PCO of 2-ethoxyethanol at 0.09 mM of Fe^{2+/3+} with TiO₂ application modes: 1 – TiO₂ Degussa P25 suspension (1 g l⁻¹); 2 – TiO₂ sprayed to the glass plate, 0.6 mg cm⁻²; 3 – TiO₂ settled at the glass plate, 0.7 mg cm⁻²; 4 – TiO₂ attached to hollow glass micro-spheres, the amount of buoyant catalyst in the reactor 50 g m⁻²; 5 – same as 4 at 25 g m⁻².

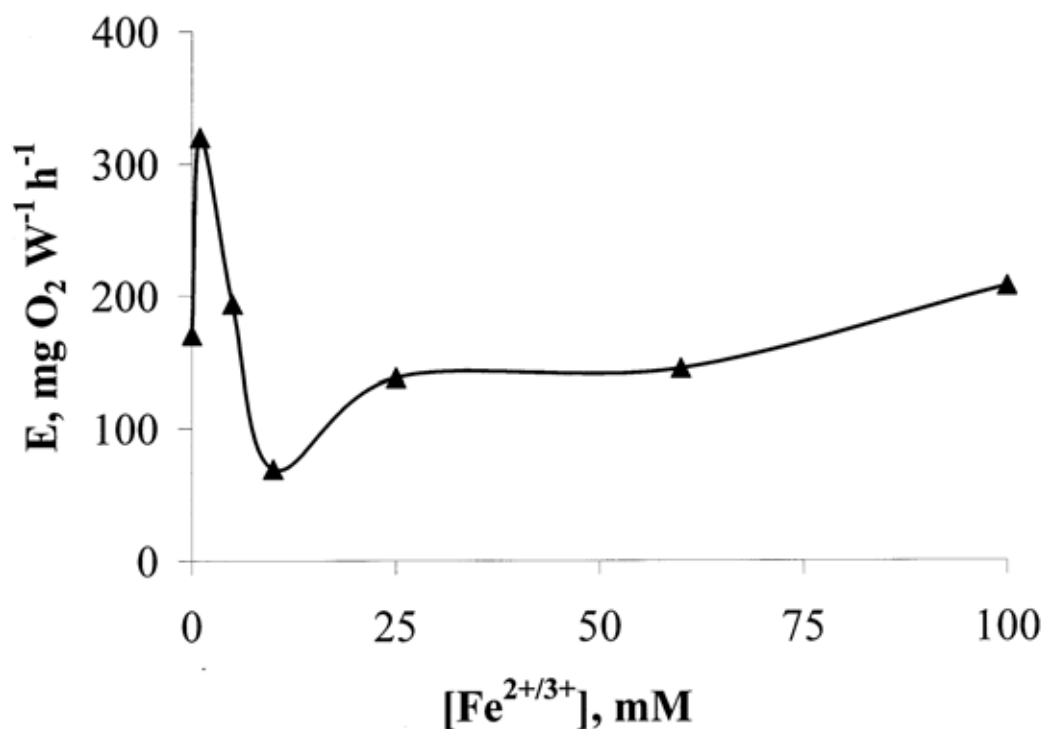


Figure 4. The efficiency of PCO of MTBE in TiO₂ slurry vs. concentration of Fe^{2+/3+}-ions at pH 3.0.

adsorption properties at the surface of the titanium dioxide.

Ferrous/ferric ions unambiguously demonstrated an inhibitory effect in the PCO of HS at all detectable concentrations (Fig. 5).

The difference in the behaviour of 2-EE, MTBE and HS can be explained by a dual mechanism of PCO [5]: 1) the adsorption of the pollutant by the surface of the titanium dioxide is followed by a direct subtraction of the pollutant's electrons, i.e. oxidation, with positively charged holes; 2) oxidation with hydroxyl radicals takes place at the catalyst surface or in its vicinity. Both reactions proceed simultaneously, although positively charged holes have an oxidation potential about 1.15 times bigger than a hydroxyl radical [17]. What mechanism dominates in PCO depends on the chemical and adsorption properties of the pollutant.

The promotion of the OH-radical was less effective in oxidation of ethylene glycol derivatives [18, 19]. The increasing PCO efficiency for 2-EE with the addition of ferrous/ferric ions in small, below 0.09 mM, concentrations may then be explained by the partial occupation of adsorption sites with Fe^{2+/3+}-ions, overpowered, however, with the electron scavenging by these ions, extending the lifetime and thus the oxidation performance of the positively charged holes. A further increase in the concentration of metallic ions results in the blockage of adsorption sites with a resultant drastic decrease in PCO efficiency. The formation of hydroxyl radicals has little effect on the overall oxidation rate.

Methyl *tert*-butyl ether is less resistant towards oxidation with a hydroxyl radical. For example, oxidation methods, such as ozonation, exhibited poor performance in the abatement of MTBE, although introduction of OH-radical promoters significantly enhanced oxidation [20]. This makes both mechanisms of PCO effective in PCO of MTBE. Small concentrations of ferrous/ferric ions therefore enhance the direct oxidation of MTBE with positively charged holes, and also the formation of OH-radicals. Radical oxidation reactions contribute to the overall oxidation rate successfully until a certain concentration of metallic ions is achieved (1 mM). Above this concentration, the formation of OH-radicals is probably obstructed by a "short-circuit" phenomenon, described in [6]: the blockage of the TiO₂ adsorption sites with ferrous/ferric ions results in reduced generation of OH-radicals. The increase of the PCO efficiency with further increasing ferrous/ferric ions concentration is consistent with the observations reported by Chu *et al.* made in UV-assisted oxidation of 2,4-dichlorophenoxy acetic acid [21] and may be explained by increased OH-radicals formation in the bulk solution initiated by the UV-irradiated Fe^{2+/3+}-ions: we also preliminarily observed MTBE oxidized to some extent under UV-irradiation in aqueous solutions containing Fe^{2+/3+}-ions with no TiO₂ present, although this reaction was beyond the scope of the present paper. In the TiO₂-free experiments the oxidation rate increased with increasing concentration of Fe^{2+/3+}-ions. The authors presume that oxidation of MTBE

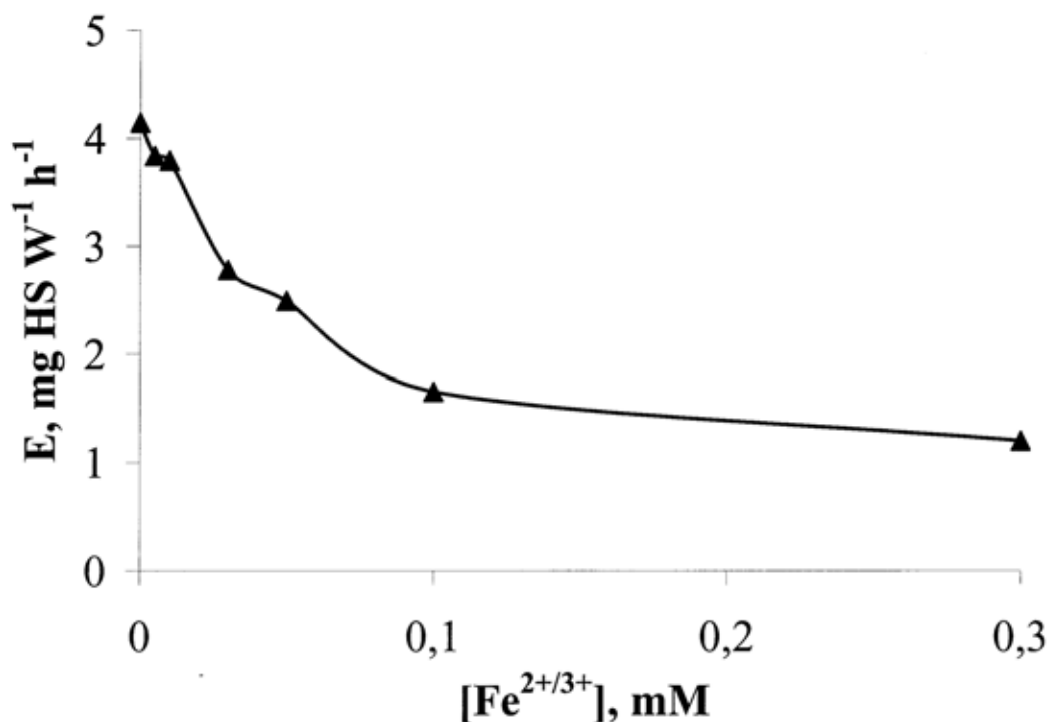


Figure 5. The efficiency of PCO of humic substances with TiO₂ attached on buoyant micro-spheres (50 g m⁻²) vs. concentration of Fe^{2+/3+}-ions at pH 3.0.

with UV-irradiated Fe^{2+/3+} may be enhanced in the presence of TiO₂. However, further experimental studies are necessary to confirm this statement.

Humic substances are known to be good scavengers of OH-radicals thus diminishing the role of radicals in the overall oxidation [22]. One could then expect an increase in PCO efficiency for HS similar to 2-EE at small concentrations of ferrous/ferric ions. The observed solely inhibitory effect of ferrous/ferric ions to the PCO efficiency of the treatment of HS solution could be explained by the complications in adsorption: not only Fe^{2+/3+}-ions block the adsorption sites at the TiO₂ surface, but also the partial chelation of carboxylic and phenolic groups of the humic molecules with the Fe^{2+/3+}-ions may obstruct their adsorption at the TiO₂ surface. Under these circumstances, the prolonged lifetime of positively charged holes may have a weakened effect due to obstructions in the adsorption of chelated humic molecules.

To support the above-mentioned hypothesis concerning the role of ferrous/ferric ions in PCO performance determined by the adsorption properties and the sensitivity of the target compounds towards radical attacks, the impact of the Fe^{2+/3+}-ions on the adsorption of a pollutant by TiO₂ was studied in a series of adsorption experiments. The ferrous/ferric ions content dependency of adsorption of 2-EE

from a solution with an equilibrium concentration of 2-EE 300 mg l⁻¹ by the TiO₂ surface was determined experimentally. As one can see from Fig. 6, the surface concentration of 2-EE steadily decreases within the Fe^{2+/3+}-ions equilibrium concentration range attributable to the peak zone of the PCO efficiency (Fig. 2).

An analogous dependence of the equilibrium surface concentration of MTBE was also observed: the MTBE surface concentration in equilibrium with an MTBE solution of 100 mg l⁻¹ decreased from 0.9 mmol g⁻¹ at zero concentration of Fe^{2+/3+}-ions to 0.5 mmol g⁻¹ at 1 mM and 0.1 mmol g⁻¹ at 10 mM of Fe^{2+/3+}-ions (Fig. 7). This explains the difference between the critical concentration values of Fe^{2+/3+}-ions for 2-EE and MTBE: the adsorption of MTBE was less affected by the presence of Fe^{2+/3+}-ions than 2-EE.

The last observation may be explained by differences in adsorption of 2-EE and MTBE. The list of carbonic acids determined qualitatively as PCO products of 2-EE include oxalic, acetic, formic and glycolic acids. The formation of glycolic acid confirms the adsorption of 2-EE by the oxygen atom of the ether group, whereas the formation of oxalic acid indicates the adsorption of 2-EE with both oxygen atoms. In general, MTBE is noticeably better adsorbed to a TiO₂ surface than 2-EE. The greater sensitivity of 2-EE to the concentration

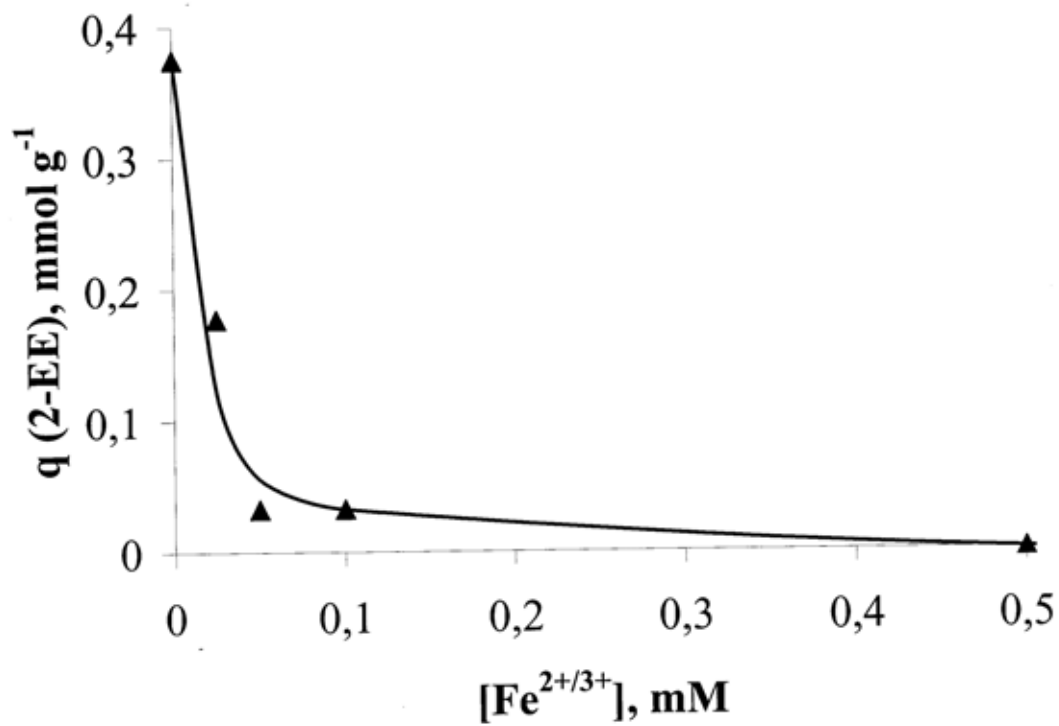


Figure 6. The surface concentration of 2-EE at TiO_2 versus $\text{Fe}^{2+/3+}$ -ions equilibrium concentration at pH 3.0 (20°C).

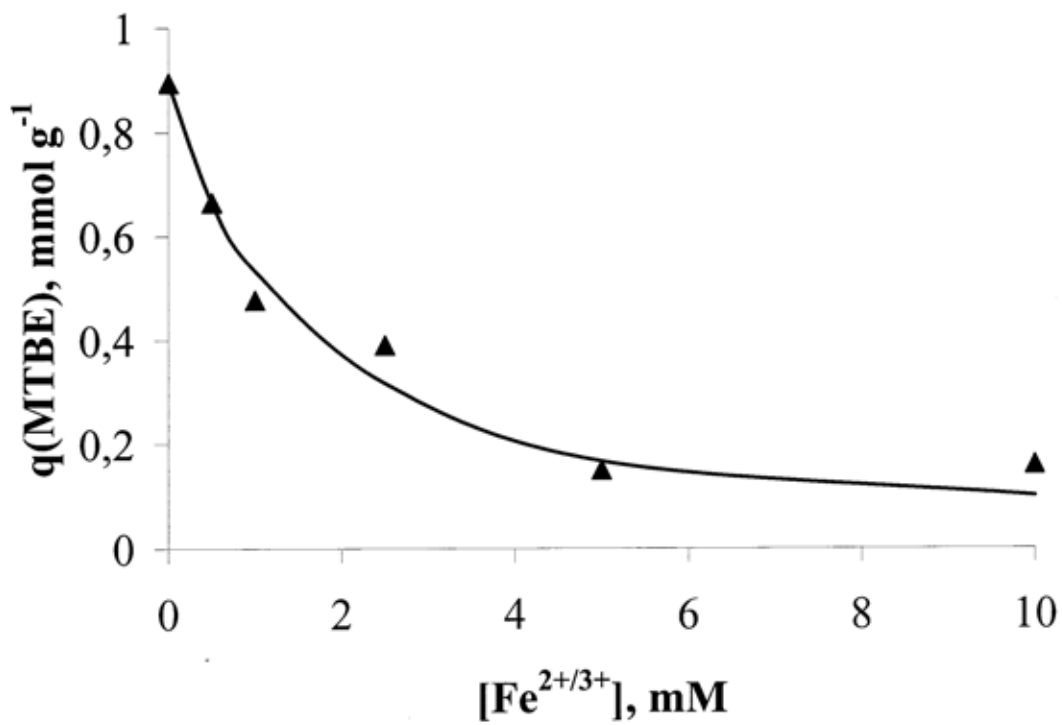


Figure 7. The surface concentration of MTBE at TiO_2 versus $\text{Fe}^{2+/3+}$ -ions concentration at pH 3.0.

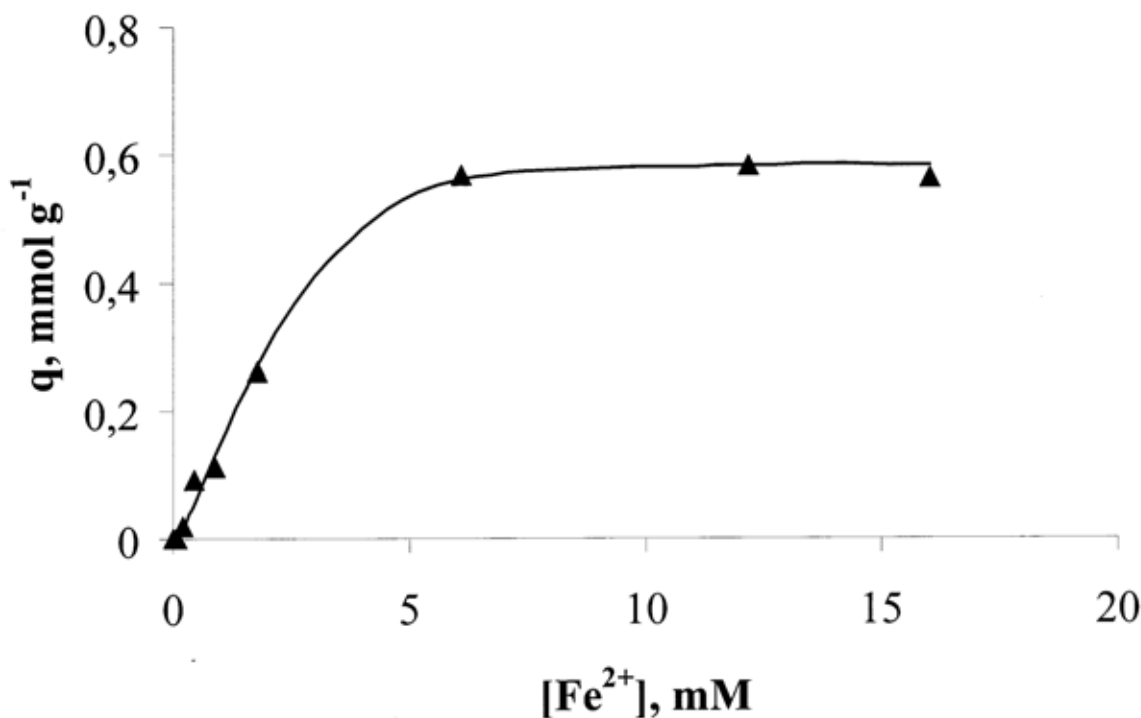


Figure 8. The surface concentration of $\text{Fe}^{2+/3+}$ -ion at TiO_2 versus $\text{Fe}^{2+/3+}$ -ions equilibrium concentration at pH 3.0 (20°C).

of $\text{Fe}^{2+/3+}$ -ions may therefore be explained by weaker adsorption of 2-EE in an acidic aqueous solution.

Humic substances were adsorbed consistently with the PCO efficiency dependence on the concentration of $\text{Fe}^{2+/3+}$ -ions: the decrease in the surface concentration with increasing ferrous/ferric ions concentration corresponds to the decrease in the HS PCO efficiency. This observation confirms the small role of OH-radicals in PCO of HS and the difficulties in adsorption can probably be accounted for by bonding of $\text{Fe}^{2+/3+}$ -ions with HS.

The adsorption of ferrous/ferric ion on the surface of titanium dioxide was also studied. The results shown in Fig. 8 are consistent with the adsorption equilibrium of MTBE: the equilibrium aqueous concentration of Fe^{2+} for the minimum adsorption of MTBE approximately coincides with the maximum adsorption of Fe^{2+} , which shows a direct connection between the occupation of adsorption TiO_2 sites with iron ions and the performance of PCO: the minimum PCO efficiency for MTBE was observed around this concentration of $\text{Fe}^{2+/3+}$.

CONCLUSIONS

The complicated influence of the addition of multivalent ferrous/ferric ions to aqueous solutions of groundwater pollutants, 2-ethoxy ethanol (2-EE), methyl *tert*-butyl ether (MTBE) and humic substances (HS), was studied

and explained. An optimum concentration range of ferrous/ferric ions was observed for 2-EE and MTBE. Ferrous/ferric ions exhibited only an inhibiting role in PCO of HS.

Evidence was found that supported the hypothesis that the optima are the result of the dual mechanism of oxidation at the surface of the TiO_2 photocatalyst, including the direct oxidation of adsorbed pollutants with positively charged holes and the radical oxidation: the PCO of 2-EE resistant to radical oxidation practically stopped when the positively charged holes at the TiO_2 surface were blocked by ferrous/ferric ions. The effective PCO of less resistant MTBE at high concentrations of $\text{Fe}^{2+/3+}$ -ions may be explained by the development of a radical oxidation mechanism. This radical mechanism exhibited poor performance with HS since they exhibit good radical scavenging ability.

ACKNOWLEDGEMENTS

The authors express their gratitude to the Estonian Science Foundation (grant 5899), Centre for International Mobility (CIMO), Finland, Ekokem Yhtiöt, Finland, and the Academy of Finland (Project 208134) for financial support of the research.

REFERENCES

1. Manahan, S.E., *Environmental Chemistry*. 6th ed. Lewis Publishers, Boca Raton, FL, USA, pp. 80-82. (1994).
2. Sax, N. I., *Dangerous Properties of Industrial Materials*. 6th ed. Van Nstrand Reinhold Co., New York, pp. 1343-1346, (1984).
3. Nitschke, L., Wagner, H., Metzner, G., Wilk, A. and Huber, L., Biological treatment of waste water containing glycols from de-icing agents. *Water Res.*, **30**, 644-648 (1996).
4. Yeh, C.K. and Novak, J.T., Anaerobic biodegradation of gasoline oxygenates in soils. *Water Environ. Res.*, **66**, 744-752 (1994).
5. Linsebigler, A. L., Lu, G. and Yates, J. T., Photocatalysis on TiO₂ surfaces: principles, mechanism and selected results. *Chem. Rev.*, **95**, 735-758 (1995).
6. Vamathevan, V., Tse, H., Amal, R., Low, G. and McEvoy, S., Effects of Fe³⁺ and Ag⁺ ions on the photocatalytic degradation of sucrose in water. *Catalysis Today*, **68**, 201-208 (2001).
7. Araña, J., González Díaz, O., Doña Rodríguez, J. M., Herrera Melian, J. A., Garriga i Cabo, C., Pérez Peña, J., Carmen Hidalgo, M. and Navío-Santos, J. A., Role of Fe³⁺/Fe²⁺ as TiO₂ dopant in photocatalytic degradation of carboxylic acids. *J. Mol. Catal. A: Chem.*, **197**, 151-171 (2003).
8. Mrowetz, M. and Selli, E., Effect of iron species in the photocatalytic degradation of an azo dye in TiO₂ aqueous suspension. *J. Photochem. Photobiol. A: Chemistry*, **162**, 89-95 (2003).
9. Brezová, V., Blazková, A., Borosová, E., Ceppan, M. and Fiala, R., The influence of dissolved metal-ions on the photocatalytic degradation of phenol in aqueous TiO₂ suspensions. *J. Mol. Catal. A: Chem.*, **98**, 109-116 (1995).
10. Beydoun, D., Tse, H., Amal, R., Low, G. and McEvoy, S., Effect of copper (II) on the photocatalytic degradation of sucrose. *J. Mol. Catal. A: Chem.*, **177**, 265-272 (2002).
11. Krichevskaya, M., Kachina, A., Malygina, T., Preis, S. and Kallas, J., Photocatalytic oxidation of fuel oxygenated additives in aqueous solutions. *Int. J. Photoenergy*, **5**, 81-86 (2003).
12. Jackson, N. B., Wang, C. M., Luo, Z., Schwitzgebel, J., Ekerdt, J. G., Brock, J. R. and Heller, A., Attachment of TiO₂ powders to hollow glass microbeads: activity of the TiO₂-coated beads in the photoassisted oxidation of ethanol to acetaldehyde. *J. Electrochem. Soc.*, **138**, 3660-3664 (1991).
13. Portjanskaja, E., Krichevskaya, M., Preis, S. and Kallas, J., Photocatalytic oxidation of humic substances with TiO₂-coated glass micro-spheres. *Environ. Chem. Letters*, **2**, 123-127 (2004).
14. Clesceri, L. S., Greenberg, A. E. and Trussel, R. R. (eds.), *Standard Methods for the Examination of Water and Wastewater*, 17th ed. APHA, AWWA, WPCF, Washington, DC, pp. 3:102-3:106 and 5:15-5:17 (1989).
15. Pohloudeck-Fabini, R. and Beyrich, T., *Organische Analyse*. Akademische Verlagsgesellschaft Geest & Portig K.-G, Leipzig (1975), pp. 145-159.
16. Catastini, C., Sarakha, M., Mailhot, G. and Bolte, M., Iron (III) aquacomplexes as effective photocatalist for the degradation of pesticides in homogeneous aqueous solutions. *Sci. Total Environ.*, **298**, 219-228 (2002).
17. Carey, J. H., An introduction to AOP for destruction of organics in wastewater. *Water Pollut. Res. J. Canada*, **27**, 1-21 (1992).
18. Takahashi, N., Ozonation of several organic compounds having low molecular weight under ultraviolet irradiation. *Ozone: Sci. Eng.*, **12**, 1-17 (1990).
19. Brezová, V., Vodny, S., Vesely, M., Ceppan, M. and Lapčík, L., Photocatalytic oxidation of 2-ethoxyethanol in a water suspension of titanium dioxide. *J. Photochem. Photobiol. A: Chem.*, **56**, 125-134 (1991).
20. Liang, S., Palencia, L. S., Yates, R. S., Davis, M. K., Bruno, J.-M. and Wolfe, R. L., Oxidation of MTBE by ozone and peroxone processes. *J. Am. Water Works Assoc.*, **91**, 11-17 (1999).
21. Chu, W., Chan, K. H., Kwan, C.Y. and Lee, C.K., The system design of UV-assisted catalytic oxidation process—degradation of 2,4-D. *Chemosphere*, **57**, 171-178 (2004).
22. Ma, J. and Graham, N.J.D., Degradation of atrazine by manganese-catalyzed ozonation: influence of humic substances. *Water Res.*, **33**, 785-793 (1999).

Article II:

Klauson, D., Preis, S. The influence of ferrous ions on the efficiency of aqueous photocatalytic oxidation of 2-ethoxy ethanol. International Journal of Photoenergy, 2005, 7 (4), pp. 175-180

The influence of ferrous ions on the efficiency of aqueous photocatalytic oxidation of 2-ethoxy ethanol

D. Klauson¹ and S. Preis^{2,†}

¹ Department of Chemical Engineering, Tallinn University of Technology, Ehitajate tee 5, Tallinn 19086, Estonia

² Department of Chemical Technology, Lappeenranta University of Technology, P.O. Box 20, FIN-53851, Lappeenranta, Finland

ABSTRACT. The complex influence of ferrous ions on the efficiency of aqueous photocatalytic oxidation (PCO) of 2-ethoxyethanol (2-EE) was examined. A drastic efficiency increase at lower concentrations of ferrous ions was observed to change to a sharp decrease at higher concentrations. An explanation was proposed for the observed phenomena based on the low sensitivity of the pollutant towards radical-oxidation reactions and the competitive adsorption of metallic ions and 2-EE on the TiO₂ surface.

1. INTRODUCTION

2-Ethoxyethanol (2-EE, CH₃-CH₂-O-CH₂-CH₂-OH) is used as a solvent, a de-icing agent for runways and aircrafts, and an antifreeze jet fuel additive. This substance is often present in groundwater as a result of leakage, accidental spillages and uncontrolled disposal of fuels and de-icing liquids. It has negative effects on the kidneys, respiratory, and reproductive systems, and also acts as a depressant of the central nervous system [1]. The de-icing agents have been proven by earlier studies to be refractory against biodegradation and thus they accumulate and remain intact in groundwater for long times [2].

The photocatalytic oxidation (PCO) of organic pollutants is based on the action of positively charged holes on the semiconductor surface [3]. However, the holes may recombine rapidly with conduction band electrons, decreasing the PCO efficiency. Prolongation of the holes' lifetime should, therefore, increase the efficiency of PCO. For this purpose, multivalent metal ions may be added to the treated solutions, or, more precisely, to the photocatalyst surface, to scavenge electrons at the surface of the titanium dioxide, thus preventing electron-hole recombination and improving the oxidation performance.

This paper analyses the influence of ferrous ion additives on the PCO of 2-EE. Several previous studies [4–6] have reported higher PCO rates following the addition of small amounts of ferrous ions. Sucrose, carboxylic acids and textile azo dye were the organic pollutants in these studies. However, higher concentrations of ferrous ion reduced the decomposition rate significantly. A similar trend was observed with other multivalent metals influencing PCO of phenol and sucrose [7, 8]. Our previous studies [9] showed the positive

role of ferrous ions at low concentrations in the efficiency of PCO of methyl *tert*-butyl ether (MTBE), although the PCO experiments with 2-EE, carried out in the same range of concentrations of Fe²⁺, indicated only a negative effect of iron ions. The results of more detailed investigation, given here, extend the knowledge of the influence of iron ions on pollutants of various types and show the complex character of the dependence of the PCO efficiency on the concentration of iron ions.

2. EXPERIMENTAL SECTION

Two 200-mL simple batch reactors with inner diameter 100 mm (evaporation dishes), aperture 40 m² m⁻³, thermostatted at 20 ± 1 °C and mechanically agitated with magnetic stirrers were used in the PCO experiments: the reactor used for the PCO was called "active" and the other, containing no photocatalyst, was called "reference". Both reactors were exposed to identical experimental conditions. The samples from the active reactor were compared to the reference samples to avoid complications caused by water evaporation. A UV-light source, Phillips TLD 15 W/05 low-pressure luminescent mercury UV-lamp with the emission maximum at 360-nm, was positioned horizontally over the reactors, providing irradiance of about 0.7 mW cm⁻² measured by the optical radiometer UVX at a distance corresponding to the level of the free surface of the reactor.

The experiments were conducted with synthetic solutions at a concentration of 300 mg L⁻¹ of 2-EE. The concentration of 2-EE was chosen to be consistent with its presence in polluted groundwater and experimental conditions applied previously [9]. All experiments were carried out at pH 3.0, adjusted with sulphuric acid. The treatment time, 24 h, was chosen to reduce

[†]E-mail: Sergei.Preis@lut.fi

the concentration of 2-EE below 50% of the residual concentration and was used in calculations of the process efficiency E (see eq. (1)). All the experiments were carried out three times under identical conditions. The average deviation of data in parallel experiments did not exceed 5%.

The experiments were performed using titanium dioxide as Degussa P25. Slurry at 1 g L^{-1} was used as a suspended catalyst option. The supported catalyst option was TiO_2 attached to buoyant hollow glass microspheres and to the surface of the glass plates. The hollow glass micro-spheres used in this study had an average diameter of 60 to 70 μm and a density 0.27 g cm^{-3} (the product of LP-ImpEx, Estonia). Titanium dioxide was attached to the surface of the micro-beads by the thermal method [10]: equal volumes of dry microspheres and aqueous suspension of titanium dioxide with a concentration of 1 g L^{-1} were mixed by stirring and sonication for 30 min. The micro-spheres were then separated from the mixture by filtration with a membrane filter, heated to dryness at 120°C and calcinated at a temperature of 300°C for 4 h. This procedure was repeated six times, which was found to be the optimum number of attachment operations [11]. Analogously, TiO_2 was attached to the surface of the glass plates (one side) in approximately equal amounts either by multiple submerging of the plates in the TiO_2 suspension with subsequent drying after each submersion, or by spraying the TiO_2 suspension over the surface of the plates and drying. TiO_2 attached to glass plates, submerged horizontally in the solution to be treated at a depth from 5 to 10 mm, was used in the PCO experiments. Since 2-EE does not absorb UV light at 360 nm, the depth of the submersion was not important within the indicated limits. This was confirmed by specially conducted experiments.

The decrease in the pollutant concentration was determined for 2-EE from the decrease in chemical oxygen demand (COD), measured by a standard method [12].

Adsorption experiments for oxygenated hydrocarbons and ferrous ion, introduced as sulphate, on the TiO_2 surface were conducted in the dark in closed flasks equipped with magnetic stirrers, thermostatted at $20 \pm 1^\circ\text{C}$ and adjusted to pH 3.0. The amount of substances adsorbed was derived from the batch mass balance: the concentration of the dissolved substance was determined before and after adsorption. The points of the isotherms are the average of three experimental sets. The concentrations of iron ions were determined by a photometric phenantrolin method described in [12].

The PCO by-products of 2-EE, mainly carbonic acids, were qualitatively determined by the methods described in [13]. 200 mg of resorcinol was added to 5 ml of the sample in a test-tube. After the resorcinol had dissolved, 10 ml of concentrated sulphuric acid was carefully inserted into the bottom of the test-tube. The coloured rings corresponding to carbonic acids ap-

peared in the following sequence: the blue ring indicating oxalic acid appeared at the liquids' interface, the red ring below the blue one indicated glycolic acid, the orange ring above the blue one corresponds to formic acid. The rings were observed distinctively and repeatedly with both synthetic solutions of the acids and the samples of PCO treated 2-EE solutions. Oxalic acid was also separated from the sample as calcium oxalate and quantitatively determined by means of titration with potassium permanganate. Acetic acid was qualitatively determined as red crystals of iron (III) acetate precipitated as a result of addition of iron (III) chloride to the sample. These identifications were available only in the absence of iron ions in the treated samples, i.e. when the samples were treated without iron ions added.

3. RESULTS AND DISCUSSION

The performance of PCO with artificial radiation sources was characterised by the process efficiency E . The efficiency E is defined as the decrease in the amount of pollutant divided by the amount of energy reaching the surface of the treated sample (eq. (1)). The efficiency values were calculated after a period of time equal to the treatment time (24 h)

$$E = \frac{\Delta c \cdot V \cdot 1000}{I \cdot s \cdot t} \quad (1)$$

where E —PCO efficiency, $\text{mg W}^{-1} \text{ h}^{-1}$; Δc —the decrease in the concentration of the pollutant, $\text{mg O}_2 \text{ L}^{-1}$ for COD of 2-EE; V —the volume of the sample to be treated, L; I —irradiance, mW cm^{-2} ; s —irradiated area, cm^2 ; t —treatment time, h.

Both ferrous and ferric ions were tested in the experiments. Sulphate was chosen as the counter-ion due to its low inhibitive effect on PCO efficiency, observed with 2-EE in [9]. The results of the experiments are shown in Figure 1. One can see a similar trend in the dependence of PCO performance on the concentrations of both ionic species. Ferric ions were seen to have the same effect as ferrous ions, which may be explained with a dynamic equilibrium established between ferrous and ferric ions at the UV-irradiated TiO_2 surface and, probably, in its closest vicinity, as described in [14].

Ferrous and ferric ions appeared to play a significant role in PCO of 2-EE. The addition of small amounts of $\text{Fe}^{2+/3+}$ -ion, up to 0.09 mM, resulted in a drastic, up to 60%, increase in the process efficiency (Figure 1). With further increase in the concentration of $\text{Fe}^{2+/3+}$, the PCO efficiency decreased dramatically. Therefore, the experiments were conducted with ferrous ions the characterisation of which at $t = 0$ and in aqueous solution was far simpler. During the PCO process, the dynamic equilibrium $\text{Fe}^{2+}/\text{Fe}^{3+}$ took place very fast.

A similar dependency pattern, in which the PCO efficiency of 2-EE had its maximum with a $\text{Fe}^{2+/3+}$

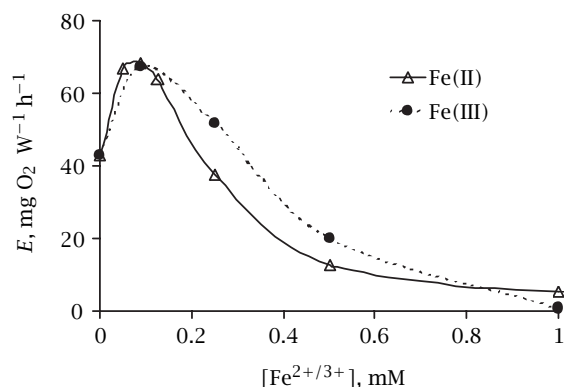


Figure 1. The efficiency of PCO of 2-ethoxyethanol in TiO₂ slurry vs. concentration of Fe²⁺ (Δ) and Fe³⁺ (●) ions at pH 3.0.

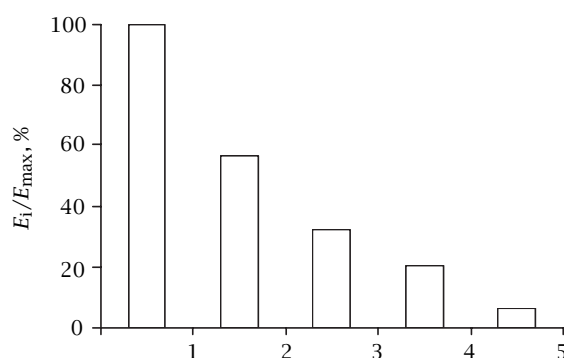


Figure 2. Efficiency of PCO of 2-ethoxyethanol at 0.09 mM of Fe²⁺ with TiO₂ application modes: 1-TiO₂ Degussa P25 suspension (1 g L⁻¹); 2-TiO₂ sprayed on the glass plate, 0.6 mg cm⁻²; 3-TiO₂ settled at the glass plate, 0.7 mg cm⁻²; 4-TiO₂ attached to hollow glass micro-spheres, the amount of buoyant catalyst in the reactor 50 g m⁻²; 5-same as 4 at 25 g m⁻².

concentration of 0.09 mM, was observed for TiO₂ attached to the glass plates, although the absolute values of the PCO efficiency were about 40 to 70% lower than with the TiO₂ slurry. Buoyant micro-beads with attached TiO₂ were the least effective (Figure 2).

Figure 2 shows that the difference in the procedure of TiO₂ attachment to the glass plates affects the PCO efficiency: attachment by spraying appeared to lead to more effective PCO. This may not be explained by the difference in the mass of TiO₂, since the attached mass was virtually the same, but is most probably due to uneven relief and porosity of the catalyst surface and, thus, a larger contact surface resulting from non-uniform spray attachment.

Methyl *tert*-butyl ether showed a trend somewhat similar to 2-EE, observed in our previous work: the drastic increase in PCO efficiency at smaller concentrations

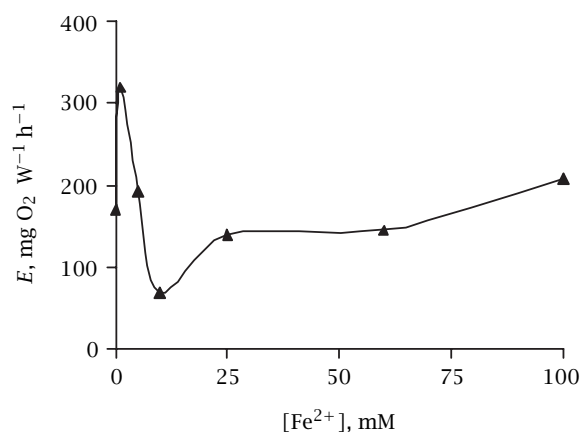


Figure 3. The efficiency of PCO of MTBE in TiO₂ slurry vs. concentration of Fe²⁺ -ions at pH 3.0.

of Fe²⁺-ions was followed by a decrease with further addition of ferrous ions (Figure 3) [9]. However, the maximum efficiency for MTBE was observed at the Fe²⁺ concentration of 1 mM, which is about ten times bigger than that for 2-EE. A further increase in the concentration of Fe²⁺-ions resulted in a gradual increase of PCO efficiency, which was not observed with 2-EE. This may be explained by the difference in the PCO mechanism of these two substances and their different adsorption properties at the surface of titanium dioxide.

The difference in the behaviour of 2-EE and MTBE can be explained by a dual mechanism [3]: (1) the adsorption of the pollutant by the surface of the titanium dioxide is followed by a direct subtraction of the pollutant's electrons, i.e. oxidation, with positively charged holes; (2) oxidation with hydroxyl radicals takes place at the catalyst surface or in its vicinity. Both reactions proceed simultaneously, although positively charged holes have an oxidation potential about 1.25 times bigger than OH-radicals [15]. Which mechanism dominates in PCO depends on the chemical and adsorption properties of the pollutant.

The promotion of the OH-radical was less effective in oxidation of ethylene glycol derivatives [16, 17]. The increasing PCO efficiency for 2-EE with the addition of ferrous ions in small, below 0.09 mM, concentrations may then be explained by the partial occupation of adsorption sites with Fe²⁺-ions, overpowered, however, with the electron scavenging by iron ions, extending the lifetime and thus the oxidation performance of the positively charged holes. A further increase in the concentration of metallic ions results in the blockage of adsorption sites with a resultant drastic decrease in PCO efficiency. The formation of hydroxyl radicals has little effect on the overall oxidation rate.

Methyl *tert*-butyl ether is less resistant towards oxidation with a hydroxyl radical. For example, oxidation methods, such as ozonation, exhibited poor

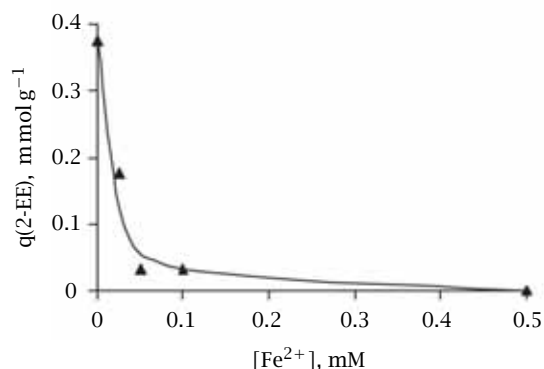


Figure 4. The surface concentration of 2-EE on TiO₂ versus Fe²⁺-ions equilibrium concentration at pH 3.0 (20 °C).

performance in the abatement of MTBE, although introduction of OH-radical promoters significantly enhanced oxidation [18]. This makes both PCO mechanisms effective in PCO of MTBE. Small concentrations of ferrous ions therefore enhance the direct oxidation of MTBE with positively charged holes, and also the formation of OH-radicals. Radical oxidation reactions contribute to the overall oxidation rate successfully until a certain concentration of metallic ions, 1 mM, is achieved (Figure 3). Above this concentration, the formation of OH-radicals is probably obstructed by a “short-circuit” phenomenon, described in [4]: the blockage of the TiO₂ adsorption sites with ferrous ions results in reduced generation of OH-radicals. The increase of the PCO efficiency with further increasing ferrous ion concentration may be explained by increased OH-radicals formation in the bulk solution initiated by the UV-irradiated Fe²⁺-ions. It was also observed that MTBE oxidized to some extent under UV-irradiation in aqueous solutions containing Fe²⁺-ions with no TiO₂ present, although this reaction was beyond the scope of the present paper. In the TiO₂-free experiments the oxidation rate increased with increasing concentration of Fe²⁺-ions. The authors presume that oxidation of MTBE with UV-irradiated Fe²⁺ may be enhanced in the presence of TiO₂. However, further experimental studies are necessary to confirm this statement.

To support the hypothesis concerning the role of ferrous ions in PCO performance determined by the adsorption properties and the sensitivity of the target compounds towards radical attacks, the impact of the Fe²⁺-ions on the adsorption of a pollutant by TiO₂ was studied in a series of adsorption experiments. The ferrous ions content dependency of adsorption of 2-EE from a solution with an equilibrium concentration of 2-EE 300 mg L⁻¹ by the TiO₂ surface was determined experimentally. As one can see from Figure 4, the surface concentration of 2-EE steadily decreased within the

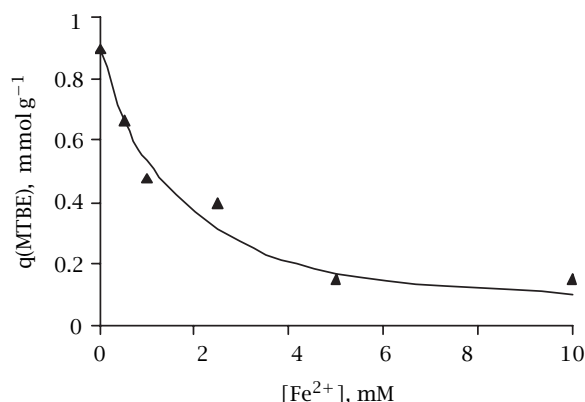


Figure 5. The surface concentration of MTBE on TiO₂ versus Fe²⁺-ions concentration at pH 3.0 (20 °C).

Fe²⁺-ions equilibrium concentration range attributable to the peak zone of the PCO efficiency (Figure 1).

An analogous dependence of the equilibrium surface concentration of MTBE was also observed: the MTBE surface concentration in equilibrium with an MTBE solution of 100 mg L⁻¹ decreased from 0.9 mmol g⁻¹ at zero concentration of Fe²⁺-ions to 0.5 mmol g⁻¹ at 1 mM and 0.1 mmol g⁻¹ at 10 mM of Fe²⁺-ions (Figure 5). This explains the difference between the critical concentration values of Fe²⁺-ions for 2-EE and MTBE: the adsorption of MTBE was less affected by the presence of Fe²⁺-ions than 2-EE.

The last observation may be explained by differences in adsorption of 2-EE and MTBE. The carbonic acids determined qualitatively as PCO products of 2-EE include oxalic, acetic, formic and glycolic acids. The possible route of the reactions is outlined in Figure 6. The presence of acetic and especially glycolic acids among the oxidation by-products indicate the adsorption of 2-EE with its etheric oxygen and, therefore, electrophilic attack of positively charged holes to the etheric bond. This results in fracture of the 2-EE molecule into two fragments, the acetic and glycolic acids (reaction A). The formation of oxalic acid appears to be possible only when both oxygen atoms in the 2-EE molecules are adsorbed on the TiO₂ surface and are under simultaneous attack of positively charged holes (reaction B). A further possible precursor of oxalic acid is glycolic acid, when the alcoholic group is oxidised (reaction C). Hypothetically, acetic acid may also be a product of 2-EE stepwise oxidation starting from the alcohol group only (reaction D) with formic acid as a product of the last reaction. The ethoxy carbonic acids were not identified and were only shown as hypothetical by-products in rectangular brackets. Further oxidation of reactive by-products, such as formic acid also observed in samples, may proceed with OH-radicals formed at the TiO₂ surface, although their formation may be

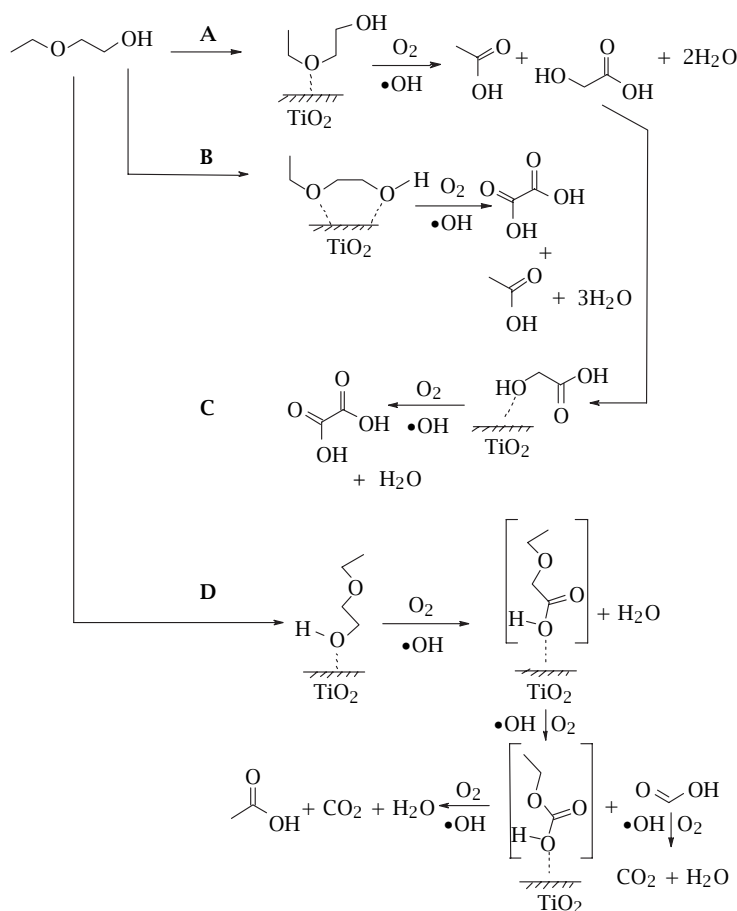


Figure 6. Outline of aqueous photocatalytic oxidation reaction of 2-ethoxy ethanol on TiO_2 .

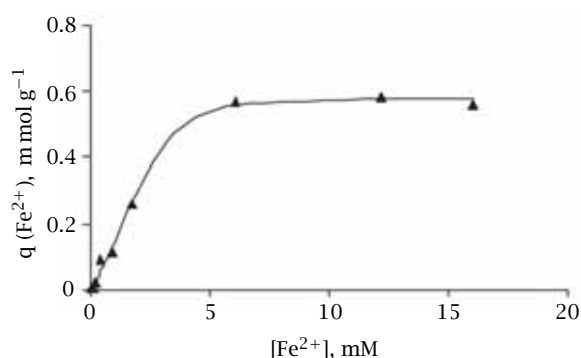


Figure 7. The surface concentration of Fe^{2+} -ions on TiO_2 versus Fe^{2+} -ions equilibrium concentration at pH 3.0 (20 °C).

suppressed in acidic media. The OH-radical, although less reactive with 2-EE, may also participate in oxidation reactions initiated by positively charged holes at the TiO_2 surface.

The adsorption of ferrous/ferric ion on the surface of titanium dioxide was also studied. The results shown in Figure 7 are consistent with the adsorption equilibrium of MTBE: the equilibrium aqueous concentration of Fe^{2+} for the minimum adsorption of MTBE approximately coincides with the maximum adsorption of Fe^{2+} , which shows a direct connection between the occupation of adsorption TiO_2 sites with iron ions and the performance of PCO—the minimum PCO efficiency for MTBE was observed around this concentration of Fe^{2+} [9].

4. CONCLUSIONS

The complicated influence of the addition of multivalent metallic ions to aqueous solutions of groundwater pollutant, 2-ethoxy ethanol (2-EE), was studied. An optimum concentration range of ferrous ions was observed.

The hypothesis was supported that the optima are the result of a dual mechanism of oxidation at the surface of the TiO_2 photocatalyst, including the direct

oxidation of adsorbed pollutants with positively charged holes and the radical oxidation: the PCO of 2-EE resistant to radical oxidation practically stopped when the positively charged holes at the TiO₂ surface were blocked by ferrous/ferric ions. The effective PCO of MTBE at high concentrations of Fe²⁺-ions observed in our previous work may be explained by the attack by hydroxyl radicals more efficient with MTBE.

ACKNOWLEDGMENTS

The authors express their gratitude to the Estonian Science Foundation (grant 5899), Centre for International Mobility (CIMO), Finland, and the Academy of Finland (Project 208134) for financial support.

REFERENCES

- [1] N. Sax, *Dangerous Properties of Industrial Materials*, 6th ed., Van Nostrand Reinhold Co., New York, 1984, pp. 1343-1346.
- [2] L. Nitschke, H. Wagner, G. Metzner, A. Wilk, and L. Huber, *Wat. Res.* **30** (1996), 644.
- [3] A. Linsebigler, G. Lu, and J. Yates, *Chem. Rev.* **95** (1995), 735.
- [4] V. Vamathevan, H. Tse, R. Amal, G. Low, and S. McEvoy, *Catalysis Today* **68** (2001), 201.
- [5] J. Araña, O. González Díaz, J. Doña Rodríguez, J. Herrera Melian, C. Garriga i Cabo, J. Pérez Peña, M. Carmen Hidalgo, and J. Navío-Santos, *J. Molecular Catalysis A: Chemical* **197** (2003), 151.
- [6] M. Mrowetz and E. Selli, *J. Photochem. Photobiol. A: Chemistry* **162** (2003), 89.
- [7] V. Brezová, A. Blazková, E. Borosová, M. Čeppan, and R. Fiala, *J. Molecular Catalysis A: Chemical* **98** (1995), 109.
- [8] D. Beydoun, H. Tse, R. Amal, G. Low, and S. McEvoy, *J. Molecular Catalysis A: Chemical* **177** (2002), 265.
- [9] M. Krichevskaya, A. Kachina, T. Malygina, S. Preis, and J. Kallas, *Int. J. Photoenergy* **5** (2003), 81.
- [10] N. Jackson, C. Wang, Z. Luo, J. Schwitzgebel, J. Ekerdt, J. Brock, and A. Heller, *J. Electrochem. Soc.* **138** (1991), 3660.
- [11] E. Portjanskaja, M. Krichevskaya, S. Preis, and J. Kallas, *Environ. Chem. Letters* **2** (2004), 123.
- [12] *Standard Methods for the Examination of Water and Wastewater* (L. Clesceri, A. Greenberg, and R. Trussel, eds.), 17th ed., APHA, AWWA, WPCF Washington, DC, 1989, pp. 3:102 and 5:15.
- [13] R. Pohloudeck-Fabini and T. Beyrich, *Organische Analyse*, Akademische Verlagsgesellschaft Geest & Portig K.-G, Leipzig, 1975, p. 145.
- [14] C. Catastini, M. Sarakha, G. Mailhot, and M. Bolte, *Sci. Total Environ.* **298** (2002), 219.
- [15] D. Bahnemann, *Solar Energy* **77** (2004), 445.
- [16] N. Takahashi, *Ozone: Sci. Eng.* **12** (1990), 1.
- [17] V. Brezová, Š. Vodný, M. Veselý, M. Čeppan, L. Lapčík, *J. Photochem. Photobiol. A: Chemical* **56** (1991), 125.
- [18] S. Liang, L. Palencia, R. Yates, M. Davis, J.-M. Bruno, and R. Wolfe, *J. Am. Wat. Works Assoc.* **91** (1999), 11.

Article III:

Klauson, D., Preis., S., The influence of iron ions on the aqueous photocatalytic oxidation of de-icing agents. International Journal of Photoenergy, 2007, 2007, Article ID 89359, pp. 1-7.

Research Article

The Influence of Iron Ions on the Aqueous Photocatalytic Oxidation of Deicing Agents

D. Klauson¹ and S. Preis²

¹ Department of Chemical Engineering, Faculty of Chemical and Materials Technology, Tallinn University of Technology, Ehitajate tee 5, 19086 Tallinn, Estonia

² Department of Chemical Technology, Lappeenranta University of Technology, P.O. Box 20, 53851 Lappeenranta, Finland

Received 13 December 2006; Revised 15 February 2007; Accepted 1 May 2007

Recommended by Terry Egerton

An experimental research into aqueous photocatalytic oxidation (PCO) of the deicing compounds, 2-ethoxyethanol (2-EE), diethylene glycol monomethyl ether (DEGMME), and ethylene glycol (EG) was undertaken. The addition of iron ions to the acidic aqueous solutions to be treated displayed complex influence on the oxidation efficiency of the above mentioned substances, resulting in a sharp increase of the PCO efficiency at smaller concentrations of iron ions followed by a drastic decrease with the increasing iron ion concentrations. The phenomena observed can be explained by the electron scavenging effect of the iron ions and the competitive adsorption of iron ions and the oxidized substances on titanium dioxide surface. The carbonic acids determined as the PCO by-products allow outlining some reaction pathways for the substances under consideration.

Copyright © 2007 D. Klauson and S. Preis. This is an open access article distributed under the Creative Commons Attribution License, which permits unrestricted use, distribution, and reproduction in any medium, provided the original work is properly cited.

1. INTRODUCTION

The photocatalytic oxidation (PCO) of organic pollutants is based on the action of positively charged holes on the semiconductor surface [1]. However, the holes may recombine rapidly with conduction band electrons, decreasing the PCO efficiency. Therefore, prolongation of the holes' lifetime should increase the efficiency of PCO. For this purpose, multivalent metal ions may be added to the treated solutions or, more precisely, to the photocatalyst surface, to scavenge electrons at the surface of the titanium dioxide, thus preventing electron-hole recombination and improving the oxidation performance.

Several previous studies [2–5] have reported higher PCO rates following the addition of small amounts of ferrous ions. Sucrose, carboxylic acids, and textile azo dye were the organic pollutants in these studies. However, higher concentrations of ferrous ion reduced the decomposition rate significantly. A similar trend was observed with other multivalent metals influencing PCO of toluene and phenol [6, 7]. Our previous results showed a peculiar influence of ferrous ions to PCO of lignin, humic acids, and some oxygenated hydrocarbons, such as methyl *tert*-butyl ether [8]. The present paper analyses the effect of iron ions addition

on the PCO efficiency of the three most used glycolic deicing agents: ethylene glycol (EG, HO-CH₂-CH₂-OH), 2-ethoxyethanol (2-EE, CH₃-CH₂-O-CH₂-CH₂-OH), and diethylene glycol monomethyl ether (DEGMME, CH₃-O-CH₂-CH₂-O-CH₂-CH₂-OH).

Ethylene glycol is mainly used as an antifreeze, although substantial amounts of EG are consumed in polymer synthesis. 2-Ethoxyethanol is used as a solvent, a deicing agent for runways and aircrafts, and a deicing additive in the jet fuel. The usage of DEGMME is similar to that of 2-EE; it is also used as a diluent for hydraulic brake fluids. Massive use of the deicing substances, their leakage, accidental spillages and uncontrolled disposal of fuels, deicing and brake liquids, and antifreezes result in their occurrence in groundwater. All these substances act as central nervous system depressants and may inflict substantial kidney damage which can be fatal; they have also negative effects on respiratory and reproductive systems [9, 10]. Glycol-based deicing agents have been proven by earlier studies to be refractory against biodegradation, and thus they accumulate and remain intact in groundwater for long times [11]. Chemical oxidation methods, such as ozonation and treatment with Fenton's reagent, have been proven inadequate in dealing with glycolic pollution [12–15], resulting in insufficient pollutant

removal and poor mineralization, not to mention high treatment cost.

2. EXPERIMENTAL SECTION

The PCO experiments were carried out in two 200 mL simple batch reactors with inner diameter 100 mm (evaporation dishes), and aperture $40 \text{ m}^2 \text{ m}^{-3}$. The reactors were thermostatted at $20 \pm 1^\circ \text{C}$ and mechanically agitated [16]. The reactor used for the PCO was called “active” and the other, containing no photocatalyst, was called “reference.” Both reactors were exposed to identical experimental conditions. The samples from the active reactor were compared to the reference samples to avoid the effect of water evaporation. A UV light source, Phillips TLD 15 W/05 low-pressure luminescent mercury UV lamp with the emission maximum at 360 nm, was positioned horizontally over the reactors, providing irradiance of about 0.7 mW cm^{-2} measured by the optical radiometer U VX at a distance corresponding to the level of the free surface of the reactor.

The experiments were carried out with synthetic solutions at a concentration of 300 mg L^{-1} of EG, 2-EE, and DEGMME. The concentrations of the substances were chosen to be consistent with their presence in polluted groundwater and experimental conditions applied previously [8]. All experiments were carried out at pH 3, adjusted with sulphuric acid. The treatment time, 24 hours, was chosen to reduce the concentration of EG, 2-EE, and DEGMME no more than 50% of the residual concentration, and was used in calculations of the process efficiency E (see (1)). All the experiments were carried out three times under identical conditions. The average deviation of data in parallel experiments did not exceed 5%.

The experiments were performed using Degussa P25 titanium dioxide as suspension at 1 g L^{-1} . Both ferric and ferrous ions were introduced as respective sulphates.

The decrease in the pollutant concentration was determined for EG, 2-EE, and DEGMME from the decrease in chemical oxygen demand (COD), measured by a standard method [17].

Adsorption experiments for glycols and ferrous ion on the TiO_2 surface were conducted in the dark in closed flasks equipped with magnetic stirrers, thermostatted at $20 \pm 1^\circ \text{C}$ and adjusted to pH 3. The amount of substances adsorbed was derived from the batch mass balance; the concentration of the dissolved substance was determined before and after adsorption. The points of the isotherms are the average of three experimental sets. The concentrations of iron ions were determined by a variation of photometric phenantrolin method described in [17], where phenantrolin was substituted by dipyritydyl.

The PCO by-products of EG, 2-EE, and DEGMME, mainly carbonic acids, were qualitatively determined by the methods described in [18]. Resorcinol in amount of 200 mg was added to 5 mL of the sample in a test tube. After the resorcinol had dissolved, 10 mL of concentrated sulphuric acid was carefully inserted into the bottom of the test-tube. The colored rings corresponding to carbonic acids appeared in

the following sequence: the blue ring indicating oxalic acid appeared at the liquids' interface, the red ring below the blue one indicated glycolic acid, the orange ring above the blue one corresponds to formic acid. The rings were observed distinctively and repeatedly with both synthetic solutions of the acids and the samples of PCO-treated glycolic solutions. Oxalic acid was also separated from the PCO-treated 2-EE solution sample as calcium oxalate, and quantitatively determined by means of titration with potassium permanganate. Acetic acid was qualitatively determined with 2-EE as red crystals of iron (III) acetate precipitated as a result of addition of iron (III) chloride to the sample. The iron ions did not show any interference in these identifications, which was verified with individual carbonic acids with and without iron ions.

3. RESULTS AND DISCUSSION

The performance of PCO with artificial radiation sources was characterised by the process efficiency E . The efficiency E is defined as the decrease in the amount of pollutant divided by the amount of energy reaching the surface of the treated sample (1). The efficiency values were calculated after a period of time equal to the treatment time of 24 hours:

$$E = \frac{\Delta c \cdot V \cdot 1000}{I \cdot s \cdot t}, \quad (1)$$

where E is the PCO efficiency, $\text{mg W}^{-1} \text{ h}^{-1}$; Δc is the decrease in the concentration of the pollutant, mg O L^{-1} for COD of EG, 2-EE, and DEGMME; V is the volume of the sample to be treated, L; I is irradiance, mW cm^{-2} ; s is irradiated area, cm^2 ; t is treatment time, hours.

Both ferrous and ferric ions were tested in the experiments with EG. Sulphate was chosen as the counter-ion due to its low inhibitive effect on PCO efficiency, observed in [8]. Previously, the indifference of the PCO towards the oxidation state of iron ions was observed in the PCO of 2-EE [16]: one could see a similar trend in the dependence of PCO performance on the concentrations of both ionic species. Ferric ions were seen to have the same effect as ferrous ions, which may be explained with a dynamic equilibrium established between ferrous and ferric ions at the UV-irradiated TiO_2 surface and, probably, in its closest vicinity, as described in [19].

In this research, the similar behaviour of iron species was observed in experiments with EG; the results are shown in Figure 1. As one can see also from Figure 2 obtained previously with 2-EE [16], ferrous and ferric ions appeared to play a significant role in PCO of EG and 2-EE. The addition of small amounts of $\text{Fe}^{2+/3+}$ -ion, up to 0.09 mM, resulted, for example, in a drastic, up to 60%, increase in the 2-EE PCO efficiency (see Figure 2).

With further increase in the concentration of $\text{Fe}^{2+/3+}$, the PCO efficiency decreased dramatically. Therefore, the experiments were conducted with ferrous ions, the characterisation of which at $t = 0$ and in aqueous solution was far simpler. During the PCO process, the dynamic equilibrium $\text{Fe}^{2+}/\text{Fe}^{3+}$ took place very fast.

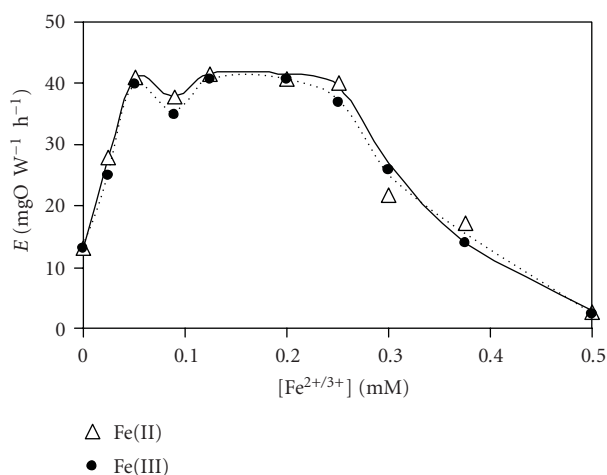


FIGURE 1: The efficiency of PCO of ethylene glycol (EG) in TiO_2 suspension versus concentration of Fe^{2+} (Δ) and Fe^{3+} (\bullet) ions at pH 3.

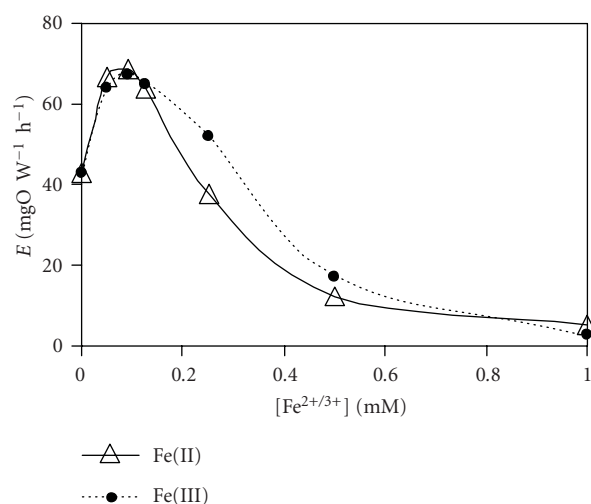


FIGURE 2: The efficiency of PCO of 2-ethoxyethanol (2-EE) in TiO_2 suspension versus concentration of Fe^{2+} (Δ) and Fe^{3+} (\bullet) ions at pH 3.

A similar dependency pattern was observed with DEGMME, although the concentration of iron ions corresponding to the efficiency peak was somewhat smaller than that of 2-EE, being 0.06 mM (Figure 3).

Ethylene glycol, however, showed a more complicated dependency of the PCO efficiency on the concentration of iron ions than 2-EE and DEGMME (see Figure 1). An initial increase in the PCO efficiency of EG at smaller iron ion concentrations (up to 0.05 mM) was followed by a minor decrease between 0.05 and 0.09 mM Fe^{2+} . The former PCO efficiency decrease was followed by yet another increase in the iron ion concentration range from 0.09 to 0.125 mM, when the efficiency returned approximately to the same values as at 0.05 mM Fe^{2+} . Between 0.125 and 0.25 mM of iron ions' concentration the efficiency value remained stable, followed

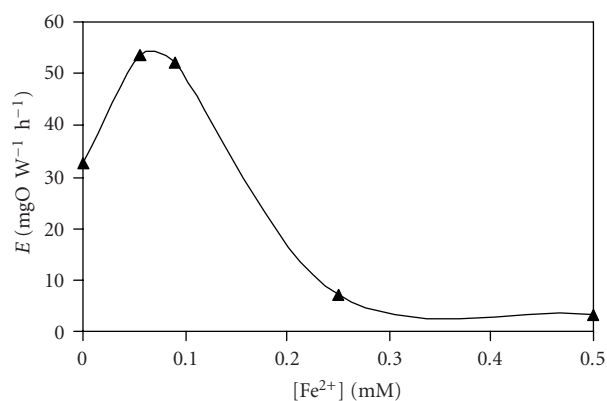


FIGURE 3: The efficiency of PCO of diethylene glycol monomethyl ether (DEGMME) in TiO_2 suspension versus concentration of Fe^{2+} ions at pH 3.

by a drastic decrease above 0.25 mM. This observation did not find a proper explanation in the present work although the decrease in the PCO efficiency at $\text{Fe}^{2+/3+}$ concentrations between 0.05 and 0.09 mM was reliably established with both iron ionic species.

Photocatalytic oxidation is known to proceed via two different mechanisms [1]: direct subtraction of the adsorbed pollutant's electrons by the positively charged holes on the surface of titanium dioxide, and oxidation with hydroxyl radicals at the catalyst surface or in its vicinity. Both reactions may proceed simultaneously, although positively charged holes have an oxidation potential about 1.25 times bigger than OH-radicals [20]. Which mechanism dominates in PCO depends on the chemical and adsorption properties of the pollutant.

Glycolic substances were shown by previous studies [21, 22] to be resistant to radical-initiated oxidation reactions. The increasing PCO efficiency for monoalcoholic 2-EE and DEGMME with the addition of ferrous ions in small concentrations (below 0.09 and 0.06 mM, resp.) may then be explained by the partial occupation of adsorption sites with Fe^{2+} -ions, overpowered, however, with the electron scavenging by iron ions, extending the lifetime and thus improving the oxidation performance of the positively charged holes. A further increase in the concentration of iron ions results in the blockage of adsorption sites with a resultant drastic decrease in PCO efficiency. The difference in the concentration of iron ions at maximum PCO efficiency for 2-EE and DEGMME may be explained by better adsorption of 2-EE (see below).

Ethylene glycol has two hydroxyl groups, which may result in a more complex mechanism of a stronger adsorption. It may be assumed that the adsorption of EG on the surface of titanium dioxide takes place partially with both hydroxyl groups. As it was shown below, the EG molecule attachment with two alcohol groups does not result in simultaneous oxidation of these groups, that is, the alcohol groups are attached with the bonds of unequal length and energy.

One can presume then that the alcohol group, which is adsorbed weaker to the photocatalyst surface, should be easier displaced from the TiO_2 surface with the increasing iron ions concentration, thus making EG exhibiting fluctuations in its PCO efficiency. The surface concentrations of EG also are dramatically bigger than those of 2-EE and DEGMME (Figure 4), which explains a wide peak of the EG PCO efficiency versus the increasing Fe^{2+} -concentration.

In order to verify the viability of the hypothesis described above, series of adsorption experiments were conducted, in which the dependence of deicing agents' adsorption on the concentration of ferrous ions was examined. Also, the adsorption isotherm of ferrous ions on the surface of titanium dioxide was constructed. The results obtained are shown in Figures 4 and 5.

As one can see, the addition of small amounts of iron ions dramatically reduced the adsorption of EG, 2-EE, and DEGMME (Figure 4) on the surface of titanium dioxide. At these concentrations of iron ions, however, the growth of the PCO efficiency of these substances was observed, confirming the hypothesis of electron scavenging by iron ions.

The adsorption mechanism of the substances under consideration may be better explained with the analysis of the carbonic acids formed in PCO. Oxidation of 2-EE in absence of iron ions resulted in formation of glycolic, oxalic, acetic, and formic acids. This indicated the possible adsorption of 2-EE molecule at the protonated TiO_2 surface with oxygen atoms of hydroxyl, ether, or both oxygenated groups. Since oxalic acid was formed in trace amounts and glycolic acid was also hardly detectable, the adsorption with the hydroxyl group appeared to predominate, although the adsorption with the ether oxygen or both oxygen atoms also took place. This found an indirect proof in the fact that in presence of iron ionic species, the PCO of 2-EE resulted in the formation of only acetic and formic acids. This may be explained by the decrease in 2-EE adsorption with iron ions adsorbed on the TiO_2 surface: the absence of oxalic and glycolic acids indicates that 2-EE was adsorbed and oxidised only on the hydroxyl group.

The PCO of DEGMME resulted in formation of only glycolic and formic acids in the absence of iron ions. One can conclude that DEGMME molecule may adsorb also with either hydroxyl or one of the ether groups. However, since no oxalic acid was observed, the adsorption can take place only with one oxygen atom at a time, possibly due to geometrical obstacles for the long-chain DEGMME molecules. The last conclusion may be derived from the absence of oxalic acid among the PCO products of DEGMME: it was shown in the experiments that the PCO of glycolic acid does not result in the formation of oxalic acid. Therefore, the simultaneous adsorption and oxidation of both oxygenated groups in DEGMME molecule appear to be a prerequisite of the formation of oxalic acid. Obviously, no adsorption with ether groups was observed in presence of iron ions since no glycolic acid was detected in the treated samples, only formic acid appeared.

It might be assumed that PCO of EG adsorbed with both oxygen atoms should result in the formation of oxalic acid.

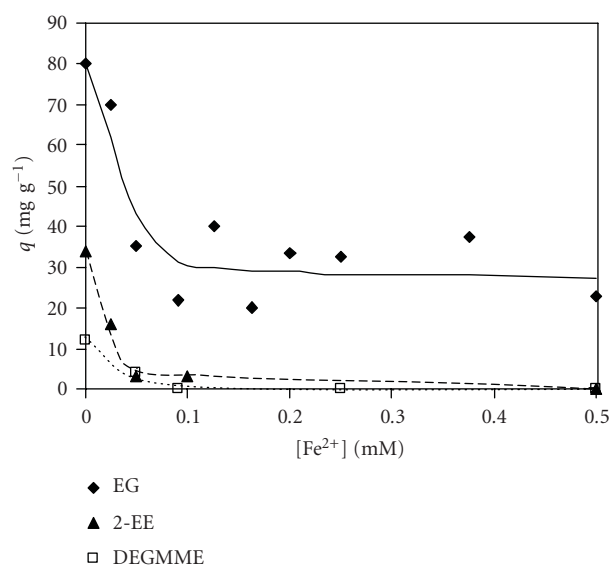


FIGURE 4: The surface concentrations of ethylene glycol (EG), 2-ethoxyethanol (2-EE) and diethylene glycol monomethyl ether (DEGMME) on TiO_2 versus Fe^{2+} -ions equilibrium concentration at pH 3 (20°C).

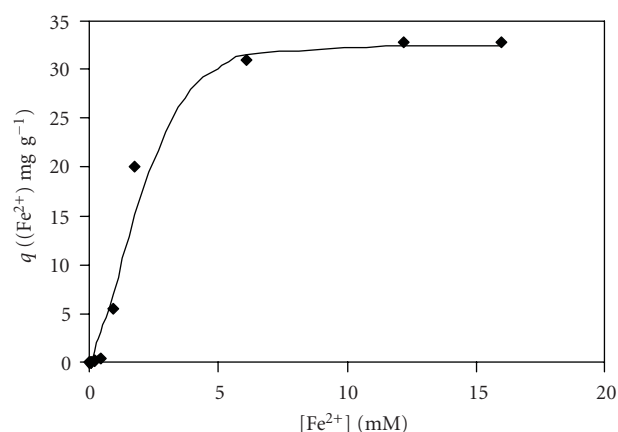


FIGURE 5: The surface concentration of Fe^{2+} -ions on TiO_2 versus Fe^{2+} -ions equilibrium concentration at pH 3 (20°C).

However, this point was overrun by the experimental data: only glycolic and formic acids were formed. Also, the PCO of glycolic acid showed no oxalic acid among the products: only formic acid was determined as the product. This circumstance indicates that the EG molecule is oxidized on only one hydroxyl group, first with subsequent oxidation of glycolic acid to formic acid and further to ultimate oxidation products, carbon dioxide and water. This is presumably possible when the EG molecule is attached to the titanium dioxide surface with only one hydroxyl group or at least when two hydroxyl groups are connected to the surface by bonds of unequal length and energy. It is worth noticing that at higher iron ion concentrations the PCO efficiency on EG is negligible, however, at the same time, the amount of EG adsorbed

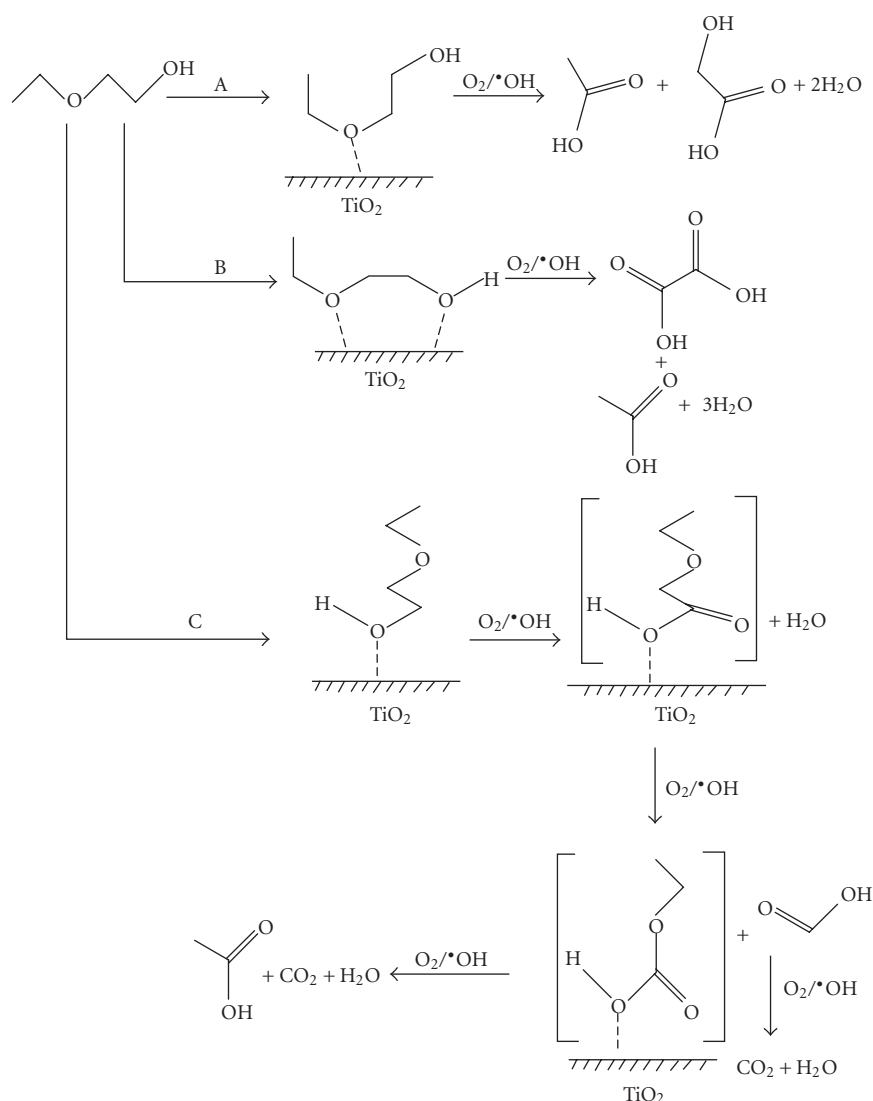


FIGURE 6: Outline of aqueous photocatalytic oxidation reaction of 2-ethoxy ethanol on TiO_2 .

on the surface of titanium dioxide is significant. This contradiction may be explained by the “short circuit” phenomenon described in [4]: iron ions adsorbed in significant amounts scavenge the electrons at the TiO_2 surface, and then are oxidised by the positively charged holes. The holes are therefore blocked by iron ions and the electrons keep circulating between iron ions and titanium dioxide. This way no pollutant oxidation can take place, regardless of its residual adsorption on the catalyst surface.

The adsorption of iron ions was of Langmuir type, reaching its maximum value at approximately $34 \text{ mg L}^{-1} \text{ Fe}^{2+}$ (see Figure 5). One can see that all the efficiency changes under the experimental conditions take place at the surface concentration of iron ions growing with their concentration in the solution.

Alongside with adsorption mechanism clarification, the determination of PCO by-products allows to outline possible reaction pathways of the substances oxidised. The presence

of acetic and glycolic acids among the oxidation by-products indicates the adsorption of 2-EE with its ether oxygen and, therefore, electrophilic attack of positively charged holes to the ether bond (see Figure 6). This results in fracture of the 2-EE molecule into two fragments, the acetic and glycolic acids (reaction A). The formation of oxalic acid appears to be possible only when both oxygen atoms in the 2-EE molecules are adsorbed on the TiO_2 surface and are under simultaneous attack of positively charged holes (reaction B). Acetic acid may also be a product of 2-EE stepwise oxidation starting from the alcohol group only (reaction C) with formic acid as a product of the last reaction. The ethoxy carbonic acids were not identified and were only shown as hypothetical by-products in rectangular brackets. It has been experimentally confirmed that glycolic acid cannot act as the precursor of oxalic acid; this circumstance brings the correction to the previously presented reaction pathway outline [23]. In presence of iron ions, the reaction may proceed only via

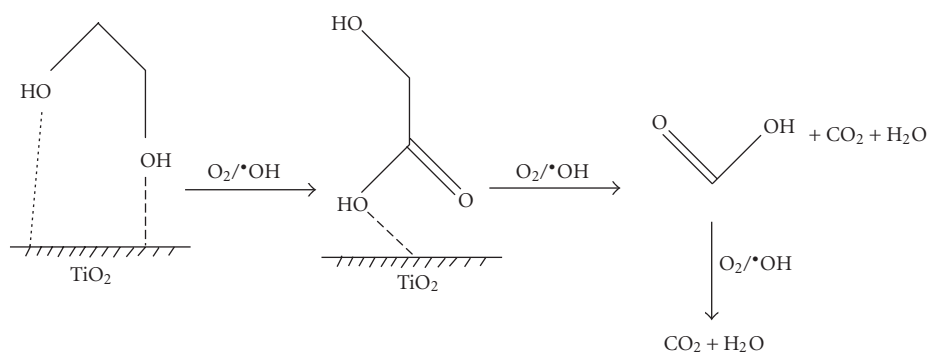


FIGURE 7: Outline of aqueous photocatalytic oxidation reaction of ethylene glycol on TiO₂.

the pathway C since formic and acetic acids were found, but neither glycolic nor oxalic acids were detected in the PCO-treated samples.

Further oxidation of reactive by-products, such as formic acid also observed in samples, may proceed with both positively charged holes and OH-radicals formed at the TiO₂ surface, although their formation may be suppressed in acidic media. The OH-radical, although less reactive with 2-EE, may also participate in oxidation reactions initiated by positively charged holes at the TiO₂ surface.

With DEGMME, adsorption of the molecule by any of the three oxygen atoms will eventually lead to the formation of glycolic and formic acids. Since no glycolic acid was observed in PCO samples in presence of iron species, no adsorption and, therefore, oxidation of ether groups took place. Formation of acetic acid was not observed as expected. Long-chain products, expected once the PCO starts fragmenting the DEGMME molecule with formation of formic acid, were not identified. Glycolic acid was presumably formed from the DEGMME molecule adsorbed with the oxygen of the ether bond in absence of iron ions.

The PCO on only one of the hydroxyl groups of EG leads to the formation of glycolic and formic acids (Figure 7). The dotted line on the figure shows the possibly weaker bond between one of the hydroxyl groups and the titanium dioxide surface, whereas the other hydroxyl group is connected to the catalyst by a shorter bond with higher energy. The addition of iron ions did not affect the composition of the PCO by-products: only glycolic and formic acids were observed with and without iron ionic species.

4. CONCLUSIONS

The complicated influence of the addition of ferrous/ferric ions to the photocatalytic oxidation of the aqueous solutions of glycolic compounds, ethylene glycol (EG), 2-ethoxy ethanol (2-EE), and diethylene glycol monomethyl ether (DEGMME) was shown and explained. An optimum concentration range of ferrous ions for the highest PCO efficiency was observed.

The hypothesis of electron scavenging by iron ions of TiO₂ surface with the increased PCO efficiency was proved.

It has been experimentally proven that the PCO efficiency optima are the result of the competitive absorption of the pollutants and iron ions on TiO₂ photocatalyst surface: the PCO of EG, 2-EE, and DEGMME practically stopped when the adsorption sites at the TiO₂ surface were blocked by iron ions.

ACKNOWLEDGMENTS

The authors express their gratitude to the Estonian Science Foundation (Grant 5899), and the Academy of Finland (project 208134) for financial support of the research.

REFERENCES

- [1] D. M. Blake, J. Webb, C. Turchi, and K. Magrini, "Kinetic and mechanistic overview of TiO₂-photocatalyzed oxidation reactions in aqueous solution," *Solar Energy Materials*, vol. 24, no. 1–4, pp. 584–593, 1991.
- [2] V. Vamathevan, H. Tse, R. Amal, G. Low, and S. McEvoy, "Effects of Fe³⁺ and Ag⁺ ions on the photocatalytic degradation of sucrose in water," *Catalysis Today*, vol. 68, no. 1–3, pp. 201–208, 2001.
- [3] D. Beydoun, H. Tse, R. Amal, G. Low, and S. McEvoy, "Effect of copper(II) on the photocatalytic degradation of sucrose," *Journal of Molecular Catalysis A: Chemical*, vol. 177, no. 2, pp. 265–272, 2002.
- [4] J. Araña, O. González Díaz, J. M. Doña Rodríguez, et al., "Role of Fe³⁺/Fe²⁺ as TiO₂ dopant ions in photocatalytic degradation of carboxylic acids," *Journal of Molecular Catalysis A: Chemical*, vol. 197, no. 1–2, pp. 157–171, 2003.
- [5] M. Mrowetz and E. Selli, "Effects of iron species in the photocatalytic degradation of an azo dye in TiO₂ aqueous suspensions," *Journal of Photochemistry and Photobiology A: Chemistry*, vol. 162, no. 1, pp. 89–95, 2004.
- [6] E. C. Butler and A. P. Davis, "Photocatalytic oxidation in aqueous titanium dioxide suspensions: the influence of dissolved transition metals," *Journal of Photochemistry and Photobiology A: Chemistry*, vol. 70, no. 3, pp. 273–283, 1993.
- [7] V. Brezová, A. Blažková, E. Borošová, M. Čeppan, and R. Fiala, "The influence of dissolved metal ions on the photocatalytic degradation of phenol in aqueous TiO₂ suspensions," *Journal of Molecular Catalysis A: Chemical*, vol. 98, no. 2, pp. 109–116, 1995.

- [8] M. Krichevskaya, A. Kachina, T. Malygina, S. Preis, and J. Kallas, "Photocatalytic oxidation of fuel oxygenated additives in aqueous solutions," *International Journal of Photoenergy*, vol. 5, no. 2, pp. 81–86, 2003.
- [9] K. Verschueren, *Handbook of Environmental Data of Organic Chemicals*, Van Nostrand Reinhold, New York, NY, USA, 1983.
- [10] N. I. Sax, *Dangerous Properties of Industrial Materials*, Van Nostrand Reinhold, New York, NY, USA, 1984.
- [11] L. Nitschke, H. Wagner, G. Metzner, A. Wilk, and L. Huber, "Biological treatment of waste water containing glycols from de-icing agents," *Water Research*, vol. 30, no. 3, pp. 644–648, 1996.
- [12] R. Andreozzi, V. Caprio, and A. Insola, "Kinetics and mechanisms of polyethyleneglycol fragmentation by ozone in aqueous solution," *Water Research*, vol. 30, no. 12, pp. 2955–2960, 1996.
- [13] V. Beschkov, G. Bardarska, H. Gulyas, and I. Sekoulov, "Degradation of triethylene glycol dimethyl ether by ozonation combined with UV irradiation or hydrogen peroxide addition," *Water Science and Technology*, vol. 36, no. 2-3, pp. 131–138, 1997.
- [14] B. D. McGinnis, V. D. Adams, and E. J. Middlebrooks, "Degradation of ethylene glycol using Fenton's reagent and UV," *Chemosphere*, vol. 45, no. 1, pp. 101–108, 2001.
- [15] T. Turan-Ertas and M. D. Gurol, "Oxidation of diethylene glycol with ozone and modified Fenton processes," *Chemosphere*, vol. 47, no. 3, pp. 293–301, 2002.
- [16] D. Klauson, S. Preis, E. Portjanskaja, A. Kachina, M. Krichevskaya, and J. Kallas, "The influence of ferrous/ferric ions on the efficiency of photocatalytic oxidation of pollutants in groundwater," *Environmental Technology*, vol. 26, no. 6, pp. 653–662, 2005.
- [17] L. Clesceri, A. Greenberg, and R. Trussell, Eds., *Standard Methods for the Examination of Water and Wastewater*, APHA-AWWA-WPCF, Washington, DC, USA, 17th edition, 1989.
- [18] R. Pohloudeck-Fabini and T. Beyrich, *Organische Analyse (Organic Analysis)*, Akademische Verlagsgesellschaft Geest & Portig K.-G., Leipzig, Germany, 1975.
- [19] C. Catastini, M. Sarakha, G. Mailhot, and M. Bolte, "Iron (III) aquacomplexes as effective photocatalysts for the degradation of pesticides in homogeneous aqueous solutions," *Science of the Total Environment*, vol. 298, no. 1–3, pp. 219–228, 2002.
- [20] D. Bahnemann, "Photocatalytic water treatment: solar energy applications," *Solar Energy*, vol. 77, no. 5, pp. 445–459, 2004.
- [21] N. Takahashi, "Ozonation of several organic compounds having low molecular weight under ultraviolet irradiation," *Ozone: Science and Engineering*, vol. 12, no. 1, pp. 1–17, 1990.
- [22] V. Brezová, Š. Vodný, M. Veselý, M. Čeppan, and L. Lapčík, "Photocatalytic oxidation of 2-ethoxyethanol in a water suspension of titanium dioxide," *Journal of Photochemistry and Photobiology A: Chemistry*, vol. 56, no. 1, pp. 125–134, 1991.
- [23] D. Klauson and S. Preis, "The influence of ferrous ions on the efficiency of aqueous photocatalytic oxidation of 2-ethoxy ethanol," *International Journal of Photoenergy*, vol. 7, no. 4, pp. 175–180, 2005.

Article IV:

Klauson, D., Portjanskaja, E., Preis, S., Visible light-assisted photocatalytic oxidation of organic pollutants using nitrogen-doped titania. *Environmental Chemistry Letters*, 2008, 6 (1), pp. 35-39.

Visible light-assisted photocatalytic oxidation of organic pollutants using nitrogen-doped titania

D. Klauson · E. Portjanskaja · S. Preis

Received: 16 February 2007 / Accepted: 18 April 2007 / Published online: 15 May 2007
© Springer-Verlag 2007

Abstract An experimental research into the aqueous photocatalytic oxidation (PCO) of organic groundwater pollutants, methyl-*tert*-butyl ether (MTBE), *tert*-butyl alcohol, phenol, humic substances, 2-ethoxy ethanol and ethylene glycol was undertaken using visible light-sensitive nitrogen-doped titanium dioxide photocatalysts. Nitrogen-doped titania proved to be an effective photocatalyst for MTBE with its action comparable to and even surpassing that of Degussa P25. In contrast, with the other substances the photocatalysts showed negligible activity. This difference was explained by the poor adsorption properties of N-doped catalysts. The predominance of different PCO mechanisms dependent of the surface properties of N-TiO₂ catalysts was elucidated.

Keywords Nitrogen-doped titania · Methyl *tert*-butyl ether (MTBE) · *tert*-Butyl alcohol (TBA)

Introduction

The present research was focused on the aqueous photocatalytic degradation of organic groundwater pollutants, such as methyl *tert*-butyl ether (MTBE; CH₃-O-C(CH₃)₃), *tert*-butyl alcohol (TBA; HO-C(CH₃)₃), phenol, humic

substances (HS), 2-ethoxy ethanol (2-EE; CH₂-CH₂-O-CH₂-CH₂-OH) and ethylene glycol (EG; HO-CH₂-CH₂-OH), using nitrogen-doped titanium dioxide as a photocatalyst that can utilise visible light.

Methyl *tert*-butyl ether, banned for its use in the USA, is still widely used as an oxygenated component of motor fuels by the rest of the world. This substance is of particular concern because of its accumulation in groundwater due to its low biodegradability (Yeh and Novak 1994). Physical removal and chemical oxidation methods, such as air stripping, activated carbon adsorption, ozonation and treatment with Fenton's reagent have been proven to be ineffective against MTBE (Johnson 1998, Xu et al. 2004; Safarzadeh-Amiri 2001).

Other substances under consideration, 2-EE and EG, are used in multiple applications in industry and transport and also may accumulate in subsurface aquifers. TBA was primarily found as a result of MTBE hydrolysis and thus also enters groundwater as an impurity of MTBE-blended motor fuels (Church et al. 1999). These substances show behaviour similar to that of MTBE towards conventional treatment methods, their photocatalytic oxidation (PCO) proceeds much slower than that of MTBE. Humic substances are also found in groundwater and known for their potential in chelation of heavy metal ions and act as carcinogenic trihalomethanes' precursors during water chlorination. Phenol was tested for its reputation of a standard substance in characterisation of PCO (Serpone et al. 1996).

The PCO of organic pollutants is based on the action of positively charged holes on the semiconductor surface. When subjected to electromagnetic irradiation, the semiconductor's electrons are displaced from the valence band to the conduction band, thus forming positively charged holes, which oxidise the organic pollutant molecules adsorbed on the photocatalyst surface. Also, the decom-

D. Klauson (✉) · E. Portjanskaja
Department of Chemical Engineering,
Tallinn University of Technology,
Ehitajate tee 5, Tallinn 19086, Estonia
e-mail: dklauson@hotmail.com

S. Preis
Department of Chemical Technology,
Lappeenranta University of Technology,
P. O. Box 20, Lappeenranta 53851, Finland

position of water molecules into hydroxyl radicals takes place on the holes.

When using titanium dioxide, one must bear in mind that only in case of ultraviolet irradiation the photons have enough energy to displace the valence band electrons, as the band-gap energy is 3.2 eV, therefore, only 4% of the solar radiation reaching the Earth surface can be utilised. The band-gap can be reduced by introducing additive atoms into titanium dioxide structure, thus, creating a crystalline structure with a misbalance in charge carriers. In case of nitrogen-doped titania, an electron-deficient structure is formed (Reddy et al. 2005), commonly described as *p*-type semiconductor, i.e. a semiconductor with an excess in positive charge carriers (holes). The holes form an acceptor band inside the band-gap, and at room temperature the electrons of the valence band have enough energy to occupy the acceptor band. The position of the latter depends on the concentration of the doping agent: with growing dopant concentration the acceptor band is shifting towards the conduction band, narrowing the band-gap and making the irradiation energy required to displace the electrons to the conduction band smaller, i.e. the useful wavelength extended to the visible light range.

The authors tested four nitrogen-doped titania visible light-sensitive photocatalysts in PCO of MTBE, TBA, 2-EE, EG and HS as groundwater pollutants, and phenol as the standard pollutant substance. The results were compared to the ones obtained with Degussa P25 titanium dioxide.

Experiments

Two thermostated at 20 ± 1 °C 200-mL simple batch reactors with inner diameter 100 mm (evaporation dishes), aperture $40 \text{ m}^2 \text{ m}^{-3}$, mechanically agitated with magnetic stirrers, were used in PCO experiments: the one used for the PCO was called "active" and the other containing no photocatalyst was called "reference". Both reactors were exposed to the identical experimental conditions. The samples from the active reactor were compared to the reference samples to avoid complications caused by water evaporation. A UV-light source, Phillips 365-nm low pressure luminescent mercury UV-lamp (15 W), was positioned horizontally over the reactors, providing the irradiance of about 0.7 mW cm^{-2} measured at a distance corresponding to the level of the free surface of the reactor by the optical radiometer Micropulse MP100 (Micropulse Technology, UK). With daylight fluorescent lamp (Phillips TL-D 15 W/33–640), the irradiance could not be directly measured. In this case, the illuminance was measured using TES 1332 luxmeter (TES Inc., Taiwan). The illuminance was 3700 lx (lm m^{-2}), which corresponds to the irradiance

of 0.5 mW cm^{-2} . The irradiance was calculated using lumen to watt ratio of 683, as the response of the human eye to the illuminance of 683 lm equals to that to the irradiance of 1 W (Kirkpatrick 2005).

The experiments were carried out using aqueous solutions of the chemicals supplied by Aldrich. The experiments were conducted with synthetic solutions of MTBE (100 mg L^{-1}), TBA (100 mg L^{-1}), phenol (50 mg L^{-1}), HS (10 mg L^{-1}), 2-EE (300 mg L^{-1}) and EG (300 mg L^{-1}). The concentrations of the pollutants were chosen consistently with their practical presence in polluted groundwater and thus experimental conditions applied previously (Krichevskaya et al. 2003). All experiments with EG derivatives were carried out at pH 3.0, adjusted with 4-*N* sulphuric acid: the indifference of these substances towards radical oxidation was established previously and, therefore, the media most beneficial for oxidation with positively charged holes, i.e. acidic, was chosen (Klauson et al. 2005). Experiments with MTBE and phenol sensitive to radical oxidation were also carried out in alkaline media, favourable to OH-radical formation. The pH value in experiments with Degussa P25 in alkaline media tended to decrease slightly; the decrease was compensated thoroughly with the addition of alkali. The treatment time was 2 h in case of MTBE, 4 h in case of TBA and 24 h with other substances. The treatment time was chosen to reduce the concentration of pollutants below 50% of the residual concentration and was used in calculations of the process efficiency *E* (see Eq. 1). All the experiments were carried out for at least three times under identical experimental conditions to derive the average value of the process efficiency. The average deviation of data in parallel experiments did not exceed 5%.

The experiments were performed using photocatalyst suspension with the concentration of 1 g L^{-1} . Titanium dioxide Degussa P25 and four nitrogen-doped catalysts synthesised on course of the research were used. Two N-doped catalysts were produced by the addition of 25 mL of aqueous solution containing 11.65 g of carbamide to 33 mL of tetrabutyl orthotitanate under constant stirring. The acquired product of hydrolysis was then dried and heated in a furnace at 400 °C. The calculated titanium to nitrogen molar ratio of the catalyst was 1:2. The cerium-containing catalyst was synthesised in a similar way, except the addition of 5 ml of ammonium cerium nitrate solution containing 200 L^{-1} in 4-*N* nitric acid. Titanium to nitrogen to cerium molar ratio was 53:120:1. Another two nitrogen-doped catalysts were synthesised by the methods described by Wang et al. (2005) and Aditi and Fernandes (2005). With these substances, calculated titanium to nitrogen ratio was 1:2.3 and 1:5, respectively.

The specific area (BET and Langmuir adsorption) and the pore volume of the catalysts were measured by the

Table 1 Surface characteristics of photocatalysts

The catalyst	BET surface area, m ² g ⁻¹	Langmuir surface area, m ² g ⁻¹	Micropore volume, mm ³ g ⁻¹
Degussa P25	49.9	67.6	2.2
N-doped TiO ₂	113.9	155.8	0
N–Ce-doped TiO ₂	156.4	213.3	0
N-doped TiO ₂ (Aditi and Fernandes 2005)	46.9	63.5	2.7
N-doped TiO ₂ (Wang et al. 2005)	127.4	174.8	0

adsorption of nitrogen using KELVIN 1042 sorptometer. The results of the measurements are presented in Table 1.

The decrease in the oxygenated hydrocarbon pollutant concentration was determined from the decrease in chemical oxygen demand (COD), measured by a standard method. COD was proved to be a universal parameter, unlike TOC, decreasing with the increasing conversion degree in oxidation reactions. Phenol was determined by the nitroaniline colorimetric method with p-nitroaniline to the 100-mL sample of treated solution 2 mL of 5% sodium carbonate and 4 mL of p-nitroaniline were added; after 15 min of the reaction the optical density at 570 nm was measured (Clesceri et al. 1989). Humic substances were determined by their absorbance at 254 nm (Clesceri et al. 1989).

Adsorption experiments with 2-EE, TBA, MTBE, HS and phenol on the photocatalyst surface were carried out at pH 3.0 in closed flasks thermostated at 20 ± 1 °C and equipped with magnetic stirrers. The adsorbed amount of substances was derived from the batch mass balance; the concentration of the dissolved substance was determined before and after adsorption.

To compare the hydrophilicities of photocatalysts the water adsorption was roughly estimated as follows. Weighed catalyst samples were dried at 105 °C to the constant mass, cooled in a desiccator and placed to 20% relative humidity at 20 °C. The tests were carried out under the daylight. Degussa P25 was also irradiated with the 365-nm UV to improve its hydrophilicity (Fujishima et al. 2000). The amount of adsorbed water was derived from the masses of dry and humidified catalysts.

Results and discussion

The performance of PCO with artificial radiation sources was characterised by the process efficiency *E*. The efficiency *E* is defined as the decrease in the amount of pollutants divided by the amount of energy reaching the surface of the treated sample (Eq. 1). The values of the

efficiency were calculated after a period of time equal to the treatment time.

$$E = \frac{\Delta c \cdot V \cdot 1,000}{I \cdot s \cdot t}, \tag{1}$$

where *E* is the PCO efficiency (mg O W⁻¹ h⁻¹); Δ*c* is the decrease in the pollutant's concentration (mg O L⁻¹) measured as COD; *V*, the volume of the sample to be treated (L); *I*, irradiance (mW cm⁻²); *s*, irradiated area (cm²); *t*, treatment time (h).

With 2-EE and EG, no degradation was noticed within the limits of analytical precision with N-doped photocatalysts of all tested kinds neither with UV-irradiation nor with visible light, although these substances were successfully oxidised on Degussa P25 (Klauson et al. 2005). Phenol and HS were degraded under the visible light in the suspensions of the photocatalyst synthesised according to Aditi and Fernandes (2005) for 9 and 13%, respectively. The result with suspended Degussa P25 with phenol was far more advanced; phenol was practically completely removed in the reference experiments under the described experimental conditions. Humic substances also readily yielded to PCO on the attached Degussa P25 surface under UV-radiation (Portjanskaja et al. 2004). The N-doped catalysts thus exhibited poor photocatalytic properties in respect to these compounds. Differently, TBA was better oxidised on N-doped TiO₂, the calculated efficiency was about 44 mg O W⁻¹ h⁻¹ in visible light range, which was similar to that on UV-irradiated Degussa P25—33 mg O W⁻¹ h⁻¹.

With MTBE, on the other hand, the N-doped catalysts showed high activity. With ultraviolet irradiation, the PCO efficiency of MTBE on doped catalysts was comparable to that achieved with Degussa P25 (see Table 2). In the PCO experiments using visible light, the activity of the N-doped catalysts was also significant; the decrease in COD in visible light was similar to that observed with UV-irradiation

Table 2 The PCO efficiency for MTBE with N-doped catalysts under UV-radiation compared to Degussa P25

The catalyst	The PCO efficiency <i>E</i> , mg O W ⁻¹ h ⁻¹	
	UV 365 nm	Visible light
Degussa P25	170 ± 5	–
N-doped TiO ₂ , Ti:N = 1:2	183 ± 8	177 ± 8
N–Ce-doped TiO ₂ Ti:N:Ce = 53:120:1	177 ± 6	188 ± 8
N-doped TiO ₂ , Ti:N = 1:5 (Aditi and Fernandes 2005)	200 ± 10	250 ± 10
N-doped TiO ₂ , Ti:N = 1:2.3 (Wang et al. 2005)	150 ± 5	160 ± 6

(Table 2). The best performance was shown by the photocatalyst with the highest content of the doping agent.

When comparing the PCO results with catalyst surface characteristics, one can notice no correlation between the performance of the catalyst and its specific area. The best results were obtained with N-TiO₂ prepared as suggested by Aditi and Fernandes (2005) having specific area and the volume of micropores similar to those of Degussa P25. In spite of the two to three times bigger specific area, the other catalysts showed lower PCO efficiency with MTBE (see Tables 1 and 2). Cerium did not appear to show any significant effect to the performance of the photocatalyst, its theoretical Ti:N molar ratio was similar to that of two other photocatalysts, and so was the performance.

The difference in the behaviour of the substances under consideration in PCO with the modified catalysts can be explained by the difference in both oxidation mechanism and adsorption properties of the substances. 2-Ethoxy ethanol and EG have been proven by earlier studies to be oxidised only on positively charged TiO₂-holes being rather immune towards radical oxidation, thus making adsorption a crucial factor in the PCO (Krichevskaya et al. 2003). On the other hand, MTBE and phenol can be oxidised by both holes and radicals, although these substances behave differently in PCO; MTBE is readily oxidised, whereas phenol yields poorly to PCO on N-TiO₂. Humic substances and TBA have been proven to act as radical scavengers; however, they yielded, although poorly, to the PCO on N-TiO₂ under visible light; TBA PCO efficiency exceeded the one of phenol for over 50 times.

The difference in PCO performance of N-TiO₂ catalysts with MTBE and TBA on one side, and phenol, HS and glycols on another side cannot be explained by the difference in the adsorption on the catalysts. The adsorption experiments with MTBE, TBA, HS, phenol and 2-EE on N-TiO₂ catalysts were carried out, in which no adsorption was observed above the limits of analytical precision. This fact explains zero PCO efficiency for glycolic compounds; no oxidation with positively charged holes is available. The zero adsorption with a good PCO performance with MTBE and TBA indicates the prevailing radical oxidation. The predominance of radical reactions in PCO of MTBE was confirmed in the experiment, in which sodium carbonate, the renowned radical scavenger, was added in amount of 20 g L⁻¹; the PCO efficiency of MTBE under visible light has drastically fallen from 189 to 16 mg O W⁻¹ h⁻¹ at pH 11.6.

However, phenol and HS should also be oxidised with OH-radicals. Their poor PCO efficiency in contrast to MTBE and TBA cannot be explained by the difference in hydrophyllicities of the catalysts. The rough estimation of the catalysts' affinity to water showed that N-doped catalysts, with one exception, exhibited about ten times higher hydrophyllicity than UV-irradiated Degussa P25 under

identical conditions. The catalyst by Aditi and Fernandes (2005), which demonstrated the best PCO performance with MTBE, was close to Degussa P25 in its affinity to water vapours.

The authors suggest that the selective PCO of MTBE and TBA could be explained by the *tert*-butyl radical in the molecular structure of these substances. Under conditions of protonated media, the surface of the catalysts is protonated, so are the molecules of phenol and HS, being electrostatically repelled from the surface. The MTBE molecule may remain, however, electrically neutral and the TBA molecule protonation may have a smaller repelling effect due to the large neutral *tert*-butyl radical. Therefore, these molecules, although not adsorbed, may approach the N-doped photocatalyst's surface close enough to react with OH-radicals more actively than phenol and HS. The surface of Degussa P25 is also protonated in acidic media, however, the adsorption of all compounds under consideration is significant, which results in a high PCO efficiency.

Conclusions

Several nitrogen-doped titanium dioxide modifications have been experimentally proven to be effective catalysts for visible-light PCO of the motor fuel additive MTBE and TBA, surpassing the performance of commercial catalyst Degussa P25 working under UV radiation. However, the PCO of 2-EE, EG, HS and phenol, did not proceed effectively. The authors find the explanation for this difference in the poor adsorption on the N-doped catalysts of all substances under consideration. Therefore, the oxidation on the N-doped photocatalysts takes place mostly with OH-radicals, which explains zero oxidation of glycolic substances. Poor oxidation of phenol and HS in contrast to the good one of MTBE and TBA is presumably explained by the electrically neutral *tert*-butyl radical in the molecular structure of latter compounds, diminishing the effect of protonation and repulsion from the catalyst's surface and, thus, enhancing radical oxidation.

Acknowledgements The authors express their gratitude to Ms. Mai Uibu, M.Sc., the Research Scientist of the Laboratory of Inorganic Materials of Tallinn University of Technology for her generous assistance in BET measurements. The gratitude for the financial support is expressed to the Estonian Science Foundation (grant 5899) and the Academy of Finland (programme "Russia in Flux", project 208134).

References

- Aditi RG, Fernandes JB (2005) A simple method to synthesize N-doped butyl titania with enhanced photocatalytic activity in sunlight. *J Solid State Chem* 178:2953–2957

- Church CD, Pankow JF, Tratnyek PG (1999) Hydrolysis of tert-butyl formate: kinetics, products, and implications for the environmental impact of methyl tert-butyl ether. *Environ Toxicol Chem* 18:2789–2796
- Clesceri LS, Greenberg AE, Trussel RR (1989) Standard methods for the examination of water and wastewater, 17th edn. APHA, AWWA, WPCF, Washington DC
- Fujishima A, Rao NT, Tryk DA (2000) Titanium dioxide photocatalysis. *J Photochem Photobiol C Photochem* 1:1–21
- Johnson P (1998) Assessment of the contribution of volatilization and biodegradation to in situ air sparging performance. *Environ Sci Technol* 32:276–281
- Kirkpatrick SJ (2005) A primer on radiometry. *Dent Mater* 21:21–26
- Klauson D, Preis S, Portjanskaja E, Kachina A, Krichevskaya M, Kallas J (2005) The influence of ferrous/ferric ions on the aqueous photocatalytic oxidation of pollutants in groundwater. *Environ Technol* 26:653–661
- Krichevskaya M, Kachina A, Malygina T, Preis S, Kallas J (2003) Photocatalytic oxidation of fuel oxygenated additives in aqueous solutions. *Int J Photoenergy* 5:81–86
- Portjanskaja E, Krichevskaya M, Preis S, Kallas J (2004) Photocatalytic oxidation of humic substances with TiO₂-coated glass micro-spheres. *Environ Chem Lett* 2:123–127. doi:10.1007/s10311-004-0078-3
- Reddy KM, Baruwati B, Jayalakshmi M., Rao MM, Manorama SV (2005) S-, N- and C-doped titanium dioxide nanoparticles: synthesis, characterization and redox charge transfer study. *J Solid State Chem* 178:3352–3358
- Safarzadeh-Amiri A (2001) O₃/H₂O₂ treatment of methyl-*tert*-butyl ether (MTBE) in contaminated waters. *Wat Res* 35:3706–3714
- Serpone N, Sauve G, Koch R, Tahiri H, Pichat P, Piccinini P, Pelizzetti E, Hidaka H (1996) Standardization protocol of process efficiencies and activation parameters in heterogeneous photocatalysis: relative photonic efficiencies $\zeta(r)$. *J Photochem Photobiol A Chem* 94:191–203
- Wang Z, Cai W, Hong X, Zhao X, Xu F, Cai C (2005) Photocatalytic degradation of phenol in aqueous nitrogen-doped TiO₂ suspensions with various light sources. *Appl Catal B Environ* 57:223–231
- Xu XR, Zhao ZX, Li XY, Gu JP (2004) Chemical oxidative degradation of methyl-*tert*-butyl ether in aqueous solution by Fenton's reagent. *Chemosphere* 55:73–79
- Yeh CK, Novak JT (1994) Anaerobic degradation of gasoline oxygenates in solids. *Wat Environ Res* 66:744–752

Article V:

Klauson D, Babkina J., Stepanova K., Krichevskaya M., Preis S., Aqueous photocatalytic oxidation of amoxicillin. *Catalysis Today*, 2010, in press, doi: 10.1016/j.cattod.2010.01.015



Contents lists available at ScienceDirect

Catalysis Today

journal homepage: www.elsevier.com/locate/cattod



Aqueous photocatalytic oxidation of amoxicillin

D. Klauson^{a,*}, J. Babkina^{a,1}, K. Stepanova^{a,1}, M. Krichevskaya^{a,1}, S. Preis^b

^a Department of Chemical Engineering, Tallinn University of Technology, Ehitajate tee 5, 19086 Tallinn, Estonia

^b Department of Chemical Engineering, Lappeenranta University of Technology, P.O. Box 20, 53851 Lappeenranta, Finland

ARTICLE INFO

Article history:
Available online xxx

Keywords:
Photocatalytic oxidation
Amoxicillin
Doped titania
Reaction pathway

ABSTRACT

Aqueous photocatalytic oxidation (PCO) of amoxicillin (AMO), a β -lactam antibiotic, was experimentally studied. Degussa P25 titanium dioxide and visible light-sensitive sol-gel synthesized carbon- and iron-doped titania were used as photocatalysts. The efficiency of PCO dependent on initial AMO concentration and pH was established. A number of organic and inorganic by-products were determined allowing construction of a possible reaction pathway.

© 2010 Elsevier B.V. All rights reserved.

1. Introduction

For the last years the interest towards the fate of medicines, especially antibiotics, has been arising. Being refractory substances [1–3], antibiotics pass the biological treatment plants intact [4], either remaining in the liquid phase or, dependent on their hydrophilicity, adsorbing to the active sludge with subsequent desorption to the environment [5]. These substances in the environment are potent in the damage of micro-flora and fauna, accumulate in food chains [6,7], and accelerate the development of resistant micro-organisms, including pathogens [8–11]. The accumulation of antibiotics in organisms may cause arthropathy, nephropathy, damages in central nervous system and spermatogenesis, mutagenic effects and light sensitivity [2].

One of the most widely used antibiotics is amoxicillin (AMO), (2S, 5R, 6R)-6-[[[(2R)-2-amino-2-(4-hydroxyphenyl)-acetyl]amino]-3,3-dimethyl-7-oxo-4-thia-1-azabicyclo[3.2.0] heptane-2-carboxylic acid, see Fig. 1), a moderate-spectrum bacteriolytic β -lactam antibiotic. There are only a few works dealing with the advanced oxidation processes (AOPs) application to the AMO degradation: Fenton oxidation [12–14] and photocatalytic oxidation (PCO) with Fluka anatase [15]. The elucidation of the AMO PCO reaction pathway makes the novelty of the present research, since the published works on the AOPs of antibiotics mainly focus on the parent compound removal and mineralization, leaving the degradation by-products unexplored.

Photocatalytic oxidation is one of AOPs based on the action of positively charged holes on the surface of illuminated semiconductor, most often titanium dioxide. Water molecules decompose on the holes to form powerful hydroxyl radicals [16]; the hole itself also can degrade the pollutant having even higher oxidation potential [17]. The electrons, excited by the UV-irradiation, also participate in the PCO, reducing dissolved oxygen resulting in the formation of other radical oxidants. The ratio of radical to hole oxidation reactions depends on the properties of the substance to be degraded. Many substances may be degraded by both mechanisms simultaneously, e.g. [18–20].

Although commercial photocatalysts, such as Degussa P25 titanium dioxide, exhibit a good performance, they can use only a small ultraviolet fraction (4%) of solar radiation reaching the earth surface due to the high energy of its band-gap [21]. This makes sensitising TiO₂-based photocatalysts to visible light the potential way of widening of utilised solar spectrum. For this purpose, titanium dioxide can be doped with various metals or non-metals, which can effectively reduce the band-gap [22–28] for excitation of electrons by lower energy photons at greater wavelength up to 540 nm as reported. However, the authors found earlier that the doped titania photocatalysts may, unlike “universal” P25, oxidise only selected pollutants [29]. This can be explained by the smaller redox potential and, possibly, faster electron-hole recombination of the catalysts with smaller band-gap [30].

2. Materials and methods

Two thermostatted at 20 ± 1 °C 200-ml batch reactors with inner diameter 100 mm (evaporation dishes), irradiated contact surface 40 m²/m³, agitated with magnetic stirrers, were used in PCO experiments: the one used for the PCO was called “active” and the

* Corresponding author. Tel.: +372 620 2857; fax: +372 620 2856.

E-mail address: deniss.klauson@ttu.ee (D. Klauson).

¹ Tel.: +372 620 2857; fax: +372 620 2856.

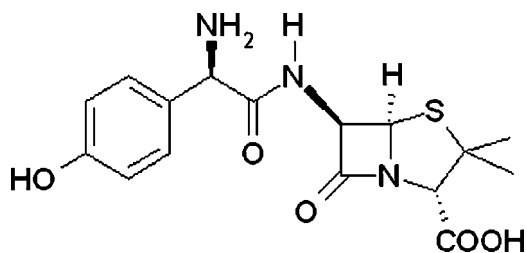


Fig. 1. Amoxicillin (AMO) molecule.

other containing no photocatalyst was called “reference”. Both reactors were exposed to the identical experimental conditions. The samples from the active reactor were compared to the reference samples to avoid complications caused by water evaporation. An artificial UV-light source, Phillips 365-nm low pressure luminescent mercury UV-lamp (15 W), was positioned horizontally over the reactors, providing the irradiance of about 0.5 mW/cm² measured at a distance corresponding to the level of the surface of the reactor by the optical radiometer Micropulse MP100 (Micropulse Technology, UK). With artificial daylight fluorescent lamp (Phillips TL-D 15W/33-640), the irradiance could not be directly measured. The illuminance was measured using TES 1332 luxmeter (TES Inc., Taiwan) reaching 3700 lx (lm/m²), which corresponds to the irradiance of 0.6 mW/cm². The irradiance was calculated using lumen to watt ratio of 684, as the response of the human eye to the illuminance of 684 lm equals to that to the irradiance of 1 W [31]. With AMO PCO experiments were conducted outdoors using natural solar radiation; the irradiance was measured by luxmeter approximating 16 mW/cm².

Titanium dioxide was used as 1 g/l slurry. The experiments were carried out with aqueous solutions of AMO supplied by Sigma–Aldrich. In the experiments, the initial concentration of AMO varied between 1 and 100 mg/l. The influence of the initial pH was studied in the range from 3 to 9, adjusted by 4N sulphuric acid or 15% sodium hydroxide. At pH higher than 9 the slurry became stable with no chance to separate it by centrifugation or filtration, making the measurements impossible. The pH was monitored throughout the experiments without adjustment. The treatment time was chosen to be 6 h under artificial light of the UV and vis lamps, and 2 h under natural solar radiation: the results in conversion degrees are reported for these times.

All the experiments were carried out for at least three times under identical experimental conditions. The average deviation of data in parallel experiments did not exceed 5%.

Amoxicillin concentration was determined photometrically, using the light absorbance at 230 nm, using Helios β spectrophotometer. Chemical oxygen demand (COD) was determined by a standard dichromate method [32], using HACH kits LCK 314 (15–150 mg O/l) and LCK 414 (5–60 mg O/l). The concentration of ammonium ion was determined photometrically using a modified version of a standard phenate method [32]. Nitrate and sulphate anions were determined using Metrohm 761 Compact IC ionic chromatograph. A Waters Aquity UPLC combined with MS and quadrupole-time of flight (Q-TOF) mass-analyzer was used for the determination of organic AMO PCO by-products. An Aquity UPLC BEH C₁₈ 1.7 μm 2.1 mm × 100 mm column was used, with water and 0.1% formic acid as eluent A (initial eluent) and acetonitrile with 0.1% formic acid as eluent B. The complete change from eluent A to B was achieved in 15 min out of 20 min run with linear gradient used. Mass spectra were acquired in a full scan mode (50–500 amu). The instrument was operated in positive ion mode, with capillary voltage of 2400 V. The mass spectrometry data was handled using MassLynx software.

The accuracy of UV-absorbance in AMO concentration measurements was checked by the parallel determination of AMO in

MS analysis of the PCO-treated samples with the AMO pre-constructed calibration curves for both methods: the difference observed between AMO concentrations determined by UV-absorbance and MS did not exceed 2% at highest, suggesting negligible amounts of UV-absorbance by PCO by-products. For this reason, the UV-absorbance was used as a simpler and less time- and resource-consuming approach than MS. It was noted that the UV-absorbance spectra of PCO-treated solutions did not exhibit a change in shape, showing no new peaks or a wavelength shift in maximum absorbance. Poor accumulation of UV-absorbing PCO by-products may be explained by their oxidation rates being comparable to or exceeding those of AMO. A similar analytical approach has been used in oxidation studies with other antibiotics of aromatic structure, such as sulphamethazine [33], chloramphenicol [11], and flumequine [34].

Adsorption experiments were carried out in closed thermostated flasks equipped with magnetic stirrers at 20 ± 1 °C. The amount of adsorbed substance was derived from the batch mass balance: the concentration of the dissolved substance was determined before and after adsorption. The adsorption equilibrium was experimentally determined to be reached in 6 h. In order to determine AMO concentration in the adsorption experiments, the UV-absorbance was used.

Six specimens of carbon-doped titania were obtained by the hydrolysis of tetrabutyl orthotitanate at room temperature without adjustment of pH being around 5.5–6.0, followed by drying and calcination at different temperatures (200–700 °C). Five iron-doped titania catalysts with calculated iron content from 0.42 to 3 at.% were prepared by the pulverisation of 75 ml of tetrabutyl orthotitanate into 1 l pre-sonicated Fe₂O₃ suspensions of various concentrations (0.1–0.7 g/l); the hydrolysis was followed by sonication, drying and calcination at 200 °C. After calcinations, all the catalysts were washed with hot (70–80 °C) distilled water applied in a sequence of 10–15 rinsing rounds (ca. 1 l per 1 g of catalyst) in order to clean the catalyst surface from water-soluble compounds.

The crystallinity of carbon-doped titania was analyzed using D5000 Kristalloflex, Siemens (Cu-Kα irradiation source) X-ray diffraction spectroscopy (XRD). Carbon content was measured with PHI 5600 X-ray photoelectron spectroscopy. The specific area (BET and Langmuir adsorption) and the pore volume of the catalysts were measured by the adsorption of nitrogen using KELVIN 1042 sorptometer.

3. Results and discussion

3.1. PCO experiments with Degussa P25

The results of AMO PCO were expressed in its concentration decrease rate and the PCO efficiency, *E*, defined as the decrease in the amount of the pollutant divided by the amount of energy reaching the surface of the treated sample. The efficiency is calculated according to the following equation [35]:

$$E = \frac{\Delta c \times V \times 1000}{I \times S \times t} \quad (1)$$

where *E*, PCO efficiency, mg/(Wh); Δ*c*, the decrease in the pollutant's concentration, mg/l, or COD, mg O/l; *V*, the volume of the sample to be treated, l (in this case, 0.2 l); *I*, irradiance, mW/cm²; *S*, irradiated area, cm²; *t*, treatment time, h.

The best performance was observed at pH 6.0, occurring naturally in the AMO solutions, followed by alkaline and acidic media. The dependence of AMO conversion *x* on its initial concentration from 1 to 100 mg/l may be seen in Fig. 2. The increase in conversion at smaller concentrations reaches its peak at approximately 10–25 mg/l (dependent on pH), and is followed by a

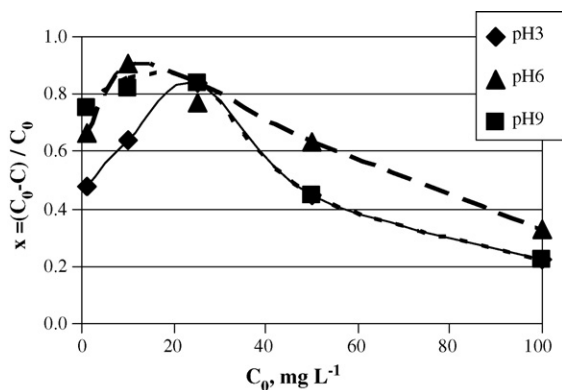


Fig. 2. The dependence of AMO conversion on its initial concentration: artificial UV, 20 °C, treatment time 6 h.

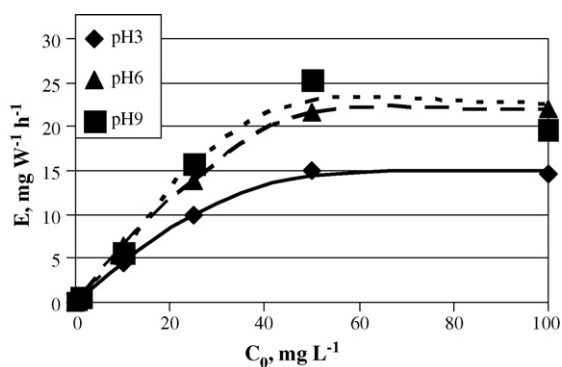


Fig. 3. The dependence of PCO efficiency on the AMO initial concentration: 20 °C.

swift decrease, which may be explained by changes in reaction rate control mechanism: the reaction rate limitation at smaller concentrations, when the active sites on the catalyst surface are only partially occupied by adsorbed AMO molecules, changes to the mass transfer limitation, when all the active sites on the photocatalyst surface are filled at higher AMO concentrations, and a new AMO molecule can be adsorbed only after desorption or complete oxidation of the degradation by-products. Thus, above 20–25 mg/l PCO efficiency and, subsequently, the absolute amount of degraded AMO (see Eq. (1)) remains constant, as one can see from Fig. 3. In the majority of the experiments, COD decrease was between 10 and 40%.

The addition of *tert*-butyl alcohol (TBA) as a radical scavenger to the solution to be treated in the amount equimolar with AMO (0.068 mM, i.e. 25 mg/l of AMO and 5 mg/l of TBA) did not alter the latter's degradation rate, which allows suggesting the dominance of hole reactions: the radical oxidation should be noticeably affected by the presence of TBA.

Since the radical reactions appeared to play a minor role in the PCO of AMO, the adsorption of the latter on the catalyst surface

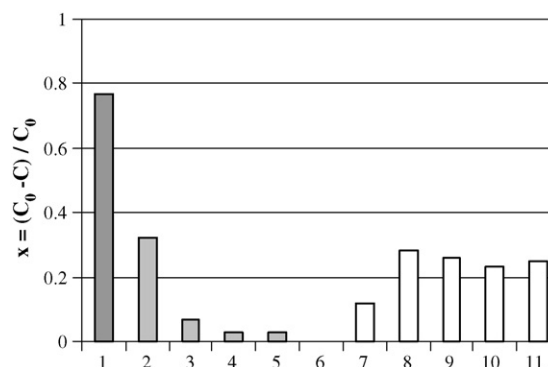


Fig. 4. AMO degradation degree at doped catalysts with visible light in 6-h treatment: 1, P25 with UV; 2, 37 at.% C, 200 °C; 3, 34.9 at.% C, 400 °C; 4, 34.9 at.% C, 500 °C; 5, 30.4 at.% C, 600 °C; 6, 34.7 at.% C, 700 °C; 7, 0.42 at.% Fe; 8, 0.89 at.% Fe; 9, 1.33 at.% Fe; 10, 2.2 at.% Fe; 11, 3.0 at.% Fe; all Fe–TiO₂ samples calcinated at 200 °C; AMO 25 mg/l; pH 6.0.

attracted an interest as a relevant circumstance: the behaviour of the oxidation efficiency consistent with the adsorption may support the hypothesis of the hole oxidation. The adsorption of AMO on TiO₂ was observed to be rather low increasing with concentration growth up to 3.5 mg/g (ca. 0.009 mmol/g) at the AMO concentration of about 100 mg/l. Judging from the PCO results fitting well to the Langmuir–Hinshelwood description (Section 3.1, Figs. 2 and 3), the adsorption of AMO fits well to the PCO performance: in the studied concentration range, the adsorption of AMO on the Degussa P25 may be adequately described by both Langmuir ($R^2 = 0.9538$) and Freundlich ($R^2 = 0.9912$) equations (Eqs. (2) and (3)), derived from the adsorption experiments data:

$$q_L = 0.011 \times \frac{15.979 \times c}{1 + 15.979 \times c} \quad (2)$$

$$q_{Fr} = 0.0145 \times c^{0.3437} \quad (3)$$

where AMO adsorption q is in mmol/g, and its concentration c is in mM.

3.2. PCO experiments with carbon- and iron-doped titania

The parameters of carbon-doped catalysts can be seen in Table 1. Under artificial visible light these catalysts showed AMO conversion around 30% at 25 mg/l (pH 6.0), whereas Degussa P25 under UV of similar intensity showed almost 80%. The best catalytic performance was achieved with the highest carbon content. AMO conversion decreased significantly with decreasing carbon content (see Fig. 4). The AMO conversion degree with iron-doped titania increased from 12 to 25% with iron content growing from 0.42 to 0.89 at.% (Fig. 4), remaining more or less unchanged with increasing iron content. The COD decrease was with doped catalysts around 10–30%. Adsorption experiments were also undertaken with doped titania samples. They showed very low

Table 1
The parameters of carbon-doped titania photocatalysts.

Calcination T, °C	Crystallographic composition, %			Composition, at. %			S_{BET} , m ² /g	S_{Langmuir} , m ² /g	Micropore area, m ² /g	Micropore volume, mm ³ /g
	Anatase	Brookite	Rutile	Ti	O	C				
200	71.9	28.1	–	17.2	45.8	37.0	202.3	278.9	0	0
400	78.1	21.9	–	18.1	46.6	34.9	105.7	144.7	4.12	1.54
500	76.9	18.2	5.0	18.5	46.6	34.9	39.45	53.85	3.95	1.39
600	74.4	25.6	–	20.0	49.6	30.4	8.81	12.08	0	0
700	–	–	100	18.0	47.3	34.7	3.52	4.81	0.20	0.07

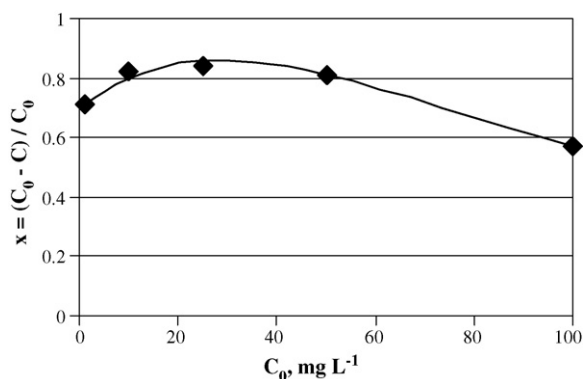


Fig. 5. AMO conversion vs. its initial concentration with Degussa P25 under solar radiation: pH 6.0, 20 °C, treatment time 2 h.

adsorption of AMO on their surface not exceeding the limits of analytical precision.

3.3. Solar PCO experiments

Amoxicillin degradation with Degussa P25 under solar radiation proceeded about three times faster than under artificial UV (Fig. 5). Since carbon-doped catalysts showed insufficient performance, only the most effective catalyst with the highest carbon content (37 at.% C, 200 °C) and iron-doped photocatalysts were used in solar PCO experiments, with which the AMO degradation proceeded also faster than with artificial light: the performance of doped catalysts was moderately inferior to that of P25 (Fig. 6). The disproportional improvement of oxidation rates, about three times for Degussa P25 and about seven times for the doped catalysts, may be explained by the difference in the

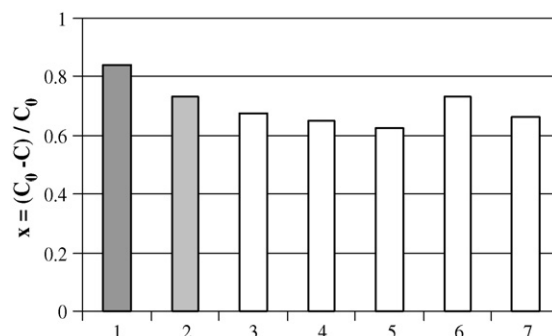


Fig. 6. AMO degradation degree at doped catalysts with solar light in 2-h treatment: 1, P25; 2, 37 at.% C; 3, 0.42 at.% Fe; 4, 0.89 at.% Fe; 5, 1.33 at.% Fe; 6, 2.2 at.% Fe; 7, 3.0 at.% Fe; AMO 25 mg/l, pH 6.0.

irradiance with UV and visible light in solar spectrum: the intensity of radiation in solar spectrum grows dramatically with increasing wavelength from 300 to 500 nm, whereas the experiments with lamps were carried out under similar irradiance conditions.

3.4. Amoxicillin PCO by-products and reaction pathway

Ammonia, nitrate and sulphate were detected in small amounts as the AMO PCO inorganic products indicating the most of nitrogen and sulphur remaining in organic by-products: nitrogen mineralized to 1.5% and sulphur to 14% extent. The COD reduction was also observed to be within 10–30% thus making the mineralization idea offered. A number of organic by-products were determined qualitatively using UPLC coupled with ESI-MS. The degradation by-products were determined for AMO concentration ranges

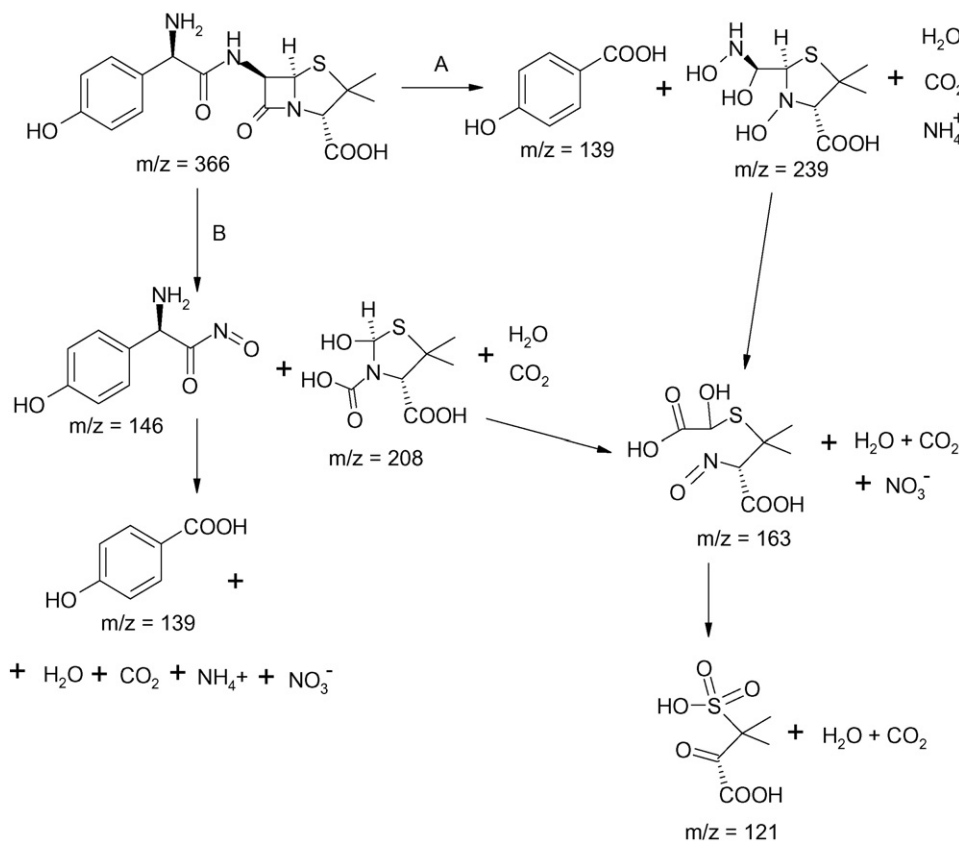


Fig. 7. PCO reaction pathway at AMO concentration of 10 mg/l (kinetic reaction rate control): pH 6.0, 20 °C.

corresponding with the different reaction rate controlling phenomena: reaction kinetics at 10 mg/l, transitional rate at 25 mg/l and mass transfer at 100 mg/l at starting pH 6.0. The organic by-products identified were somewhat different in those cases, although some were common for all the concentrations.

Judging from the identified by-products, the following reaction pathways for AMO PCO may be proposed. Under kinetics rate control at 10 mg/l (Fig. 7), the reaction has two clearly observable pathways, where AMO molecule is cleaved initially with the release of *p*-hydroxybenzoic acid ($m/z = 139$, pathway A) or of a more complex compound ($m/z = 146$, pathway B), with its subsequent degradation to a product with $m/z = 121$. In transitional reaction at 25 mg/l (Fig. 8), also, two separate reaction pathways may be proposed. The first one (Fig. 8, A) is initiated by AMO molecule fragmentation at the peptide bond that is closer to the aromatic cycle, forming *p*-hydroxybenzoic acid ($m/z = 139$) and

a bicyclic lactamic product with $m/z = 160$. The latter is subsequently degraded into an open-chain structure ($m/z = 114$), which was the ultimate AMO PCO by-product detected in this instance. The other pathway (Fig. 8, B) begins with the destruction of lactamic bond and is then followed by the destruction of the same peptide bond as in the first stage of pathway A. In the mass transfer-controlled reaction at 100 mg/l (Fig. 9), there are four possible reaction pathways detected: the first one (Fig. 9, A) is initiated by the AMO molecule cleavage, whereas the other one (Fig. 9, B) appears to begin with the break-away of the primary amino group and its subsequent replacement with the oxygen atom ($m/z = 365$). The pathway C is similar to A, however, the lactamic group remains intact after the initial molecule break-up. Pathway D is initiated by the hydroxylation of the aromatic cycle. Interesting is the increased number of different reaction pathways in the mass transfer-controlled reaction: since the AMO molecules

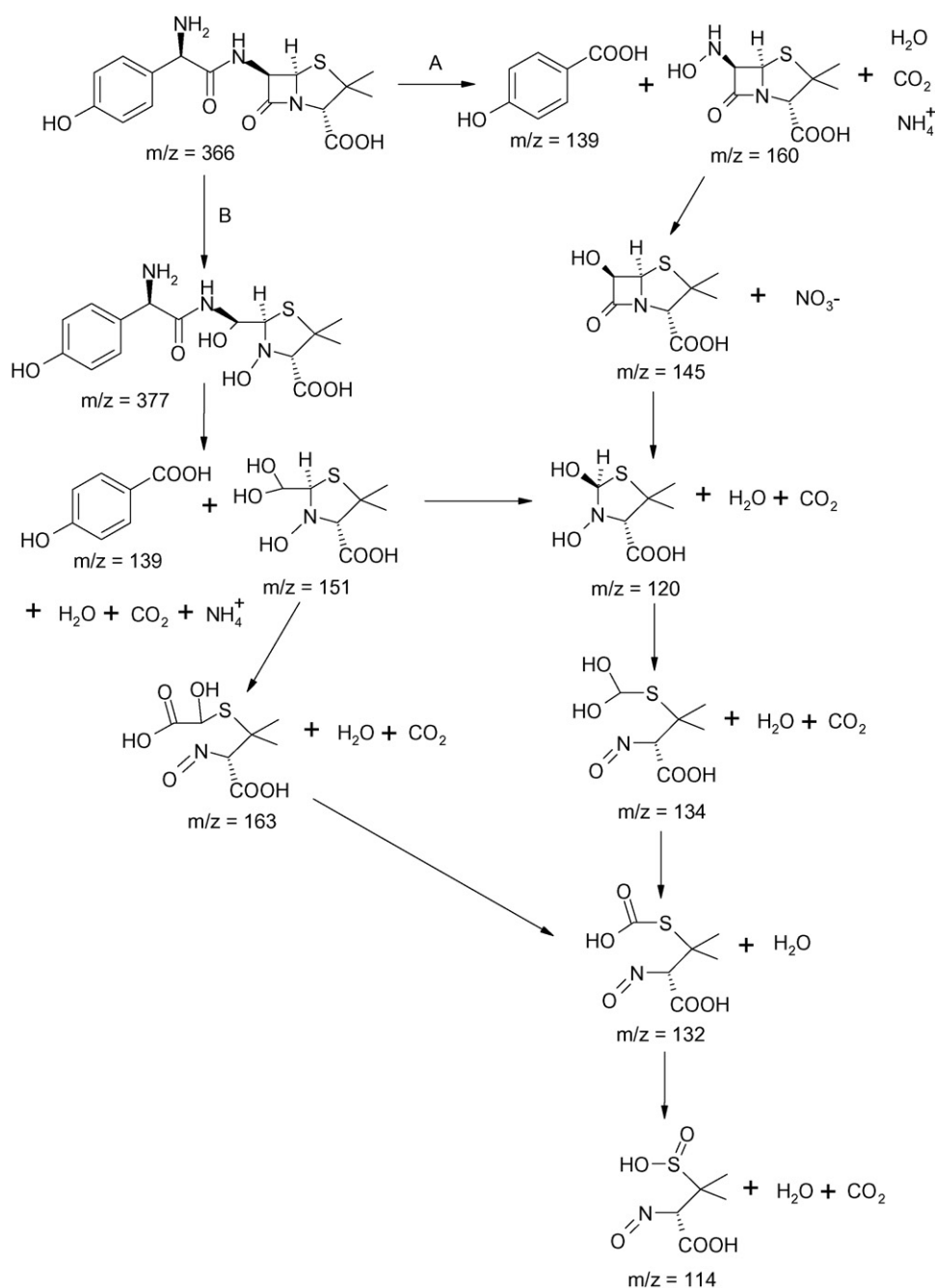


Fig. 8. PCO reaction pathway at AMO concentration of 25 mg/l (transition reaction rate control): pH 6.0, 20 °C.

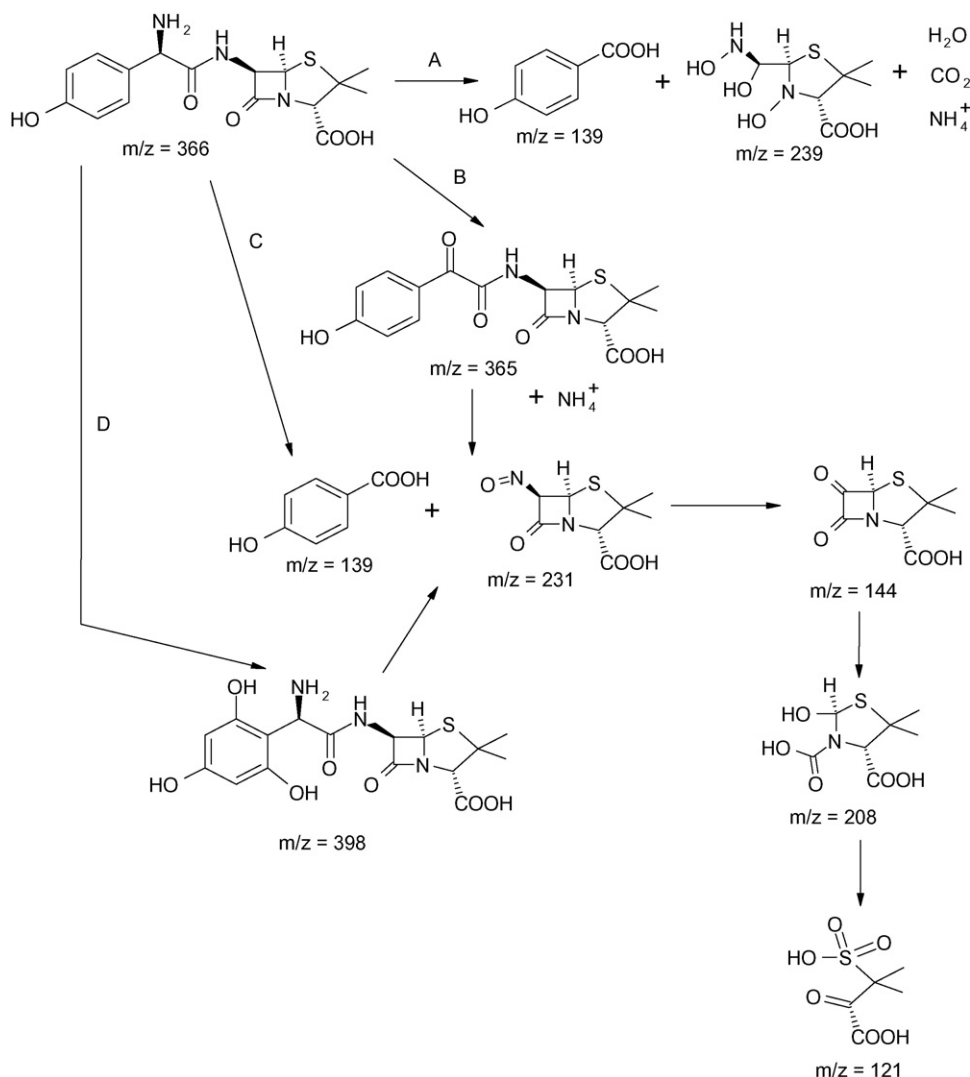


Fig. 9. PCO reaction pathway at AMO concentration of 100 mg/l (mass transfer reaction rate control): pH 6.0, 20 °C.

compete to adsorb on active sites on the surface, steric obstacles from the neighbouring AMO molecules lead to their adsorption by various functional groups, hence resulting in wider diversity of PCO reaction products and pathways.

4. Conclusions

Aqueous photocatalytic oxidation (PCO) of a widely used β -lactam antibiotic, amoxicillin (AMO) was studied using Degussa P25 titanium dioxide and visible light-sensitive synthetic sol-gel titania catalysts doped with carbon and iron. Although yielding to P25 under artificial light, doped catalysts were close by their efficiency to Degussa catalyst under solar radiation. The PCO of AMO proceeds with maximum efficiency in neutral solutions. The PCO efficiency increases with growing concentration of AMO achieving maximum at 50 mg/l and remaining constant with further concentration increase. The PCO products, determined under various AMO concentration conditions, allow the suggestion of possible reaction pathways.

Acknowledgements

The authors would like to thank Mr. Petri-Jaan Lahtvee and Ms. Liisa Arike, Competence Centre of Food and Fermentation

Technology, for their help in UPLC-MS analyses, Dr. Mai Uibu, Laboratory of Inorganic Materials, Tallinn University of Technology, for the measurements of the photocatalysts' surface area, the team of Prof. Dr.-Ing. Joachim Deubener, Division of Glass and Glass Technology, Institute of Nonmetallic Materials of the Technical University of Clausthal and especially Dr. Anna Moiseev for providing XRD measurements, Mr. Andrew S. Cavanaugh, the University of Colorado at Boulder, for providing XPS measurements. The authors express their gratitude to the Estonian Science Foundation (grant 7541), and the United States Civilian Research and Development Foundation (grant US16062) for financial support of the research.

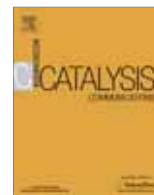
References

- [1] A. Al-Ahmad, F.D. Daschner, K. Kümmerer, Biodegradability of cefotiam, ciprofloxacin, meropenem, penicillin G, and sulfamethoxazole and inhibition of wastewater bacteria, *Arch. Environ. Contam. Toxicol.* 37 (1999) 158–163.
- [2] K. Kümmerer, A. Al-Ahmad, V. Mersch-Sundermann, Biodegradability of some antibiotics, elimination of their genotoxicity and affection of wastewater bacteria in a simple test, *Chemosphere* 40 (2000) 701–710.
- [3] R. Alexy, T. Kumpel, K. Kümmerer, Assessment of degradation of 18 antibiotics in the Closed Bottle Test, *Chemosphere* 57 (2004) 505–512.
- [4] T. Herberer, Occurrence, fate, and removal of pharmaceutical residues in the aquatic environment: a review of recent research data, *Toxicol. Lett.* 131 (2002) 5–17.

- [5] M.N. Abellan, B. Bayarri, G. Gimenez, J. Costa, Photocatalytic degradation of sulfamethoxazole in aqueous suspension of TiO₂, *Appl. Catal. B* 74 (2007) 233–241.
- [6] B. Halling-Sørensen, S. Nors Nielsen, P.F. Lanzky, F. Ingerslev, H.C. Holten Lützhøft, S.E. Jørgensen, Occurrence, fate and effects of pharmaceutical substances in the environment—a review, *Chemosphere* 36 (1998) 357–393.
- [7] C. Hartig, T. Storm, M. Jekel, Detection and identification of sulphonamide drugs in municipal waste water by liquid chromatography coupled with electrospray ionisation mass spectrometry, *J. Chromatogr. A* 845 (1999) 163–173.
- [8] S. Kim, P. Eichhorn, J.N. Jensen, A.S. Weber, D.S. Aga, Removal of antibiotics in wastewater: effect of hydraulic and solid retention times on the fate of tetracycline in the activated sludge process, *Environ. Sci. Technol.* 39 (2005) 5816–5823.
- [9] W. Baran, J. Sochacka, W. Wardas, Toxicity and biodegradability of sulfonamides and products of their photocatalytic degradation in aqueous solutions, *Chemosphere* 65 (2006) 1295–1299.
- [10] H. Sørum, in: F.M. Aarestrup (Ed.), *Antimicrobial Resistance in Bacteria of Animal Origin*, American Society for Microbiology Press, Washington, DC, 2006.
- [11] A. Chatzikakias, C. Berberidou, I. Paspaltsis, G. Kyriakou, T. Sklaviadis, I. Poullos, Photocatalytic degradation and drug activity reduction of Chloramphenicol, *Water Res.* 42 (2008) 386–394.
- [12] E.S. Emolla, M. Chaudhuri, Degradation of the antibiotics amoxicillin, ampicillin and cloxacillin in aqueous solutions by the photo-Fenton process, *J. Hazard. Mater.* 172 (2009) 1476–1481.
- [13] C. Mavronikola, M. Demetriou, E. Hapeshi, D. Partassides, C. Michael, D. Mantzavinos, D. Kassinos, Mineralisation of the antibiotic amoxicillin in pure and surface waters by artificial UVA- and sunlight-induced Fenton oxidation, *J. Chem. Technol. Biotechnol.* 84 (2009) 1211–1217.
- [14] A.G. Trovó, S.A. Santos Melo, R.F. Pupo Nogueira, Photodegradation of the pharmaceuticals amoxicillin, bezafibrate and paracetamol by the photo-Fenton process—application to sewage treatment plant effluent, *J. Photochem. Photobiol. A* 198 (2008) 215–220.
- [15] E.S. Elmolla, M. Chaudhuri, Photocatalytic degradation of amoxicillin, ampicillin and cloxacillin antibiotics in aqueous solutions using UV/TiO₂ and UV/H₂O₂/TiO₂ photocatalysis, *Desalination*, 252 (2010) 46–52.
- [16] B. Sun, M. Seto, J.S. Clements, Optical study of active species produced by a pulsed corona discharge in water, *J. Electrostat.* 39 (1997) 189–202.
- [17] D. Bahnemann, Photocatalytic water treatment: solar energy applications, *Sol. Energy* 77 (2004) 445–459.
- [18] R.W. Matthews, Photo-oxidation of organic material in aqueous suspensions of titanium dioxide, *Water Res.* 20 (1986) 569–578.
- [19] V. Brezova, Š. Vodny, M. Vesely, M. Ceppan, L. Lapcik, Photocatalytic oxidation of 2-ethoxyethanol in a water suspension of titanium dioxide, *J. Photochem. Photobiol. A* 56 (1991) 125–134.
- [20] J. Chen, D.F. Ollis, W.H. Rulkens, H. Bruning, Photocatalysed oxidation of alcohols and organochlorides in the presence of native TiO₂ and metallized TiO₂ suspensions. Part II: photocatalytic mechanisms, *Water Res.* 33 (1999) 669–676.
- [21] Y. Zhang, J.C. Crittenden, D.W. Hand, D.L. Perram, Fixed-bed photocatalysts for solar decontamination of water, *Environ. Sci. Technol.* 28 (1994) 435–442.
- [22] C. Lettmann, K. Hildenbrand, H. Kisch, W. Macyk, W.H. Maier, Visible light photodegradation of 4-chlorophenol with a coke-containing titanium dioxide photocatalyst, *Appl. Catal. B* 32 (2001) 215–227.
- [23] E. Arpac, F. Sayilkan, M. Asiltürk, P. Tatar, N. Kiraz, H. Sayilkan, Photocatalytic performance of Sn-doped and undoped TiO₂ nanostructured thin films under UV and vis-lights, *J. Hazard. Mater.* 140 (2007) 69–74.
- [24] T. Ihara, M. Miyoshi, Y. Iriyama, O. Matsumoto, S. Sugihara, Visible-light active titanium dioxide realized by an oxygen-deficient structure and by nitrogen doping, *Appl. Catal. B* 42 (2003) 403–409.
- [25] S.D. Sharma, D. Singh, K.K. Saini, C. Kant, V. Sharma, S.C. Jain, C.P. Sharma, Sol-gel-derived super-hydrophilic nickel doped TiO₂ film as active photo-catalyst, *Appl. Catal. A* 314 (2006) 40–46.
- [26] D. Li, H. Haneda, Sh. Hishita, N. Ohashi, Visible-light-driven nitrogen-doped TiO₂ photocatalysts: effect of nitrogen precursors on their photocatalysis for decomposition of gas-phase organic pollutants, *Mater. Sci. Eng. B* 117 (2005) 67–75.
- [27] Z. Wang, W. Cai, X. Hong, X. Zhao, F. Xu, C. Cai, Photocatalytic degradation of phenol in aqueous nitrogen-doped TiO₂ suspensions with various light sources, *Appl. Catal. B* 57 (2005) 223–231.
- [28] T. Ohno, M. Akiyoshi, T. Umebayashi, K. Asai, T. Mitsu, M. Matsumura, Preparation of S-doped TiO₂ photocatalysts and their photocatalytic activities under visible light, *Appl. Catal. A* 265 (2004) 115–121.
- [29] D. Klauson, S. Preis, Visible light-assisted aqueous photocatalytic oxidation of organic pollutants using nitrogen-doped titania, *Environ. Chem. Lett.* 6 (2008) 35–39.
- [30] Z. Liu, D.D. Sun, P. Guo, J.O. Leckie, One-step fabrication and high photocatalytic activity of porous TiO₂ hollow aggregates by using a low-temperature hydrothermal method without templates, *Chem. Eur. J.* 13 (2007) 1851–1855.
- [31] S.J. Kirkpatrick, A primer on radiometry, *Dent. Mater.* 21 (2005) 21–26.
- [32] L.S. Clesceri, A.E. Greenberg, R.R. Trussel, *Standard Methods for the Examination of Water and Wastewater*, 17th ed., APHA, AWWA, WPCF, Washington, DC, 1989.
- [33] S. Kaniou, K. Pitarakis, I. Barlagianni, I. Poullos, Photocatalytic oxidation of sulfamethazine, *Chemosphere* 60 (2005) 372–380.
- [34] R. Palominos, J. Freer, M.A. Mondaca, H.D. Mansilla, Evidence for hole participation during the photocatalytic oxidation of the antibiotic flumequine, *J. Photochem. Photobiol. A* 193 (2008) 139–145.
- [35] S. Preis, M. Krichevskaya, Y. Terentyeva, A. Moiseev, J. Kallas, Treatment of phenolic and aromatic amino compounds in polluted waters by photocatalytic oxidation, *J. Adv. Oxid. Technol.* 5 (2002) 77–84.

Article VI:

Klauson D., Portjanskaja E., Budarnaja O., Krichevskaya M., Preis S., The synthesis of sulphur and boron-containing titania photocatalysts and the evaluation of their photocatalytic activity. *Catalysis Communications*, 2010, 11 (8), pp. 715-720, doi: 10.1016/j.catcom.2010.02.001



The synthesis of sulphur and boron-containing titania photocatalysts and the evaluation of their photocatalytic activity

Deniss Klauson^{a,*}, Elina Portjanskaya^a, Olga Budarnaja^a, Marina Krichevskaya^a, Sergei Preis^b

^a Department of Chemical Engineering, Tallinn University of Technology, Ehitajate Tee 5, 19086 Tallinn, Estonia

^b Department of Chemical Engineering, Lappeenranta University of Technology, P.O. Box 20, 53851 Lappeenranta, Finland

ARTICLE INFO

Article history:

Received 30 December 2009

Received in revised form 28 January 2010

Accepted 1 February 2010

Available online 6 February 2010

Keywords:

Photocatalytic oxidation

Sulphur-containing titania

Boron-containing titania

Methyl-*tert*-butyl ether

tert-Butyl alcohol

i-Propanol

2-Ethoxy ethanol

p-Toluidine

Phenol

ABSTRACT

Aqueous photocatalytic oxidation of methyl-*tert*-butyl ether, *p*-toluidine, *tert*-butyl alcohol, *i*-propanol, 2-ethoxy ethanol and phenol, was studied using sulphur and boron-containing titania photocatalysts, active in visible light. The activity of the catalysts, compared to commercial Degussa P25, was tested in PCO of the pollutants dependent on the admixture content. The performance of S- and B-TiO₂ under visible light in PCO of MTBE, TBA and *i*-propanol was surpassing that of P25 under UV. However, in respect of *p*-toluidine and phenol both S- and B-containing titania showed an inferior, although comparable, performance, to that of P25. Experiments were carried out under artificial and solar light.

© 2010 Elsevier B.V. All rights reserved.

1. Introduction

Aqueous photocatalytic oxidation (PCO) of organic groundwater pollutants, methyl-*tert*-butyl ether (MTBE, CH₃-O-C(CH₃)₃), *tert*-butyl alcohol ((H₃C)₃C-OH, TBA), *i*-propanol (H₃C-CH(OH)-CH₃), 2-ethoxy ethanol, *p*-toluidine, and phenol, was studied using two series of titania photocatalysts, synthesised by sol-gel method, doped with sulphur and boron active in visible light.

Methyl-*tert*-butyl ether, banned for its use in the USA, is still widely used as an oxygenated component of motor fuels by the rest of the world. Water pollution with MTBE may occur due to traffic accidents, fuel leaks or inappropriate fuel disposal. This substance is of particular concern because of its accumulation in groundwater due to its low biodegradability [1]. Physical removal and chemical oxidation methods, such as air stripping, activated carbon adsorption, ozonation and treatment with Fenton's reagent have been proven to be ineffective against MTBE [2–4].

p-Toluidine is a widely used industrial chemical, with its use ranging from a component of several jet and rocket fuels to applications in paint and pharmaceutical industries [5]. Also, at former munitions sites *p*-toluidine is a degradation intermediate of *p*-nitrotoluene, and occurs in tobacco smoke [6]. Thus, the pollution

of soil and groundwater with *p*-toluidine occurs at the military sites; industrial emissions are also possible. Non-biodegradable *p*-toluidine may accumulate in groundwater aquifers in toxic amounts. Conventional water treatment methods have been shown to be inadequate against *p*-toluidine pollution [7].

Phenol, being a substantial environment pollutant of, for example, oil shale industry [8], has a reputation of a standard model contaminant used to test the activity of various oxidation methods and catalysts. *tert*-Butyl alcohol (TBA) can be primarily found in the groundwater as a result of MTBE hydrolysis; it may also enter groundwater as an impurity of MTBE-blended motor fuels [9]. 2-Ethoxy ethanol is used in multiple applications in industry and transport and also may accumulate in subsurface aquifers. The main interest in *i*-propanol, however, was to study the PCO of secondary carbon atom when compared to primary carbon of 2-EE, tertiary carbon atom of MTBE and TBA and aromatic structures of phenol and *p*-toluidine. Thus the choice of model pollutants was serving the systematic study of the catalysts' performance on pollutant substances of different molecular structure found simultaneously in polluted groundwater. Although dyes are often used as test objects for novel photocatalysts, the authors believe that the performance of the latter would better be checked by real and chemically stable pollutants, unlike dyes that can spontaneously decompose under visible irradiation. Also, often the modified catalysts exhibit dramatically different performance with different

* Corresponding author.

E-mail address: dklauson@hotmail.com (D. Klauson).

substances [10]. In case when various pollutants can be found simultaneously in, for example, fuel-polluted groundwaters, the knowledge of photocatalytic activity against multiple targets is necessary.

Subjected to electromagnetic irradiation of appropriate energy, the excited semiconductor's valence band electrons are displaced to the conduction band, forming positively charged holes oxidizing the water molecules into hydroxyl radicals reacting with the pollutant. Also, the direct oxidation of organic pollutant adsorbed on the photocatalyst surface by the positively charged holes takes place.

Most commonly used titanium dioxide photocatalysts can be excited only by ultraviolet irradiation, as the band-gap energy of TiO_2 is 3.2 eV. This way, only 4% of the solar radiation reaching the Earth surface can be used. However, the semiconductor band-gap can be reduced by doping, i.e. introducing additive atoms into titanium dioxide structure, thus forming a crystalline structure with a misbalance in charge carriers. These charge carriers, either electrons or holes, have enough energy to create a new energetic level inside the band-gap (named either donor or acceptor level, depending on whether it is formed by electrons or holes respectively), which is occupied at room temperature by electrons. When subjected to electromagnetic irradiation, the electrons of donor or acceptor level can be excited and displaced to the conduction band from an energetic level inside the band-gap with less energy required for electron excitation, i.e. light with greater wavelength may be utilised.

Sulphur- and boron-containing titania visible light-sensitive photocatalysts were synthesised using sol-gel method and tested in PCO of the abovementioned pollutants. An undoped titania sample synthesised by the same pattern was used as a reference. The performance of the modified catalysts, dependent on the admixture content, was compared to one another and to that of Degussa P25 titanium dioxide.

2. Experimental

Two thermostatted at 20 ± 1 °C 200-mL simple batch reactors with inner diameter 100 mm (evaporation dishes), aperture $40 \text{ m}^2 \text{ m}^{-3}$, mechanically agitated with magnetic stirrers, were used in PCO experiments: the one used for the PCO was called "active" and the other containing no photocatalyst was called "reference". Both reactors were exposed to identical experimental conditions. The samples from the active reactor were compared to the reference samples to avoid complications caused by water evaporation. A UV-light source, Philips 365-nm low pressure luminescent mercury UV-lamp (Sylvania Blacklight F 15 W 350 BL-T8), was positioned horizontally over the reactors, providing the irradiance of about 0.7 mW cm^{-2} measured at a distance of 25 cm, corresponding to the level of the free surface of the reactor by the optical radiometer Micropulse MP100 (Micropulse Technology, UK). With daylight fluorescent lamp (Philips TLD 15 W/33–640), the irradiance was measured indirectly, being calculated from the illuminance, measured by TES luxmeter (TES Inc., Taiwan), using lumen to watt ratio of 684, as the response of human eye to light with the illuminance of 684 lumens (lm) equals to that to the irradiance of 1 W [11]. With Philips TLD lamp, the amount of UV-irradiation was also specifically measured using the above-mentioned Micropulse radiometer for 254 and 365 nm and total amount of UV by using Ocean Optics USB2000 + UV-VIS spectrometer. Only negligibly small fraction of UV around 365–400 nm was observed. These measurements are also confirmed by the publicly available data from the lamp manufacturer [12]. Thus, any noticeable action of the photocatalyst when using Philips TLD lamp as the irradiation source may not be attributed to the UV fraction emitted by the lamp but is clearly due to the activity of the catalysts in

visible light region. There were also some experiments conducted outdoors, using natural solar irradiation. A schematic representation of the experimental setup can be seen in Fig. 1.

The experiments were carried out using aqueous solutions of the chemicals supplied by Aldrich. With all chemicals except 2-EE, the experiments were conducted with synthetic solutions (i.e. the pollutants dissolved in distilled water) at 100 mg L^{-1} ; with 2-EE the concentration was higher, being 300 mg L^{-1} . The concentrations were chosen with reference to those that may be found in real contaminated aquifers used in previously conducted experiments [7,13]. The experiments were carried out in acidic (pH 3), natural (pH 6.5) and alkaline (pH 11) media, adjusted either by 4 N sulphuric acid or 15% sodium hydroxide. The treatment time for MTBE was 2 h under artificial light and 30 min under solar radiation. With *i*-propanol, treatment time was also 2 h. For *p*-toluidine and phenol, treatment time was 24 h. TBA solutions were treated for 4 h. Treatment time for 2-EE was chosen to be 24 h under artificial and 5 h under solar light. The treatment time in every case was chosen to reduce the concentration of pollutants below 50% of the residual concentration and was used in calculations of the process efficiency E (see Eq. (1)). All the experiments were carried out for at least three times under identical experimental conditions to derive the average value of the process efficiency. The average deviation of data in parallel experiments did not exceed 5%.

Adsorption experiments with the pollutants on the photocatalyst surface were carried out at respective pH in closed flasks thermostatted at 20 ± 1 °C and equipped with magnetic stirrers. The adsorbed amount of substances was derived from the batch mass balance: the concentration of the dissolved substance was determined before and after adsorption.

Titanium dioxide Degussa P25, eight sulphur-containing and five boron-containing synthetic catalysts were used. Sulphur-containing photocatalysts were prepared by the hydrolysis of titanium tetrabutoxide with addition of a pre-calculated amount of 0.1 N sodium thiosulphate as sulphur source, followed by calcination at 400 °C for 4 h. After this, the catalyst was washed with hot distilled water applied in a sequence of 10–15 rinsing rounds (ca. 1 L per 1 g of catalyst) in order to clean the catalyst surface from water-soluble compounds. In case of boron-containing photocatalysts, sodium tetraborate was used as boron source. An additional catalyst was synthesised using the same pattern, although without the addition of sulphur or boron sources. The experiments were performed in photocatalyst suspensions of 1 g L^{-1} .

Many authors indicate complete transformation of sulphide to sulphate at calcination temperature in air from 300 to 500 °C [14]. For verification of the catalysts stability, the S-modified catalyst was suspended in distilled water in amount of 1 g L^{-1} under the UV light for 24 h. The sulphate determination was carried out with the IC (Dionex DX-120) with no corresponding peaks observed at the sensitivity of 10 ppb. As for carbon, the available

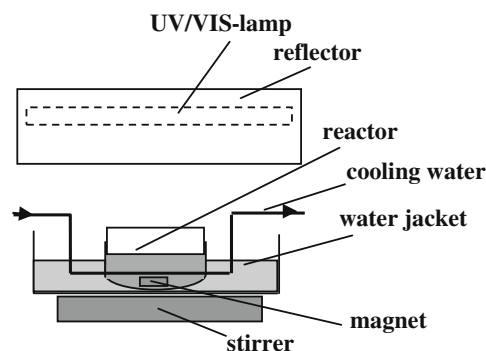


Fig. 1. Experimental setup.

Table 1
Main characteristics of sulphur- and carbon-doped photocatalysts.

Composition (at.%)					S_{BET}	S_{Langmuir}	$S_{\text{millipores}}$	$V_{\text{millipores}}$
S	Ti	O	C	Impurities	$\text{m}^2 \text{g}^{-1}$	$\text{m}^2 \text{g}^{-1}$	$\text{m}^2 \text{g}^{-1}$	$\text{mm}^3 \text{g}^{-1}$
0	18.1	46.6	33.9	0	105.7	144.7	4.1	5.1
0.8	17.9	47.5	32.8	1.0	93.8	126.7	1.7	0.6
1.1	17.5	46.2	34.1	1.1	129.0	176.0	0	0
1.4	18.1	47.1	33.4	0	170.7	234.0	0	0
1.7	16.6	46.1	34.3	1.4	164.5	219.2	10.5	3.4
1.7	18.5	50.5	28.0	1.3	132.0	178.4	4.7	1.7
2.5	17.7	49.9	28.7	1.6	141.9	149.3	58.3	20.6
2.8	18.7	48.1	28.9	1.6	163.6	222.7	6.1	2.1
B	Ti	O	C	Impurities				
1.1	17.3	47.1	34.0	0.6	150.7	206.1	10.3	3.6
1.5	12.3	34.2	51.1	0.8	112.6	156.6	0	0
2.0	9.9	35.0	53.1	0	272.4	380.1	0	0
3.2	9.7	33.7	53.4	0.06	242.5	337.8	0	0
3.8	12.1	37.5	46.5	0	78.2	107.8	0	0

knowledge shows that when preparing titania photocatalysts by sol–gel method, it is impossible to completely eliminate carbon originating from tetrabutyl orthotitanate even when calcining the catalysts at high temperatures, where free and organic carbon, and also carbonate, would already decompose. This suggests that the amounts of carbon that can be present in the sol–gel prepared photocatalysts after calcinations and thorough washing are incorporated in a stable form into titanium dioxide crystal lattice [15].

In order to evaluate the stability of the photocatalysts, every experiment was carried out using at least three times under identical conditions using the same portion of the photocatalyst. The difference between the results of single experiments was even in case of 24-h experiments well within the parallel experiments deviation (under 5%) with no tendencies observed.

The crystallinity of modified titania photocatalysts was analysed using X-ray diffraction (XRD) spectroscopy D5000 Kristalloflex, Siemens (Cu K α irradiation source). Elements content was measured with X-ray photoelectron spectroscopy PHI 5600. The specific area (BET and Langmuir adsorption) and the pore volume of the catalysts were measured by the adsorption of nitrogen using Kelvin 1042 sorptometer.

The decrease of MTBE, TBA, 2-EE and *i*-propanol concentrations was determined from the decrease in chemical oxygen demand (COD), measured by a standard method. This parameter, unlike TOC, was proven to be universal, decreasing with the increased conversion degree in oxidation reactions. Also, with several randomly selected doped catalysts, the decrease of MTBE concentration was measured by gas chromatography, which showed that MTBE was totally degraded in about 1 h time regardless the catalyst used, however, COD decrease, i.e. the degradation of MTBE PCO by-products, proceeded differently; this was another reason for choosing COD decrease to evaluate PCO performance. Concentrations of *p*-toluidine were measured photometrically after diazotization and reaction with phenol at 490 nm, and those of phenol were determined photometrically after reaction with *p*-nitroaniline at 570 nm using Helios β spectrophotometer together with the COD. In case of *p*-toluidine, the evolution of nitrite and nitrate ions was also determined using Metrohm 761 Compact IC ion chromatograph.

The performance of PCO under artificial radiation was characterised by the process efficiency E defined as the decrease in the amount of pollutants divided by the amount of energy reaching the surface of the treated sample within the treatment time (Eq. (1)).

$$E = \frac{\Delta C \times V \times 1000}{I \times S \times t} \quad (1)$$

where E – PCO efficiency, $\text{mg W}^{-1} \text{h}^{-1}$; ΔC – the decrease in the pollutant's concentration mg L^{-1} or mg O L^{-1} measured as COD; V – the volume of the sample to be treated, L; I – irradiance, mW cm^{-2} ; S – irradiated area, cm^2 ; t – treatment time, h.

3. Results and discussion

3.1. Photocatalyst characterisation

Table 1 shows the composition and surface properties of S- and B–TiO₂. As one can see, beyond the primary admixtures, i.e. sulphur and boron, there is also some amount of carbon, the presence of which is inevitable in sol–gel synthesis even at high calcinations temperatures (over 1000 °C). The first row of the table shows the reference catalyst synthesised without sulphur or boron precursors. Nitrogen and silica were detected by XPS in small amounts as impurities. Judging from the XRD analysis, anatase prevailed in all doped catalysts.

The specific surface area of both catalyst types shows a tendency to pass a maximum with growing concentration of doping elements. The changes in Millipore area and volume, on the other hand, are far less systematic. It should be also noted that S–TiO₂ catalyst samples tended to give acidic and B–TiO₂ – alkaline reaction when suspended in water after thorough wash before use, which should be attributed to the functional groups at the catalysts' surface, as the catalysts were thoroughly washed after calcination (see Section 2).

3.2. Photocatalytic oxidation experiments

3.2.1. Sulphur-containing titania

The PCO of MTBE under artificial visible light (Philips TLD 15 W fluorescent lamp) with S–TiO₂ proceeds best in acidic media, followed by alkaline and neutral ones (Fig. 2a). This pattern was observed for all S-containing catalysts. For this reason, further experiments with MTBE on the impact of admixture content were conducted in acidic media (pH 3.0). Here the efficiency increased with the increasing sulphur content up to 1.5 at.% and then steadily decreased (see Fig. 3a). The values of MTBE PCO efficiency observed with S-doped catalysts were up to two times higher than with Degussa P25 (350 compared to 170 $\text{mg O W}^{-1} \text{h}^{-1}$) [13]. With the photocatalyst containing 1.7 at.% S, COD of the treated solutions reached zero in time, i.e. not only MTBE was oxidized but also its by-products were totally mineralized. Some of the S-containing catalyst specimens under UV-radiation (Sylvania Blacklight lamp) showed activity similar to the one of Degussa P25 (see Fig. 3a).

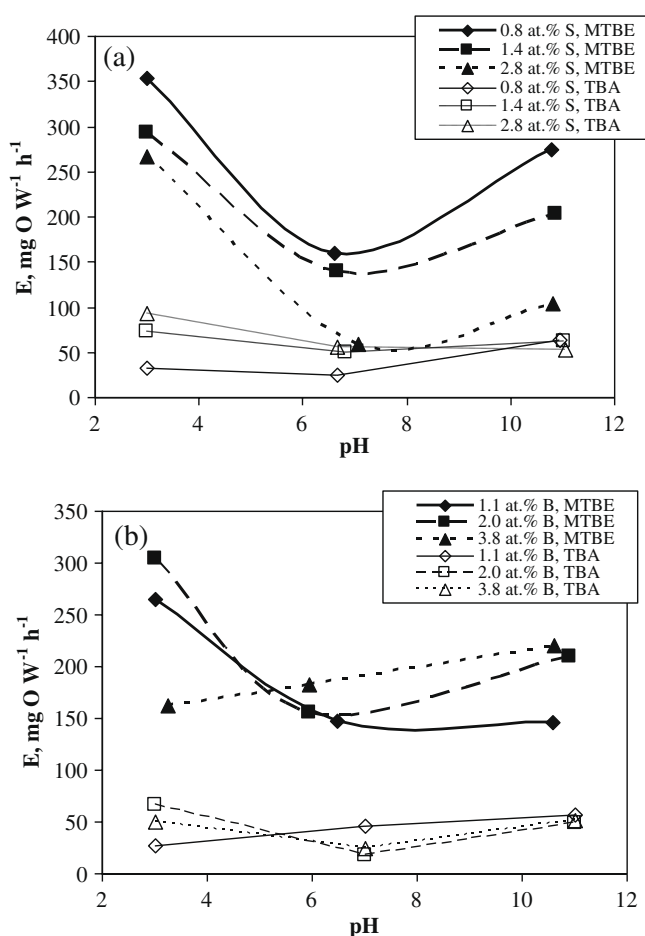


Fig. 2. The dependence of efficiency of PCO of MTBE and TBA on the initial solution pH with the sulphur (a) and boron-modified (b) photocatalysts, pH 3.0, 20 °C, visible light.

The efficiencies achieved with S-containing catalysts in TBA oxidation were also up to three times higher than those with Degussa P25 (90 compared to 33 mg O W⁻¹ h⁻¹ [13]). The dependency of TBA PCO efficiency on pH differed from the pattern of MTBE: under alkaline conditions the catalysts showed similar efficiencies invariant of S-content, although acidic media still seem to be superior, followed by alkaline and neutral media (Fig. 2a). Interestingly, the PCO efficiency of TBA under visible light increased almost linearly with growing sulphur content in the catalysts (Fig. 3a), whereas under UV the dependence of PCO efficiency on dopant concentration was similar to that observed with MTBE, having a maximum at around 1.4 at.% S. The values of PCO efficiency under UV-radiation were similar to the one achieved with Degussa P25.

The degradation of COD of MTBE solutions treated under the solar light proceeded faster with Degussa P25, although the performance of some sulphur-containing photocatalysts was close to that.

Sulphur-containing titania catalysts exhibited poor performance in PCO of phenol: only 3% of phenol in 100-ppm solution was degraded with visible light under experimental conditions in 24 h; under UV-radiation the result was slightly better – 19%. The PCO efficiency in visible light, measured in COD units, was thus only 0.5 mg O W⁻¹ h⁻¹. The efficiency of Degussa P25 in phenol PCO was 10 mg O W⁻¹ h⁻¹ under similar experimental conditions.

The sulphur-containing catalysts showed poor performance both under artificial and solar radiation in 2-EE PCO. With another aliphatic alcohol *i*-propanol, however, the PCO efficiency with S-TiO₂ under visible light was almost two times higher than the

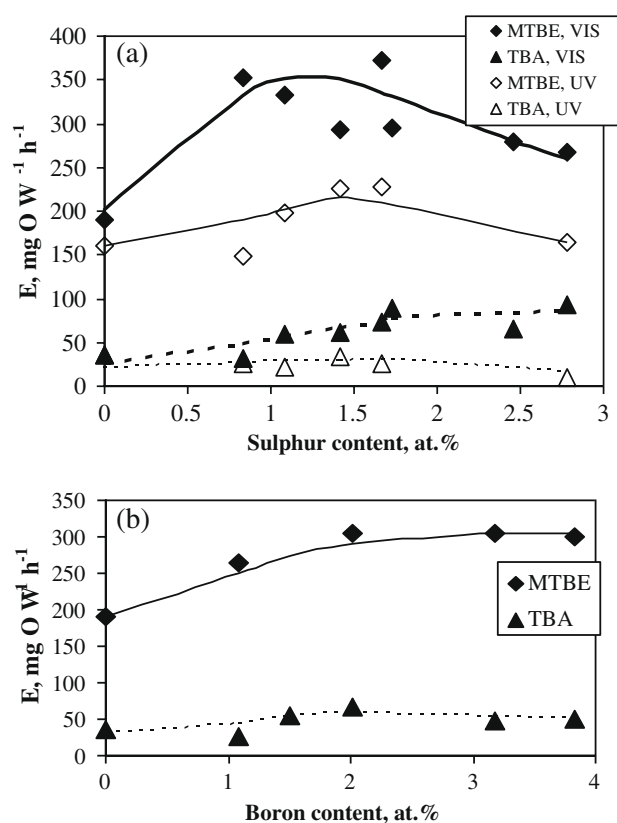


Fig. 3. The dependence of the efficiency of MTBE (a) and TBA (b) PCO on the sulphur content in the photocatalysts, pH 3.0, 20 °C, UV and visible light.

one achieved with Degussa P25 under UV, 69 and 38 mg O W⁻¹ h⁻¹, respectively.

The best performance in *p*-toluidine PCO with S-TiO₂ was observed under alkaline pH (see Fig. 4a), where the experiments were subsequently carried out. Under acidic and neutral conditions, *p*-toluidine PCO did not proceed with the sulphur-containing photocatalysts. The efficiency of S-TiO₂ catalysts in alkaline media under visible light in PCO of *p*-toluidine was comparable to the one of commercial Degussa's under UV, which was 4 mg W⁻¹ h⁻¹ or 8 mg O W⁻¹ h⁻¹. However, the variation in sulphur content in the photocatalysts did not affect much the efficiency numbers.

3.2.2. Boron-containing titania

With B-TiO₂, the dependence of the efficiency of MTBE and TBA PCO on pH was similar to that of S-TiO₂ (see Fig. 2b). Under visible radiation at pH 3.0 an increasing trend in PCO efficiency was observed with the boron content increasing to 2 at.%; above that content, the efficiency remained at a constant level (Fig. 3b). Under visible light with B-TiO₂ the efficiency of PCO of both MTBE and TBA exceeded the one achieved with Degussa P25 under UV for about two times (Fig. 3).

Contrary to the S-TiO₂ catalysts, the boron-containing titania exhibited the fastest *p*-toluidine PCO in acidic media followed by neutral and basic ones (Fig. 4b). The PCO efficiency with B-TiO₂ in acidic media under visible light exceeded the one of Degussa's under UV by a factor 1.5 for *p*-toluidine and 2.0 for COD degradation. It is noticeable that in neutral and alkaline media the PCO efficiency decreases slightly with the increase in the boron content in the catalysts (rather similar to the effect observed with S-TiO₂), however, the trend is quite contrary in case of acidic media, where certain growth can be observed. The reason behind this observation is the different behaviour in acidic media of the catalyst

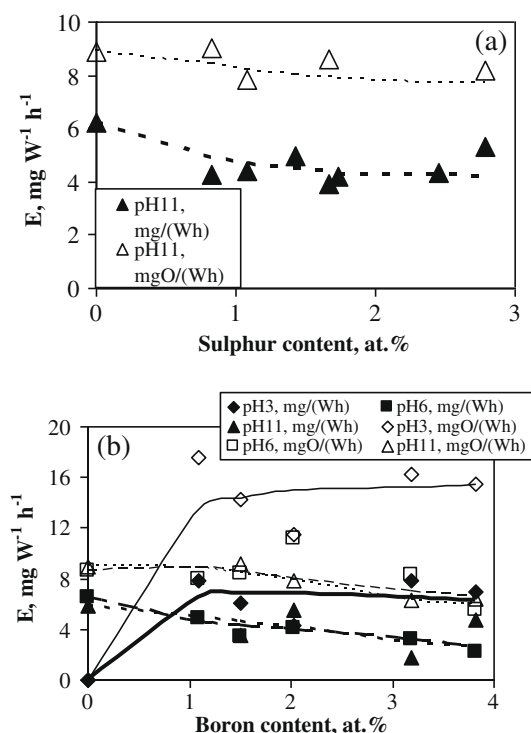


Fig. 4. The dependence of the *p*-toluidine PCO efficiency on the initial solution pH with the sulphur (a) and boron-modified (b) photocatalysts: pH 3.0, 20 °C, visible light.

containing only carbon as opposed to those containing boron and carbon.

The adsorption of substances under scope on the surface of both doped catalyst types was found to be insignificantly small, ranging around a few mg g^{-1} of titania. This makes the major part of degradation proceeding through hydroxyl radical reactions.

3.3. Discussion

The dependence of efficiency of MTBE PCO on the S-admixture concentration passing through the maximum at 1.5–1.7 at.% can be explained by the decrease in catalyst redox potential accompanying the decrease in the band-gap energy with growing dopant concentration [16]. Under visible light, at first, the decrease in the band-gap enhances the PCO performance. With the growing admixture content, however, the decrease in the redox potential overpowers the positive effect of the decreased band-gap, resulting in the PCO efficiency decrease. Slight PCO efficiency growth between 0.8 and 1.5 at.% S may be attributed to the growth of the catalysts' contact surface area. Even though the substances' adsorption does not greatly improve due to this, greater area is illuminated, which may result in a better hydroxyl radical production. The linear growth of PCO efficiency of TBA with growing content of sulphur within the experimental limits could be explained by the turning point laying at higher dopant concentrations.

It may be seen that with aliphatic substances the modified catalysts showed the best performance with MTBE and TBA, followed by *i*-propanol and 2-EE. Since the adsorption of substances under scope on the surface of the catalysts was found to be negligible, the PCO is assumed to proceed here mainly as a nucleophilic attacks of hydroxyl radicals. Nucleophilic attack proceeds upon the carbon atom having the highest partial positive charge. In ethers and alcohols this is a carbon atom located next to oxygen due to oxygen being more electronegative: with 2-EE, the nucleophilic attack proceeds on both C1 and C2 atoms [17], although an attack

on C1 tends to prevail. With *i*-propanol, a secondary carbon atom connected to the hydroxyl group is under attack, in TBA and MTBE molecules hydroxyl radical attacks tertiary carbon atom, connected to the hydroxyl and methoxy groups, respectively, although an attack on the methyl group in MTBE may also take place. Despite obvious geometric obstruction, the nucleophilic attack on tertiary carbon atom is the most effective, followed by secondary and finally by the primary atom, as one can see from the present results. This is to be explained by greater charge localisation on tertiary and secondary carbon atoms: tertiary carbon's electron cloud is pulled to oxygen atom on one hand and to three comparatively electronegative methyl groups on the other hand. The secondary carbon atom is less affected by methyl groups, and the C-atoms in 2-EE are least affected.

The difference observed in the behaviour of S-TiO₂ and B-TiO₂ in PCO of *p*-toluidine and phenol may be explained by the different nature of functional groups attached to the aromatic ring: the PCO is known to proceed first through the oxidation of functional groups followed by the ring rupture, which is harder than the first step. In *p*-toluidine amino and methyl groups are both less electronegative than hydroxyl group of phenol. Also, it is far easier to oxidize amino or methyl group than the hydroxyl one, as the latter process means in fact breaking the aromatic ring.

The overall performance of S-TiO₂ is slightly better than that of B-TiO₂, however, when the dependence of PCO efficiency on admixture concentration is examined, the trends observed with oxygenated hydrocarbons are similar. Also, with both catalyst types the best performance was observed in acidic media, despite the fact that PCO of the substances under scope appears to proceed mainly through radical reactions, which should be favoured by basic media. The only exception in terms of pH is *p*-toluidine with S-containing titania: the best performance was in alkaline conditions, and the efficiency was higher with B-containing titania. This may be explained by the fact that S-TiO₂ surface had acidic reaction, while B-TiO₂ ones had alkaline; thus, pH of the solutions each time shifted towards neutral reaction during PCO experiments with *p*-toluidine.

4. Conclusions

Aqueous photocatalytic oxidation (PCO) of methyl-*tert*-butyl ether (MTBE), *tert*-butyl alcohol (TBA), 2-ethoxy ethanol (2-EE), *i*-propanol, *p*-toluidine and phenol was undertaken using visible light-sensitive sulphur- and boron-containing titania. Those photocatalysts have proven to be effective against MTBE, TBA and *i*-propanol, with respective PCO efficiencies under visible light exceeding those of commercial photocatalyst Degussa P25 under UV. The performance of S- and B-TiO₂ with *p*-toluidine was less efficient but still comparable to that of Degussa P25. In case of 2-EE and phenol, however, the performance of both photocatalyst types was clearly insufficient.

Acknowledgements

The authors would like to thank the team of Prof. Dr.-Ing. Joachim Deubener, Division of Glass and Glass Technology, Institute of Nonmetallic Materials of the Technical University of Clausthal and especially Dr. Anna Moiseev for providing XRD measurements, Mr. Andrew S. Cavanaugh, the University of Colorado at Boulder, for providing XPS measurements, and Dr. Mai Uibu, the Laboratory of Inorganic Materials of Tallinn University of Technology, for providing specific surface area measurements of the catalysts. The authors would also like to thank Estonian Science Foundation (Grant G7541) and United States Civilian Research and Development

Foundation (Grant US16062) for the financial support of the research.

References

- [1] C.K. Yeh, J.T. Novak, *Water Environ. Res.* 66 (1994) 744–752.
- [2] P. Johnson, *Environ. Sci. Technol.* 32 (1998) 276–281.
- [3] A. Safarzadeh-Amiri, *Water Res.* 35 (2001) 3706–3714.
- [4] X.R. Xu, Z.X. Zhao, X.Y. Li, J.P. Gu, *Chemosphere* 55 (2004) 73–79.
- [5] K.K. Papok, E.G. Semenid, *Motor, Jet and Rocket Fuels (Motornye, reaktivnye i raketnye topliva)*, Gostoptehizdat, Moscow, 1962 (in Russian).
- [6] I. Schmeltz, D. Hoffmann, *Chem. Rev.* 77 (1977) 295–311.
- [7] S. Preis, M. Krichevskaya, Y. Terentyeva, A. Moiseev, J. Kallas, *J. Adv. Oxidation Technol.* 5 (2002) 77–84.
- [8] A. Kahru, A. Maloverjan, H. Sillak, L. Pollumaa, *Environ. Sci. Pol. Res.* 1 (2002) 27–33.
- [9] C.D. Church, J.F. Pankow, P.G. Tratnyek, *Environ. Toxicol. Chem.* 18 (1999) 2789–2796.
- [10] D. Klauson, E. Portjanskaja, S. Preis, *Environ. Chem. Lett.* 6 (2008) 35–39.
- [11] S.J. Kirkpatrick, *Dent. Mater.* 21 (2005) 21–26.
- [12] Royal Philips. Available from: <http://www.prismaecat.lighting.philips.com/FredhopperPDFWebServiceInter/docts/f38f1cfb-c971-4d99-87eb-c718c1020c4b/product.pdf>.
- [13] M. Krichevskaya, A. Kachina, T. Malygina, S. Preis, J. Kallas, *Int. J. Photoenergy* 5 (2003) 81–86.
- [14] M. Raileanu, M. Crisan, N. Dragan, D. Crisan, A. Galtayries, A. Braileanu, A. Ianculescu, V.S. Teodorescu, I. Nitoi, M. Anastasescu, *J. Sol–Gel Sci. Technol.* 51 (2009) 315–329.
- [15] S.U.M. Khan, M. Al-shahry, W.B. Ingler Jr., *Science* 297 (2002) 2243–2244.
- [16] Z. Liu, D.D. Sun, P. Guo, J.O. Leckie, *Chem. Eur. J.* 13 (2007) 1851–1855.
- [17] D. Klauson, S. Preis, *Environ. Technol.* 7 (2005) 175–180.

Article VII:

Klauson D., Krichevskaya M., Borissova M., Preis S., Aqueous photocatalytic oxidation of sulphamethizole, *Environmental Technology*, 2010, in press

Aqueous photocatalytic oxidation of sulfamethizole

D. Klauson^{1*}, M. Krichevskaya¹, M. Borissova², S. Preis³

¹ Department of Chemical Engineering, Tallinn University of Technology, Ehitajate tee 5, Tallinn 19086, Estonia

² Department of Chemistry, Tallinn University of Technology, Akadeemia tee 15, 12618, Tallinn, Estonia

³ LUT Chemistry, Lappeenranta University of Technology, P. O. Box 20, Lappeenranta 53851, Finland

Tel.: +372 620 2857, fax: +372 620 2856, e-mail: deniss.klauson@ttu.ee

(Received xxx 2010; final version received xxx 2010)

Aqueous photocatalytic oxidation (PCO) of a non-biodegradable sulphonamide antibiotic sulfamethizole was studied. The impacts of photocatalyst dose, initial pH, and substrate concentration in the range from 1 to 100 mg L⁻¹ were examined with a number of organic and inorganic by-products determined, suggesting a the initial break-up of the SMZ molecule at the sulphonamide bond. The experiments were carried out under artificial near-UV and visible light, and solar radiation using Degussa P25 and less efficient visible light-sensitive C-doped titanium dioxide as photocatalysts.

Keywords: sulphamethizole, SMZ, PCO, Langmuir-Hinshelwood kinetics, reaction pathway

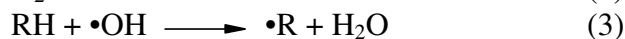
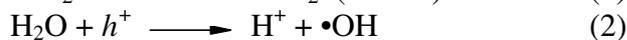
Introduction

In recent years, there has been growing interest in emerging aqueous pollutants, including antibiotic medicaments having strong antimicrobial activity and extensively used in antibacterial chemotherapy. Strong antimicrobial activity, although beneficial for therapy, becomes a major concern for the environment. Antibiotic substances are not readily biodegradable and either pass through biological treatment plants intact [1], or adsorb to the active sludge with subsequent desorption [2], accumulating in the environment [3-5]. The accumulation of antibiotics in organisms may cause arthropathy, nephropathy, damage to the central nervous system and spermatogenesis, mutagenic effects, and light sensitivity [4]. A further and possibly far greater threat is, however, possible development of antibiotic-resistant micro-organisms, including pathogens [6, 7]. Taking all this into consideration, there is clear need for an effective chemical oxidation method for the abatement of antibiotics.

1
2
3 Sulphonamides constitute a synthetic antibiotics class widely used as both human and
4
5
6 veterinary medicine against a majority of Gram-positive and many Gram-negative micro-
7
8 organisms and protozoa. In livestock and poultry production, these are used also in growth
9
10 promoting. The residues of sulphonamides can be found in animal products for human
11
12 consumption, such as honey, milk, eggs, fish or meat [8]. Most sulphonamides have a
13
14 relatively long half-life, generating on accumulation serious unwanted effects on human
15
16 health, such as allergic or toxic reactions [9] and there have already been reports of
17
18 sulphonamides [10-12] and sulphonamide-resistant micro-organisms being encountered in the
19
20 environment [13]. Sulfamethizole ((4-amino-N-(5-methyl-1,3,4-thiadiazole-2-yl)-
21
22 benzenesulfonamide, SMZ; Fig. 1), a common sulphonamide antibiotic effective against
23
24 *Escherichia coli*, is under consideration in this study. The elucidation of the SMZ PCO
25
26 reaction pathway makes the novelty of the present research, since the published works on the
27
28 AOPs of antibiotics mainly focus on the parent compound removal and mineralization,
29
30 leaving the degradation by-products unexplored.
31
32
33
34
35

36 Photocatalytic oxidation (PCO) is considered in this study as an alternative method for
37
38 abatement of non-biodegradable antibiotics. It is an advanced oxidation process (AOP) based
39
40 on the action of positively charged holes (h^+), created by the illumination of semiconductor
41
42 either directly on its surface or having moved there due to the existence of electrical field on
43
44 the interface of the catalyst and the solution [14]. Water molecules decompose on the holes to
45
46 form hydroxyl radicals, which have a high oxidation potential [15]; the hole itself is an even
47
48 more powerful oxidant that can degrade the pollutant directly [16]. Electrons (e^-), excited by
49
50 the UV-irradiation, also participate in the PCO, reducing dissolved oxygen and leading thus to
51
52 the formation of more radical oxidants. The proportion of radical *versus* hole oxidation
53
54 depends on the physico-chemical properties of the substance to be degraded. The evidence of
55
56 the surface reactions dominating was present by [17]. Many substances may be degraded by
57
58
59
60

1
2
3 both mechanisms simultaneously. The following reactions are the main ones that take place
4
5 during PCO [18, 19]:
6



14
15 The amount of hydroxyl radicals is replenished by the creation of new radicals by
16
17 reaction (2) and by the reactions initiated by the reduction of dissolved oxygen by the
18
19 photoelectrons [20].
20
21

22 Commercial photocatalysts, such as Degussa P25 titanium dioxide, although showing
23
24 good performance, can utilise only ultraviolet light comprising a small fraction (4%) of solar
25
26 radiation reaching the Earth surface due to the high energy of its band gap [21]. This makes
27
28 sensitising TiO_2 -based photocatalysts to visible light a potential way of widening the utilised
29
30 solar spectrum and improving the performance of the catalyst. For this purpose, titanium
31
32 dioxide can be doped by various metals or non-metals, which can effectively lead to reduction
33
34 of the band-gap [22-28]. This, subsequently, leads to the excitation of electrons by photons of
35
36 lower energy, i.e. with greater wavelength; wavelengths up to 540 nm have been reported to
37
38 be effective. The authors' previous experience shows, however, that doped titania
39
40 photocatalysts may, unlike "universal" Degussa P25, oxidise only selected pollutants [29].
41
42 This may be explained by the smaller red-ox potential and, possibly, faster electron-hole
43
44 recombination of catalysts with a smaller band-gap energy [30].
45
46
47
48
49

50 Photocatalytic oxidation seems to be an effective method for degrading many
51
52 otherwise persistent pollutants, including antibiotics [5, 31, 32] and several works have
53
54 demonstrated the degradation of various sulphonamides [2, 33, 34].
55
56
57
58
59
60

Materials and methods

Two thermostatted at $20 \pm 1^\circ\text{C}$ 200-mL batch reactors with inner diameter 100 mm, irradiated plane surface $40 \text{ m}^2 \text{ m}^{-3}$, with magnetic stirrers, were used: the one used for the PCO called “active” and the other containing no photocatalyst called “reference”, exposed to the identical conditions. The samples from both reactors were compared to avoid errors caused by water evaporation. A UV-light source, Phillips Sylvania Blacklight low pressure luminescent mercury UV-lamp (15 W) with maximum emission around 365-nm was positioned horizontally over the reactors, providing the irradiance of 0.5 mW cm^{-2} at their surface, measured by the radiometer Micropulse MP100. With the daylight fluorescent lamp (Phillips TL-D 15W/33-640), the illuminance was measured using TES 1332 luxmeter reaching 3,700 lx (lm/m^2), which corresponds to the irradiance of 0.6 mW/cm^2 . The irradiance was calculated using a lumen to watt ratio of 683, as the response of the human eye to the illuminance of 683 lm equals that to the irradiance of 1 W [35]. The same calculation pattern applies to solar irradiation with the illuminance averaging most of the times around 100,000 lx, i.e. 15 mW cm^{-2} .

The initial SMZ (Sigma-Aldrich) concentrations from 1 to 100 mg L^{-1} were applied at the initial pH from 3 to 11 adjusted with sulphuric acid for sulphate having minimum impact to PCO [36] and sodium hydroxide solutions. pH was monitored, not altered. In order to achieve a considerable degree of conversion of SMZ, the experimental time was chosen to be 6 h with artificial light sources and 2 h with solar irradiation. All the experiments were tripled under identical experimental conditions; the average deviation did not exceed 5%.

The influence of the Degussa P25 catalyst dose in slurry was examined in the range from 0.25 to 1.5 g L^{-1} . With doped catalysts, only the loading of 1 g L^{-1} was used, which was, similarly to [2], found to be optimum for P25.

1
2
3 Adsorption experiments were carried out in thermostatted flasks with magnetic stirrers
4
5 at $20\pm 1^\circ\text{C}$. The amount of adsorbed substance was derived from the mass balance by
6
7 determining the concentration of the dissolved substance before and after adsorption at the
8
9 equilibrium reached in 1 h.
10
11

12
13 Sulfamethizole concentrations were determined photometrically using a Helios β
14
15 spectrophotometer, measuring light absorbance at 279 nm. A Q-Star Elite mass-spectrometer
16
17 (MS) (Applied Biosystems, Germany) equipped with an electrospray ionization (ESI) source
18
19 and a quadrupole-time of flight (Q-TOF) mass-analyzer was used for determination of organic
20
21 by-products of SMZ PCO. Samples were diluted with 50% MeOH containing 0.1%
22
23 CH_3COOH and injected directly into the MS using a syringe pump with a flow rate of $7.0\ \mu\text{L}$
24
25 min^{-1} . Mass spectra were acquired in a full scan mode (30-500 amu). The instrument was
26
27 operated in positive ion mode under the following conditions: ionspray voltage 4500 V;
28
29 curtain gas, 20 arbitrary units; nebulizer gas, 23 arbitrary units. The MS data were treated
30
31 using Analyst QS 2.0 software.
32
33
34
35

36
37 The accuracy of UV-absorbance in SMZ concentration measurements was verified by
38
39 the parallel determination of SMZ in MS analysis of the PCO-treated samples at different pH
40
41 values with the SMZ pre-constructed calibration curves for both methods: the difference
42
43 observed between SMZ concentrations determined by UV-absorbance and MS did not exceed
44
45 2% at highest, suggesting negligible amounts of UV-absorbance by PCO by-products. For this
46
47 reason, the UV-absorbance was used as a simpler and less time- and resource-consuming
48
49 approach than MS. The UV-absorbance spectra of PCO-treated solutions did not change in
50
51 shape, showing no new peaks or a wave-length shift in maximum absorbance. Poor
52
53 accumulation of UV-absorbing PCO by-products may be explained by their oxidation rates
54
55 being comparable to or exceeding those of SMZ. A similar analytical approach has been used
56
57
58
59
60

1
2
3 in oxidation studies with other antibiotics of aromatic structure, such as sulphamethazine [37],
4
5 chloramphenicol [32], and flumequine [38].
6
7

8 Chemical oxygen demand (COD) was determined by a standard dichromate method
9
10 [39], using HACH kits LCK 314 (15 to 150 mg O L⁻¹) and LCK 414 (5 to 60 mg O L⁻¹). The
11
12 concentration of ammonium was determined photometrically using a modified version of a
13
14 standard phenate method [39]. Five-day biochemical oxygen demand (BOD₅) was also
15
16 determined by a standard method [39]. Nitrate and sulphate anions were determined using a
17
18 Metrohm 761 Compact IC ionic chromatograph.
19
20
21

22 Carbon-doped titania was obtained by the hydrolysis of tetrabutyl orthotitanate at
23
24 room temperature at pH 5.5 to 6.0, followed by drying and calcination at 200, 300 and 500°C.
25
26 After calcinations, the catalysts were washed with hot (70-80°C) distilled water applied in a
27
28 sequence of 15 rinsing rounds (ca 1 L per 1 g of catalyst) to clean the catalyst from water-
29
30 soluble compounds.
31
32
33

34 The crystallinity of carbon-doped titania was analysed using D5000 Kristalloflex,
35
36 Siemens (Cu K α irradiation source) X-ray diffraction spectroscopy (XRD). Carbon content
37
38 was measured with PHI 5600 X-ray photoelectron spectroscopy. The specific area (BET and
39
40 Langmuir adsorption) and the pore volume were measured by the adsorption of nitrogen using
41
42 KELVIN 1042 sorptometer. The composition and the surface properties of the catalysts are
43
44 shown in Table 1.
45
46
47

48 To express the results of SMZ PCO, the PCO efficiency E , defined as the decrease in
49
50 the pollutant amount divided by the amount of energy reaching the treated sample, was
51
52 calculated according to Equation 5:
53
54

$$E = \frac{\Delta c \cdot V \cdot 1000}{I \cdot s \cdot t}, \quad (5)$$

55
56
57
58
59
60

1
2
3 where E – PCO efficiency, $\text{mg W}^{-1} \text{h}^{-1}$; Δc – the decrease in the pollutant's concentration, mg
4 L^{-1} , or COD, mg O L^{-1} ; V – the volume of the sample to be treated, L (in this case, 0.2 L); I –
5 irradiance, mW cm^{-2} ; s – irradiated area, cm^2 ; t – treatment time, h.
6
7
8
9

10 11 12 **Results and discussion**

13 *Sulfamethizole PCO kinetics*

14
15 Photocatalytic oxidation was found to be to be an effective method to degrade SMZ:
16
17 PCO efficiency as high as $15 \text{ mg W}^{-1} \text{h}^{-1}$ ($22 \text{ mg O W}^{-1} \text{h}^{-1}$) was achieved at the initial
18
19 concentration of 100 mg L^{-1} , removing 25% of SMZ. At concentrations below 5 mg L^{-1} , all
20
21 SMZ was eliminated in 6 h with an efficiency of $4 \text{ mg W}^{-1} \text{h}^{-1}$ ($5 \text{ mg O W}^{-1} \text{h}^{-1}$).
22
23
24

25
26 The influence of pH was studied at the SMZ initial concentration of 25 mg L^{-1} . No
27
28 significant impact of pH on SMZ degradation was observed within the pH range 3 to 11
29
30 similarly to PCO of sulfamethoxazole [2]. The adsorption of SMZ, however, slightly
31
32 increased with pH, which may suggest predominant oxidation with the surface reactions since
33
34 radical oxidation should show improved performance in alkaline media due to hydroxide ions
35
36 acting as a hydroxyl radical source [40]. This study did not find any results which support
37
38 more complex interaction between PCO and adsorption with possible mutual compensations:
39
40 the addition of *tert*-butyl alcohol (TBA) as a radical scavenger [40] to the solution to be
41
42 treated in an amount equimolar with sulfamethizole resulted in an insignificant decrease in
43
44 sulfamethizole removal: after 6 h, 75% degraded in the presence of TBA compared to 78% in
45
46 its absence, supporting the hypothesis of prevailing surface oxidation.
47
48
49
50

51
52 Evaluation of the effect of SMZ initial concentration was carried out at pH 5.0 within
53
54 a concentration range from 1 to 100 mg L^{-1} . At lower SMZ concentrations (below 25 mg L^{-1}),
55
56 the decrease of concentration over time was exponential, suggesting a first order of reaction.
57
58 Above 25 mg L^{-1} , however, the oxidation rate was observed to stay at an approximately
59
60 constant level, about 3 to $4 \text{ mg L}^{-1} \text{h}^{-1}$ (Fig. 2), suggesting zero order. The decreasing relative

1
2
3 conversion rate (%) with increased initial concentration indicates that the process limitation is
4
5 the rate of the reaction described by a kinetic equation with an order greater than one. The
6
7 oxidation rate, measured over 6 h as the COD decline, increased from 33 to 60% with
8
9 increasing concentration of SMZ from 1 to 5 mg L⁻¹, and then decreased to 12% as the
10
11 concentration increased further to 100 mg L⁻¹. The efficiency of PCO thus increased with
12
13 increasing SMZ concentration up to 50 mg L⁻¹ and then remained constant at about 21 mg W⁻¹
14
15 h⁻¹ for SMZ oxidation and 15 mg O₂ W⁻¹ h⁻¹ for COD decrease (Fig. 3).
16
17
18
19

20 At the SMZ concentrations within the experimental range, the adsorption on TiO₂
21
22 showed an almost linear growing trend with the SMZ concentration growth. This can be best
23
24 described by a Freundlich isotherm (Eq. 6), with $R^2 = 0.9859$. The values of adsorption in Eq. 2
25
26 are in mmol g⁻¹. The adsorption of SMZ exhibited an increasing trend with the growth of pH.
27
28 This may be explained by the protonation of SMZ molecule in acidic media, which makes the
29
30 molecule positively charged, as is the surface of titanium dioxide, which is also protonated
31
32 under these conditions. This way, the adsorption is somewhat decreased due to the
33
34 electrostatic repulsion. With the increase of pH both SMZ and TiO₂ lose these additional
35
36 protons and their charge, increasing SMZ adsorption.
37
38
39
40

$$q = 0.993 \times c^{0.272} \quad (6)$$

41
42
43
44
45 Biochemical oxygen demand (BOD) of the initial SMZ solution (25 mg L⁻¹) was zero,
46
47 and with progressing PCO it showed, similar to sulfamethoxazole [4], a minor increase, since
48
49 not all the antibiotic was degraded. This finding points to the major difficulty in measuring
50
51 the BOD₅ of SMZ: being zero at higher residual concentrations, BOD₅ is low in solutions
52
53 with effectively degraded SMZ due to the small amount of biodegradable products present,
54
55 resulting in negligible changes in dissolved oxygen concentration in BOD tests. The
56
57 observation also indicates problematic improvement of the biodegradability of antibiotic
58
59 solutions treated by PCO.
60

1
2
3 Experiments with carbon-doped titania were undertaken under artificial visible light.
4
5 These results were less efficient and showed a maximum 10% conversion for a 25 mg L⁻¹
6
7 SMZ solution in 6 h, compared to almost 80% degraded SMZ with UV-irradiated Degussa
8
9 P25 under similar conditions.
10
11

12 A series of experiments using both Degussa P25 titanium dioxide and C-doped titania
13
14 photocatalysts were conducted under solar radiation, the intensity of which was
15
16 overwhelmingly higher than that of artificial light sources with a wider range of wavelengths.
17
18 Solar PCO of SMZ proceeded faster; exponential curves were observed even with SMZ
19
20 concentrations that exhibited zero order-like behaviour with artificial UV-light (Fig. 4).
21
22 Doped titania also showed better PCO performance under solar radiation with 75% SMZ
23
24 removal from the initial solution of 25 mg L⁻¹, although still less efficient than Degussa P25.
25
26
27
28

29 It appeared that the performance of the carbon-doped catalysts in SMZ PCO has a
30
31 negative trend in respect to calcination temperature from 200 to 500°C (Fig. 5). This can be
32
33 explained by the bigger loss of carbon and the contact surface at higher temperature and, thus,
34
35 a commensurate decrease in activity under visible light.
36
37

38 A monomolecular Langmuir-Hinshelwood (L-H) model with substrate decomposition
39
40 on the catalyst surface and immediate by-product desorption was chosen for description of the
41
42 SMZ PCO kinetics. The reaction rate and adsorption constants obtained from the
43
44 experimental data with their standard deviations are given in Table 2, with Figure 6 providing
45
46 the $1/r_0$ vs. $1/C_0$ plot used to calculate these values. It can be seen that the adsorption
47
48 constants obtained from different series of experiments remain close to each other, whereas
49
50 the reaction rate constant under solar radiation noticeably exceeds that of experiments under
51
52 artificial UV. This suggests that the L-H model is a logical data fit for the reaction under
53
54 consideration.
55
56
57
58
59
60

Sulfamethizole PCO by-products and a possible reaction pathway

Ammonia, nitrate and sulphate anions were detected as the SMZ PCO inorganic products.

A number of organic SMZ PCO by-products were determined qualitatively using ESI-MS.

Inorganic ions were detected in small amounts since most nitrogen and sulphur remained in the organic by-products; a result seen also for sulfamethoxazole [33], and amoxicillin [41]. Based on the identified by-products, two possible reaction pathways for SMZ PCO may be proposed (Fig. 7). Both proceed through the break-up of the SMZ molecule at the sulphonamide bond in the early stage. However, the appearance of product with $m/z=287$ suggests preliminary hydroxylation of the SMZ molecule. Consequently, pathway A leads to the formation of a product with $m/z=168$. After the release of sulphate, aminophenol ($m/z=124$) is formed. Along pathway B, the SMZ molecule is cleaved similarly to pathway A, however, the aromatic by-product formed is stabilised into a quinon precursor ($m/z=156$) due to the charge transfer effect. The precursor on the course of its subsequent degradation releases sulphate, giving the quinonic product $m/z=108$, which is further hydroxylated ($m/z=139$). Both aminophenol ($m/z=124$, pathway A) and the hydroxylated imidic derivative of quinone ($m/z=139$, pathway B) seem to be the ultimate clearly detectable products of the respective pathways, and these products undergo subsequent decomposition into smaller fragments, some of which were also identified. Both pathways appear to yield a product with $m/z=116$ (2-amino-5-methyl-1,3,4-thiadiazole), which was observed accumulating in sequential samples.

Conclusions

Photocatalytic oxidation is an effective means for degrading SMZ; at smaller concentrations, total SMZ degradation was achieved together with a significant degree of mineralization. Sulfamethizole PCO seems to proceed mainly through surface reactions. Visible light-sensitive carbon-doped titania showed inadequate PCO performance when compared to Degussa P25. Several SMZ PCO by-products were identified and allowed

1
2
3 construction of possible reaction pathways. The kinetics of SMZ PCO can be datafitted
4
5
6 with the monomolecular Langmuir-Hinshelwood model.
7

8 Acknowledgements

9 The authors express their gratitude to the Estonian Science Foundation (grant 7541), and the United States
10 Civilian Research and Development Foundation (grant US16062) for financial support of the research.
11

12 Table 1. Composition, crystallographic and surface properties of carbon-doped titania
13

14 Table 2. Parameters of Langmuir-Hinshelwood equation calculated for sulfamethizole PCO at
15 Degussa P25 for artificial UV and natural solar radiation
16

17
18 Figure 1. Structural formula of sulfamethizole
19

20 Figure 2. The dependence of sulfamethizole degradation on time at various initial
21 concentrations: pH 5, 20°C
22

23
24 Figure 3. The dependence of sulfamethizole PCO efficiency on its initial concentration: pH 5,
25 20°C
26

27 Figure 4. The dependence of sulfamethizole degradation under natural solar radiation on time
28 at various initial concentrations: pH 5, 20°C
29

30 Figure 5. The effect of calcination temperature on the performance of carbon-doped titania
31 under solar radiation; pH 5, 20°C
32

33 Figure 6: Reciprocal PCO rate vs. reciprocal SMZ initial concentration for artificial UV and
34 solar light at Degussa P25 catalyst for L-H parameters (the point $C_0^{-1} = 315 \text{ mM}^{-1}$
35 corresponding to 1 mg L^{-1} for artificial UV is not shown)
36

37
38 Figure 7. Sulfamethizole PCO reaction pathway.
39

40 D. Klauson (born 1983) is a final year doctoral student at Tallinn University of Technology (TUT), Estonia,
41 Department of Chemical Engineering. His academic grades are Bachelor of Science (2005) and Master of Science
42 (2006). Currently, he is employed at TUT at the position of Engineer.
43

44 M. Krichevskaya (born 1974) is a Senior Researcher at the department of Chemical Engineering, TUT. She
45 received her PhD degree in 2003.
46

47 M. Borissova (born 1977) is a Research Scientist at the department of Chemistry, Tallinn University of
48 Technology. She received her PhD degree in 2007.
49

50 S. Preis (born 1959) is an Associate Professor at Lappeenranta University of Technology (LUT), Finland. His
51 academic degrees are Doctor in Environmental Engineering (TUT, 1988) and Doctor in Chemical Engineering
52 (LUT, 2002).
53

54 55 References

- 56
57 [1] T. Herberer, *Occurrence, fate, and removal of pharmaceutical residues in the aquatic*
58 *environment: A review of recent research data*, Toxicol. Lett. 131 (2002), pp. 5-17
59 [2] M.N. Abellan, B. Bayarri, G. Gimenez, and J. Costa, *Photocatalytic degradation of*
60 *sulfamethoxazole in aqueous suspension of TiO₂*, Appl. Catal. B-Environ. 74 (2007),
pp. 233-241

- 1
2
3 [3] B. Halling-Sørensen, S. Nors Nielsen, P.F. Lanzky, F. Ingerslev, H.C. Holten Lützhof, and S.E. Jørgensen, *Occurrence, fate and effects of pharmaceutical substances in the environment – A review*, Chemosphere 36 (1998), pp. 357-393
- 4
5
6
7 [4] K. Kümmerer, A. Al-Ahmad, and V. Mersch-Sundermann, *Biodegradability of some antibiotics, elimination of their genotoxicity and affection of wastewater bacteria in a simple test*, Chemosphere 40 (2000), pp. 701-710
- 8
9
10 [5] R. Alexy, T. Kümpel, and K. Kümmerer, *Assessment of degradation of 18 antibiotics in the Closed Bottle test*, Chemosphere 57 (2004), pp. 505-512
- 11
12
13 [6] S. Kim, P. Eichhorn, J.N. Jensen, A.S. Weber, and D.S. Aga, *Removal of antibiotics in wastewater: Effect of hydraulic and solid retention times on the fate of tetracycline in the activated sludge process*, Environ. Sci. Technol. 39 (2005), pp. 5816-5823
- 14
15
16 [7] W. Baran, J. Sochacka, and W. Wardas, *Toxicity and biodegradability of sulfonamides and products of their photocatalytic degradation in aqueous solutions*, Chemosphere 65 (2006), pp. 1295-1299
- 17
18
19 [8] S. Wang, H.Y. Zhang, L. Wang, Z.J. Duan, and I. Kennedy, *Analysis of sulfonamide residues in edible animal products: A review*, Food Addit. Contam. 23 (2006), pp. 362-384
- 20
21
22 [9] J.P. Sanderson, D.J. Naisbitt, and B.K. Park, *Role of bioactivation in drug-induced hypersensitivity reactions*, AAPS J, 8 (2006), pp. E55-E64
- 23
24
25 [10] J.F. Jen, H.L. Lee, and B.N. Lee, *Simultaneous determination of seven sulphonamide residues in swine wastewater by high-performance liquid chromatography*, J. Chromatogr. A 793 (1998), pp. 378-382
- 26
27
28 [11] M.Y. Haller, S.R. Müller, C.S. Mc Ardell, A.C. Alder, and M.J.-F. Suter, *Quantification of veterinary antibiotics (Sulfonamides and Trimethoprim) in animal manure by liquid chromatography - mass spectrometry*, J. Chromatogr. A 952 (2002), pp. 111-120
- 29
30
31 [12] C. Hartig, T. Storm, and M. Jekel, *Detection and identification of sulphonamide drugs in municipal waste water by liquid chromatography coupled with electrospray ionisation tandem mass spectrometry*, J. Chromatogr. A 854 (2003), pp. 163-173
- 32
33
34 [13] M.S. Diaz-Cruz and D. Barcelo, *LC-MS² trace analysis of antimicrobials in water, sediment and soil*, Trends Anal. Chem. 24 (2005), pp. 645-657
- 35
36
37 [14] A. Mills, and S Le Hunte, *An overview of semiconductor photocatalysis*, J. Photochem. Photobiol. A 108 (1997), pp. 1-35
- 38
39
40 [15] B. Sun, M. Seto, and J.S. Clements, *Optical study of active species produced by a pulsed corona discharge in water*, J. Electrostat. 39 (1997), pp. 189-202
- 41
42
43 [16] D. Bahnemann, *Photocatalytic water treatment: Solar energy applications*, Sol. Energy 77 (2004), pp. 445-459
- 44
45
46 [17] K. Ichibashi, A. Fujishima, T. Watanabe, and K. Hashimoto, *Quantum yields of active oxidative species formed on TiO₂ photocatalyst*, J. Photochem. Photobiol. A 134 (2000), pp. 139-142
- 47
48
49 [18] R. W. Matthews, *Photo-oxidation of organic material in aqueous suspensions of titanium dioxide*, Water Res. 30 (1986), pp. 569-578
- 50
51
52 [19] V. Brezova, Š. Vodny, M. Vesely, M. Ceppan, and L. Lapcik, *Photocatalytic oxidation of 2-ethoxyethanol in a water suspension of titanium dioxide*, J. Photochem. Photobiol. A 56 (1991), pp. 125-134
- 53
54
55 [20] A. Fujishima, T.N. Rao, and D. Tryk, *Titanium dioxide photocatalysis*, J. Photochem. Photobiol. C 1 (2000), pp. 1-21
- 56
57
58 [21] Y. Zhang, J.C. Crittenden, D.W. Hand, and D.L. Perram, *Fixed-bed photocatalysts for solar decontamination of water*, Environ. Sci. Technol. 28 (1994), pp. 435-442
- 59
60

- 1
2
3 [22] C. Lettmann, K. Hildenbrand, H. Kisch, W. Macyk, and W.H. Maier, *Visible light*
4 *photodegradation of 4-chlorophenol with a coke-containing titanium dioxide*
5 *photocatalyst*, Appl. Catal. B-Environ. 32 (2001), pp. 215-227
6
7 [23] T. Ihara, M. Miyoshi, Y. Iriyama, O. Matsumoto, and S. Sugihara, *Visible-light active*
8 *titanium dioxide realized by an oxygen-deficient structure and by nitrogen doping*,
9 Appl. Catal. B-Environ. 42 (2003), pp. 403-409
10
11 [24] T. Ohno, M. Akiyoshi, T. Umabayashi, K. Asai, T. Mitsu, and M. Matsumura,
12 *Preparation of S-doped TiO₂ photocatalysts and their photocatalytic activities under*
13 *visible light*, Appl. Catal. A-Gen. 265 (2004), pp. 115-121
14
15 [25] D. Li, H. Haneda, S. Hishita, and N. Ohashi, *Visible-light-driven nitrogen-doped TiO₂*
16 *photocatalysts: Effect of nitrogen precursors on their photocatalysis for decomposition*
17 *of gas-phase organic pollutants*, Mater. Sci. Eng. B-Solid 117 (2005), pp. 67-75
18
19 [26] Z. Wang, W. Cai, X. Hong, X. Zhao, F. Xu, and C. Cai, *Photocatalytic degradation of*
20 *phenol in aqueous nitrogen-doped TiO₂ suspensions with various light sources*, Appl.
21 Catal. B-Environ. 57 (2005), pp. 223-231
22
23 [27] S.D. Sharma, D. Singh, K.K. Saini, C. Kant, V. Sharma, S.C. Jain, and C.P. Sharma, *Sol-*
24 *gel-derived super-hydrophilic nickel doped TiO₂ film as active photo-catalyst*, Appl.
25 Catal. A-Gen. 314 (2005), pp. 40-46
26
27 [28] E. Arpac, F. Sayilkan, M. Asiltürk, P. Tatar, N. Kiraz, and H. Sayilkan, *Photocatalytic*
28 *performance of Sn-doped and undoped TiO₂ nanostructured thin films under UV and*
29 *vis-lights*, J. Hazard. Mater. 140 (2007), pp. 69-74
30
31 [29] D. Klauson and S. Preis, *Visible light-assisted aqueous photocatalytic oxidation of*
32 *organic pollutants using nitrogen-doped titania*, Environ. Chem. Lett. 6 (2008), pp.
33 35-39
34
35 [30] Z. Liu, D.D. Sun, P. Guo, and J.O. Leckie, *One-step fabrication and high photocatalytic*
36 *activity of porous TiO₂ hollow aggregates by using a low-temperature hydrothermal*
37 *method without templates*, Chem. Eur. J. 13 (2007), pp. 1851-1855
38
39 [31] A. Al-Ahmad, F.D. Daschner, and K. Kümmerer, *Biodegradability of cefotiam,*
40 *ciprofloxacin, meropenem, penicillin G, and sulfamethoxazole and inhibition of*
41 *wastewater bacteria*, Arch. Environ. Contamin. Toxicol. 37 (1999), pp. 158-163
42
43 [32] A. Chatzikakis, C. Berberidou, I. Paspaltsis, G. Kyriakou, T. Sklaviadis, and I. Poulios,
44 *Photocatalytic degradation and drug activity reduction of Chloramphenicol*, Water
45 Res. 42 (2008), pp. 386-394
46
47 [33] M.N. Abellan, J. Gimenez, and S. Esplugas, *Photocatalytic degradation of antibiotics:*
48 *The case of sulfamethoxazole and trimethoprim*, Cat. Today 144 (2009), pp. 131-136
49
50 [34] L. Hu, P.M. Flanders, P.L. Millerm, and T.J. Strathmann, *Oxidation of sulfamethoxazole*
51 *and related antimicrobial agents by TiO₂ photocatalysis*, Water Res. 41 (2007), pp.
52 2612-2626
53
54 [35] S.J. Kirkpatrick, *A primer on radiometry*, Dent. Mater. 21 (2005), pp. 21-26
55
56 [36] M. Krichevskaya, A. Kachina, T. Malygina, S. Preis, and J. Kallas, *Photocatalytic*
57 *degradation of fuel oxygenated additives in aqueous solutions*, Int. J. Photoenergy 5
58 (2003), pp. 81-86
59
60 [37] S. Kaniou, K. Pitarakis, I. Barlagianni, and I. Poulios, *Photocatalytic oxidation of*
sulfamethazine, Chemosphere 60 (2005), pp. 372-380
[38] R. Palominos, J. Freer, M.A. Mondaca, and H.D. Mansilla, *Evidence for hole*
participation during the photocatalytic oxidation of the antibiotic flumequine, J.
Photochem. Photobiol. A 193 (2008), pp. 139-145
[39] L.S. Clesceri, A.E. Greenberg, and R.R. Trussel, *Standard methods for the examination*
of water and wastewater, APHA, AWWA, WPCF Washington, DC, 1989

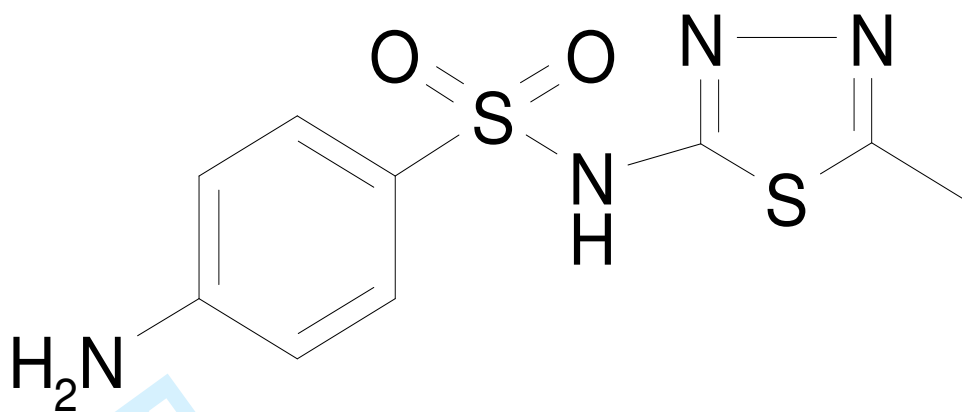
- 1
2
3 [40] Y.F. Sun, and J.J. Pignatello, Evidence for a surface dual hole-radical mechanism in the
4 TiO₂ photocatalytic oxidation of 2,4-dichlorophenoxyacetic acid, *Env. Sci. Technol.*
5 29 (1995), pp. 2065-2072
6
7 [41] D. Klauson, J. Babkina, K. Stepanova, M. Krichevskaya, and S. Preis, *Aqueous*
8 *photocatalytic oxidation of amoxicillin*, *Cat. Today*, in press (2010), doi:10.1016/
9 j.cattod.2010.01.015
10
11
12
13
14
15
16
17
18
19
20
21
22
23
24
25
26
27
28
29
30
31
32
33
34
35
36
37
38
39
40
41
42
43
44
45
46
47
48
49
50
51
52
53
54
55
56
57
58
59
60

For Peer Review Only

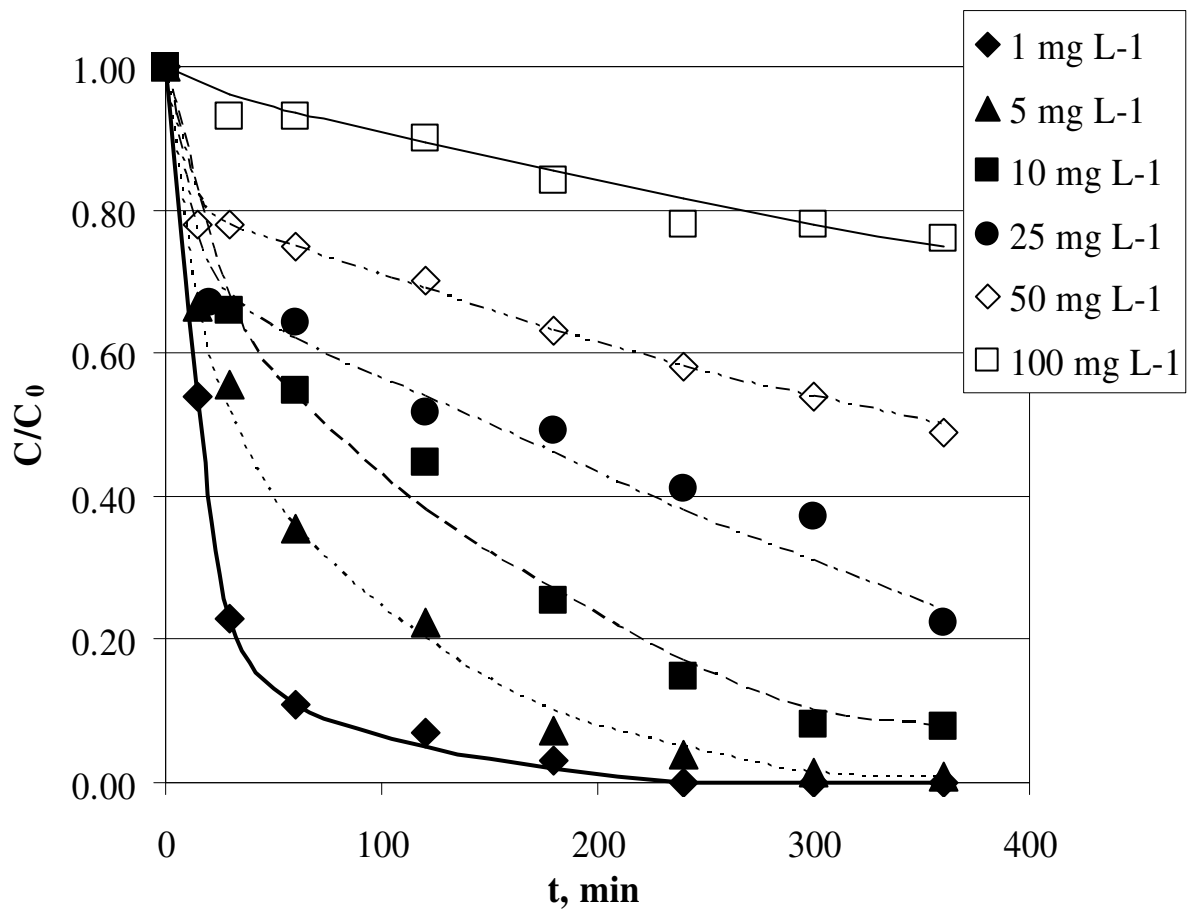
Calcination T, °C	Crystallographic composition, %			Composition, at. %			S _{BET} , m ² /g	S _{Langmuir} , m ² /g	Micropore area, m ² /g	Micropore volume, mm ³ /g
	Anatase	Brookite	Rutile	Ti	O	C				
200	71.9	28.1	-	17.2	45.8	37.0	202.3	278.9	0	0
300	67.5	10.1	22.4	17.9	45.6	36.5	157.2	215.8	0.42	0.15
500	76.9	18.2	5.0	18.5	46.6	34.9	39.45	53.85	3.95	1.39

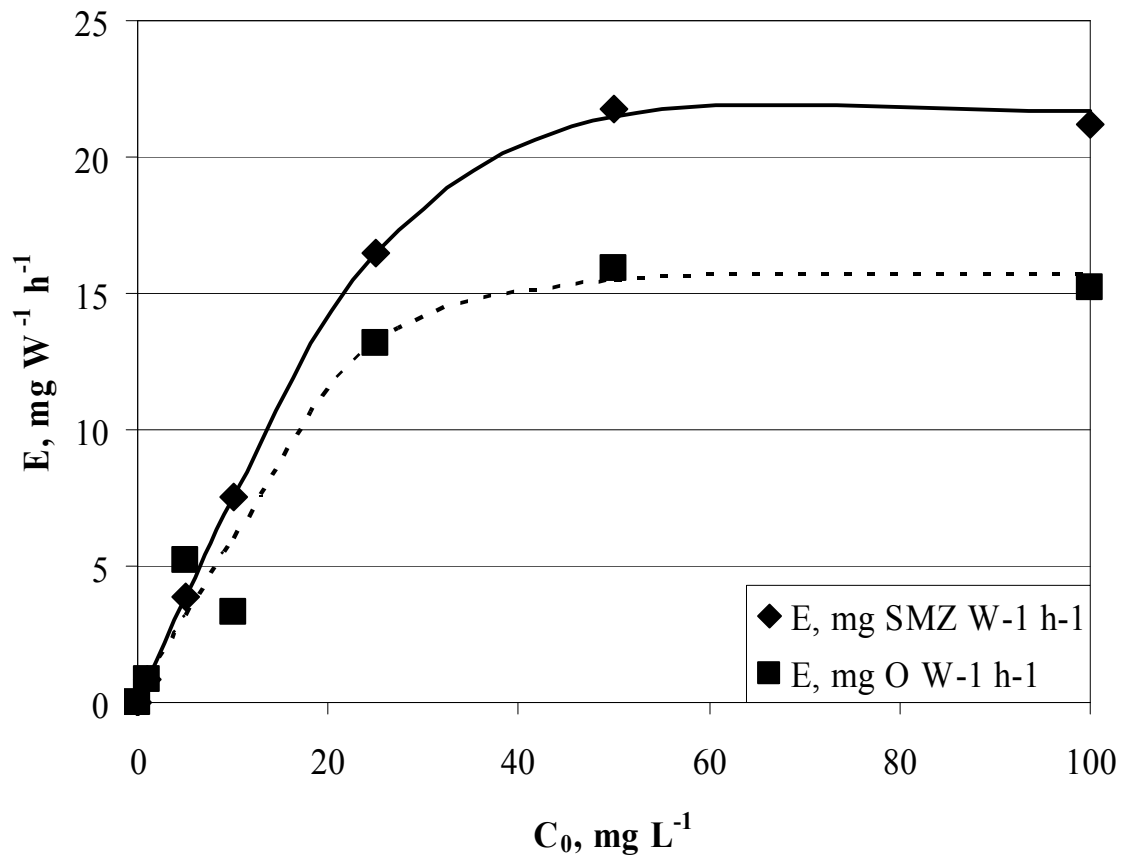
	k, mM ⁻¹ min ⁻¹	K, mM	R ²
Artificial UV	0.29	25.45	0.9921
Solar radiation	2.15	25.05	0.9903

For Peer Review Only

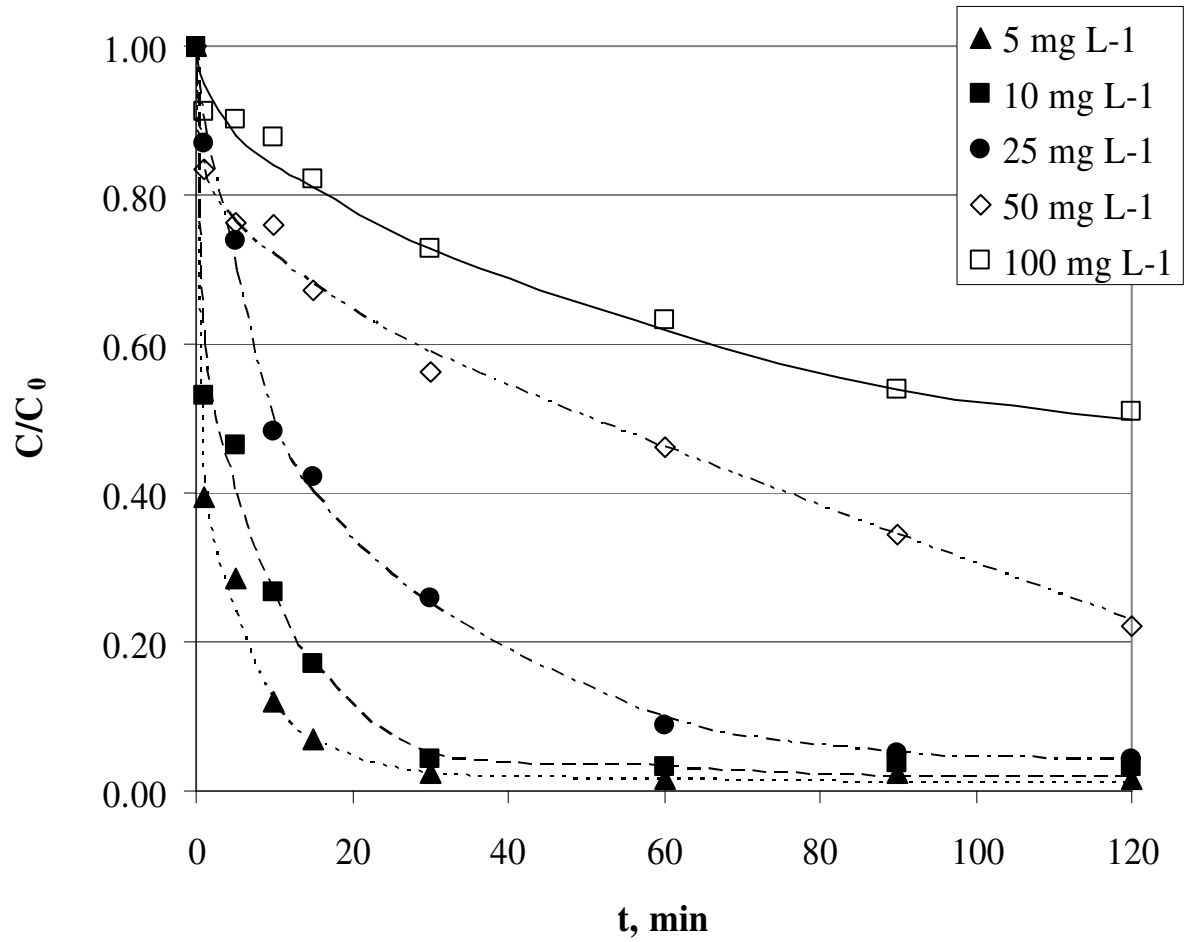


For Peer Review Only

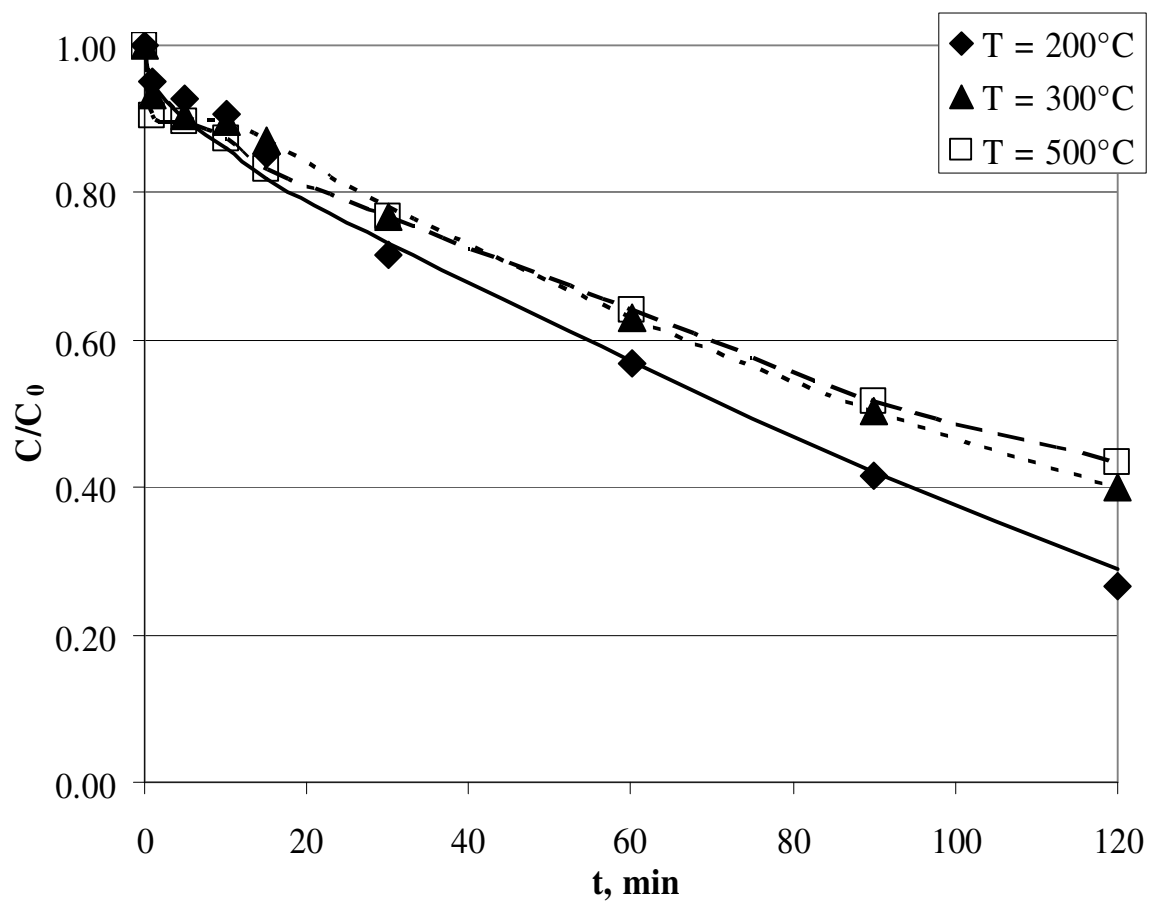


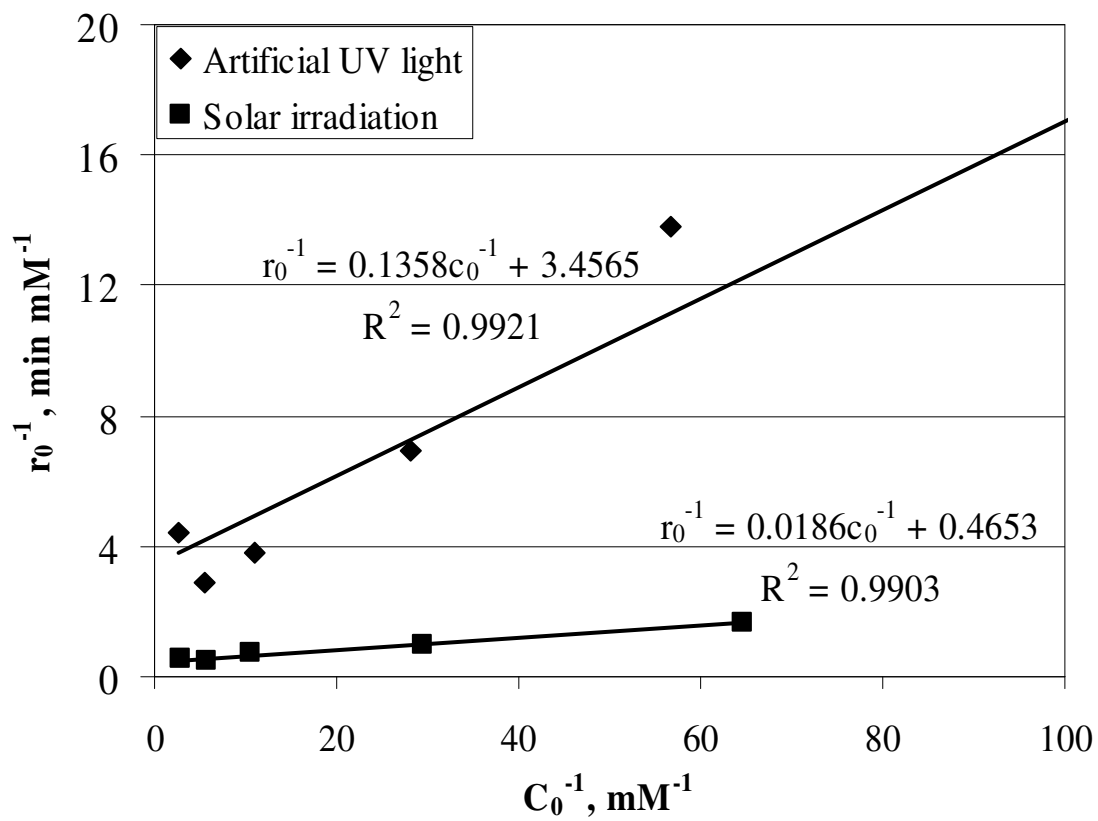


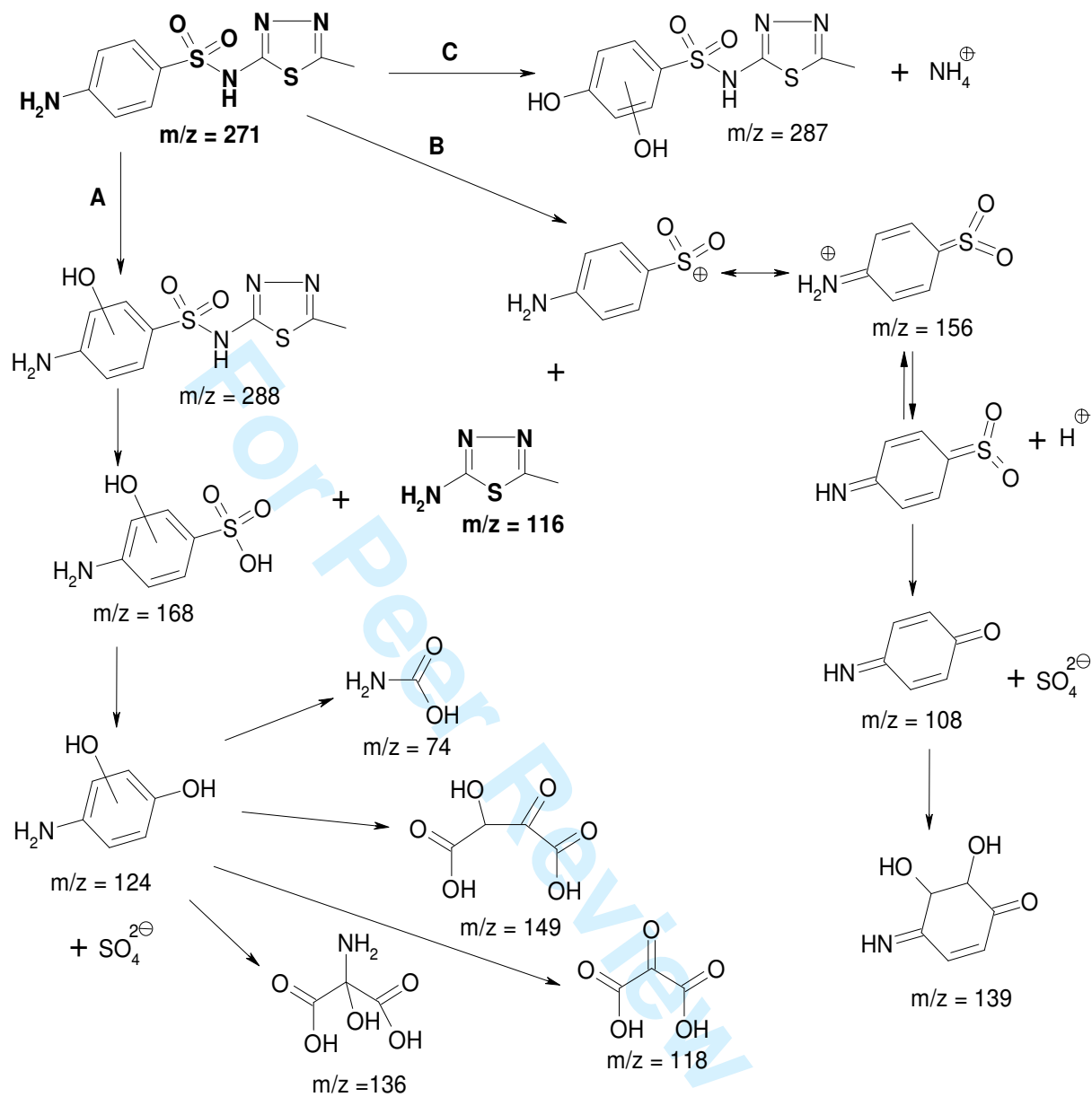
Review Only



View Only







APPENDIX II
SUPPLEMENTARY MATERIALS

Article VIII:

Klauson D., Poljakova A., Krichevskaya M., Preis S., Aqueous photocatalytic oxidation of doxycycline, submitted to Journal of Photochemistry and Photobiology A (as of 14.04.2010)

Aqueous photocatalytic oxidation of doxycycline

Deniss Klauson¹, Alissa Poljakova¹, Marina Krichevskaya¹ and Sergei Preis²

¹Department of Chemical Engineering, Tallinn University of Technology, Ehitajate tee 5, 19086 Tallinn, Estonia
Fax: +372 620 2856; tel. +372 620 2857; e-mail: deniss.klauson@ttu.ee

²LUT Chemistry, Lappeenranta University of Technology, P.O. Box 20, 53851 Lappeenranta, Finland

Abstract

The research into the aqueous photocatalytic oxidation of doxycycline was undertaken with Degussa P25 titanium dioxide and visible light-sensitive sol-gel synthesized carbon-containing titania as photocatalysts. The effect of titanium dioxide concentration, initial doxycycline concentration, pH and the catalysts properties on the photocatalytic oxidation efficiency was examined. Identified doxycycline photocatalytic oxidation by-products allowed proposal of a possible doxycycline degradation pathway.

Keywords: oxidation pathway, tetracycline antibiotics, doped titania, calcinations, advanced oxidation process

1. Introduction

Antibiotics in wastewaters are refractory substances [1-3] passing the biological treatment plants intact [4], remaining in the liquid phase or adsorbing to the active sludge [5]. They pose a threat to micro-flora and fauna, accumulate in food chains [6, 7], and develop resistant micro-organisms, including pathogens [8-11]. Doxycycline (DC, (4*S*,4*aR*,5*S*,5*aR*,6*R*,12*aS*)-4-(dimethylamino)-3,5,10,12,12*a*-pentahydroxy-6-methyl-1,11-dioxo-1,4,4*a*,5,5*a*,6,11,12*a*-octahydrotetracene-2-carboxamide) is a tetracycline antibiotic used against bacteria, protozoa and helminths. Since DC is used against some of the most hazardous diseases, i.e. bubonic plague and anthrax [12, 13], its prevention from entering the environment is of great importance.

Photocatalytic oxidation (PCO) is based on the action of positively charged holes on the illuminated semiconductor, most often TiO₂. Water molecules decompose on the holes forming hydroxyl radicals [14]; the hole, having even higher oxidation potential [15], can also degrade pollutants. The ratio of radical to hole oxidation depends on the adsorptive and reactive properties of pollutants [16-18]. The elucidation of the DC PCO reaction pathway was one of the main objectives of the present research, since the published works on the oxidation of antibiotics mainly focus on the parent compound removal and mineralization.

Titania photocatalysts can use only UV fraction (4%) of solar radiation due to the high band gap energy [19]. This makes sensitising TiO₂ to visible light the way of widening of utilised solar spectrum. TiO₂ can be doped with various elements reducing the band-gap [20-26] for excitation of electrons by lower energy photons. However, the authors found that the doped titania photocatalysts may oxidise only selected pollutants [27-30]. This can be explained by the smaller redox potential and, possibly, faster electron-hole recombination [31].

Several works regarding the degradation of tetracycline, compound belonging to the same family of antibiotics as DC, have been published up to date [32-34]. The main novelty of the present research and its difference from these works is the research into the PCO degradation pathways with the aid of UPLC-MS (see Materials and Methods), which allowed to identify DC degradation mechanisms and their dependence on the substance's adsorption on the catalyst surface. Another major novelty is the departure from already well-established practice of using solely UV-sensitive commercial catalysts in the PCO of antibiotics, and the application of efficient visible light-sensitive photocatalysts that are able to degrade DC much better than these.

2. Materials and methods

Two thermostatted at 20±1°C 200-mL batch reactors with inner diameter 100 mm, irradiated plane surface 40 m² m⁻³, with magnetic stirrers, were used: the one used for the PCO called "active" and the other containing no photocatalyst called "reference", exposed to the identical conditions. The samples from both reactors were compared to avoid errors caused by water evaporation. A UV-light source, Phillips Actinic BL low pressure luminescent mercury UV-lamp (15 W) with maximum emission around 365-nm was positioned horizontally over the reactors, providing the irradiance of 1.5 mW cm⁻² at their surface, measured by the radiometer Micropulse MP100. With the daylight fluorescent lamp (Phillips TL-D 15W/33-640), the illuminance was measured using TES 1332 luxmeter reaching 3,700 lx (lm/m²), which corresponds to the irradiance of 0.6 mW cm⁻² [35].

Titanium dioxide was used as slurry (0.5 to 1.5 g L⁻¹). The DC (Sigma-Aldrich) concentration varied from 10 to 100 mg L⁻¹. The pH impact was studied in the range from 3 to 7, adjusted by sulphuric acid or sodium hydroxide. The treatment time was from 1 to 4 h to achieve at least 50% reduction of the initial DC concentration. Experiments were carried out for three times under identical conditions with the average deviations under 5%.

To determine the DC concentration, two methods were compared in PCO experiments: photometrical determination of specific UV-absorption (SUVA) at 346 nm using Helios β spectrophotometer, and the Waters Aquity UPLC combined with MS and quadrupole-time of flight (Q-TOF) mass-analyzer used for the determination of organic DC PCO by-products. An Aquity UPLC BEH C₁₈ 1.7 μm 2.1×100 mm column was used with 0.1% formic acid aqueous solution, eluent A (initial one), and 0.1% formic acid acetonitrile solution, eluent B. The complete change from A to B was programmed for 15 min out of 20 min run with linear gradient. Mass spectra were acquired in full scan mode (50-500 amu), the MS operated in positive ion mode and capillary voltage of 2400 V. The MS-data were handled using MassLynx software. The reason for using two methods was the ease of spectrophotometric determination, provided no or little interference of the UV-absorbing DC PCO by-products. UV-absorbance proved its applicability with sufficient accuracy for negligible differences between the concentration values obtained in PCO experiments. The by-products of DC PCO were identified using the same UPLC-MS method.

Chemical oxygen demand (COD) was determined by a standard dichromate method [36], using HACH kits LCK 314 (15 to 150 mg O L⁻¹) and LCK 414 (5 to 60 mg O L⁻¹). The concentration of ammonium ion was determined photometrically using a modified version of a standard phenate method [36]. Anions were determined using Metrohm 761 Compact IC ionic chromatograph.

Adsorption experiments were carried out in thermostatted flasks with magnetic stirrers at 20±1°C. The amount of adsorbed substance was derived from the mass balance by determining the concentration of the dissolved substance before and after adsorption at the equilibrium reached in 2 h.

Specimens of carbon-doped titania were obtained by the hydrolysis of tetrabutyl orthotitanate at room temperature with unadjusted pH around 5.5 to 6.0, followed by calcination from 200 to 800°C. After calcinations, the catalysts were washed with hot (70-80°C) distilled water applied in a sequence of 15 rinsing rounds (ca 1 L per 1 g of catalyst) to clean the catalyst from water-soluble compounds.

The crystallinity of carbon-doped titania was analysed using D5000 Kristalloflex, Siemens (Cu Kα irradiation source) X-ray diffraction spectroscope (XRD). Carbon content was measured with PHI 5600 X-ray photoelectron spectroscope. The specific area (BET and Langmuir adsorption) and the pore volume were measured by the adsorption of nitrogen using KELVIN 1042 sorptometer.

To express the results of DC PCO, the PCO efficiency E , defined as the decrease in the pollutant amount divided by the amount of energy reaching the treated sample, was calculated according to Equation 1 [37]:

$$E = \frac{\Delta c \cdot V \cdot 1000}{I \cdot s \cdot t}, \quad (1)$$

where E – PCO efficiency, mg W⁻¹ h⁻¹; Δc – the decrease in the pollutant's concentration, mg L⁻¹, or COD, mg O L⁻¹; V – the volume of the sample to be treated, L (in this case, 0.2 L); I – irradiance, mW cm⁻²; s – irradiated area, cm²; t – treatment time, h.

3. Results and discussion

3.1. PCO experiments with Degussa P25

The best PCO performance was observed at pH 4.4, occurring naturally in the DC solutions, followed closely by neutral and acidic media, i.e. the pH-dependence was weakly pronounced. Optimum catalyst dose was expectedly determined to be 1 g L⁻¹.

Figure 1 shows the dependence of PCO efficiency on the DC initial concentration, calculated for 1 h treatment: E increases with the increased initial DC concentration assuming the description of the DC PCO using Langmuir-Hinshelwood (L-H) model of monomolecular surface reaction, followed by the products desorption (Eq. 2). The equation, derived from the experimental data via the $1/r_0 = f(1/c_0)$ dependence (plot not shown), has average square deviation $R^2=0.9877$, supporting the proposed L-H data fit. The reaction rate equation

$$r_0 = k \frac{Kc_0}{1 + Kc_0}, \quad (2)$$

where r_0 is the reaction rate, mM min^{-1} ; k – reaction rate constant, $\text{mM}^{-1} \text{min}^{-1}$; K – adsorption constant, mM ; c_0 – initial DC concentration, mM , gives $k = 0.002 \text{ mM}^{-1} \text{ min}^{-1}$ and $K = 10.2 \text{ mM}$.

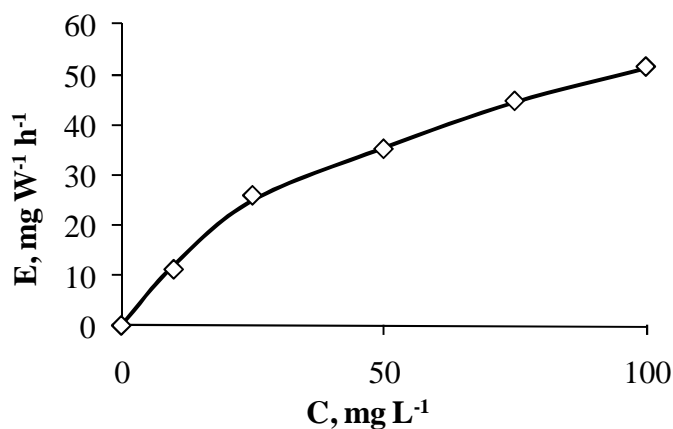


Figure 1. The dependence of DC PCO efficiency on the DC initial concentration with 1 g L^{-1} Degussa P25 TiO_2 (1 h treatment time, pH 4.4)

With the addition of *tert*-butyl alcohol (TBA) as a radical scavenger in the amount equimolar with DC (0.056 mM, i.e. 25 mg/l of DC and 4.2 mg L^{-1} of TBA), the DC degradation rate decreased by a very small amount, comparable to the accuracy limit in parallel experiments, which, together with the indifference towards pH, allows suggesting the dominance of hole oxidation reactions.

The DC adsorption on the P25 was from 5.9 mg g^{-1} at the initial DC concentration of 10 mg L^{-1} to 20 mg g^{-1} at 100 mg L^{-1} . Similar to the PCO results fitting to the L-H model, the adsorption experimental data fit well to the Langmuir equation (Eq. 3, $R^2=0.9836$):

$$q_L = q_{\max} \frac{Kc_0}{1 + Kc_0}, \quad (3)$$

where q – adsorption, mmol g^{-1} ; q_{\max} – theoretical maximal adsorption, mmol g^{-1} , giving $q_{\max} = 0.08 \text{ mmol g}^{-1}$ and $K = 9.2 \text{ mM}$. The K -values obtained from PCO and adsorption experiments demonstrate consistency.

The percent of degraded COD was reasonably high at smaller concentrations: e.g. at 10-25 mg DC L^{-1} , up to 80% COD was degraded in 2 h. However, with 100 mg DC L^{-1} , only 7% of COD was degraded in 4 h. The disproportion observed at higher concentrations may be explained by the accumulation of non-aromatic by-products (see Fig. 3). This assumption is consistent with the minor discrepancy between the UV-absorbance at 346 nm and the UPLC-MS measurements of the DC concentration in PCO-treated solutions (Section 2). Also, the low mineralization degree of nitrogen is consistent with accumulation of organic by-products at higher DC concentrations (Section 3.3).

3.2. PCO experiments with carbon-containing titania

The parameters of carbon-doped catalysts can be seen in Table 1. The catalysts performance was tested with DC solutions of 25 mg L^{-1} at pH 4.4. Under visible light the catalyst calcinated at 200°C , having the highest carbon content and the contact surface, showed performance superior to that of Degussa P25: if P25 removed 19.5 mg L^{-1} , C- TiO_2 calcinated at 200°C degraded 23.2 mg L^{-1} under visible light of 2.5 times lower irradiance, making the PCO efficiency about three times higher. With the increased catalysts' calcination temperature, their performance decreased (Fig. 2).

T(calcination), °C	Crystallographic composition, %			Composition, at. %			S(BET), m ² g ⁻¹	S(Langmuir), m ² g ⁻¹	Micropore area, m ² g ⁻¹	Micropore volume, mm ³ g ⁻¹
	Anatase	Brookite	Rutile	Ti	O	C				
200	71.9	28.1	-	17.2	45.8	37.0	202.3	278.9	0	0
400	78.1	21.9	-	18.1	46.6	34.9	105.7	144.7	4.12	1.54
500	76.9	18.2	5.0	18.5	46.6	34.9	39.45	53.85	3.95	1.39
600	74.4	25.6	-	20.0	49.6	30.4	8.81	12.08	0	0
700	-	-	100	18.0	47.3	34.7	3.52	4.81	0.20	0.07
800	0.8	-	99.2	19.3	52.3	28.4	3.75	5.14	0.13	0.05

Table 1. Composition and surface properties of carbon-containing photocatalysts dependent on calcinations temperature

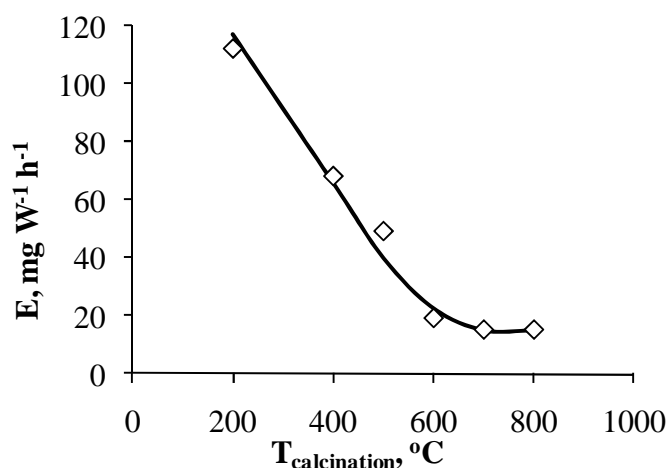


Figure 2. The dependence of DC PCO efficiency on the calcinations temperature of the carbon-modified titania (1 g L⁻¹): 25 mg L⁻¹, pH 4.4

3.3. Doxycycline PCO reaction pathway

Ammonia, nitrite and nitrate in trace amounts were detected, indicating the most of nitrogen remaining in organic by-products. The determined by-products allow distinguishing three simultaneous PCO pathways (Fig. 3). Two of them, A and C, begin with oxidation of the terminal parts of the DC molecule ($m/z=445$): in pathway A, aromatic ring is destroyed forming the identified product with $m/z=409$, whereas pathway C begins with the subtraction of dimethyl amino- and amino groups and their replacement by hydroxyl group, together with phenolic cycle hydroxylation ($m/z=435$). Pathway B proceeds through the cleavage of DC molecule in two fragments, $m/z=183$ and $m/z=273$. In pathway A, the product $m/z=409$ goes through oxidation of the part adjacent to the degraded phenolic ring, forming monocyclic product $m/z=273$. The latter is also formed in pathway B. Pathway C proceeds with oxidation of the product with $m/z=435$ to the ones with $m/z=224$ and, subsequently, 255. Products $m/z=183$, 255 and 273 are the ultimate detectable by-products, likely degrading into small unidentified fragments.

The variety of the pathways may be explained by the DC molecule adsorption at the phenolic (A), alcohol (B) or amino group (C). Due to minor presence of the mineral nitrogen and the minority of aromatic products, the minor importance of the pathway C may be assumed.

4. Conclusions

Aqueous PCO of DC was studied using Degussa P25 and visible light-sensitive synthetic sol-gel titania catalysts doped with carbon. The titania sample with the highest carbon content and contact surface showed performance surpassing the one of P25. The performance of carbon-containing titania decreased with the increasing calcination temperature, i.e. decreasing carbon content and contact surface. The PCO of DC appeared to be less sensitive towards the pH and presence of a radical scavenger suggesting DC PCO likely proceeding mainly through hole reactions. The PCO efficiency increases with the DC increasing concentration, although the PCO by-products accumulate at higher pollutant concentration. The character of the DC PCO by-products allows suggesting predominant decomposition of aromatic ring.

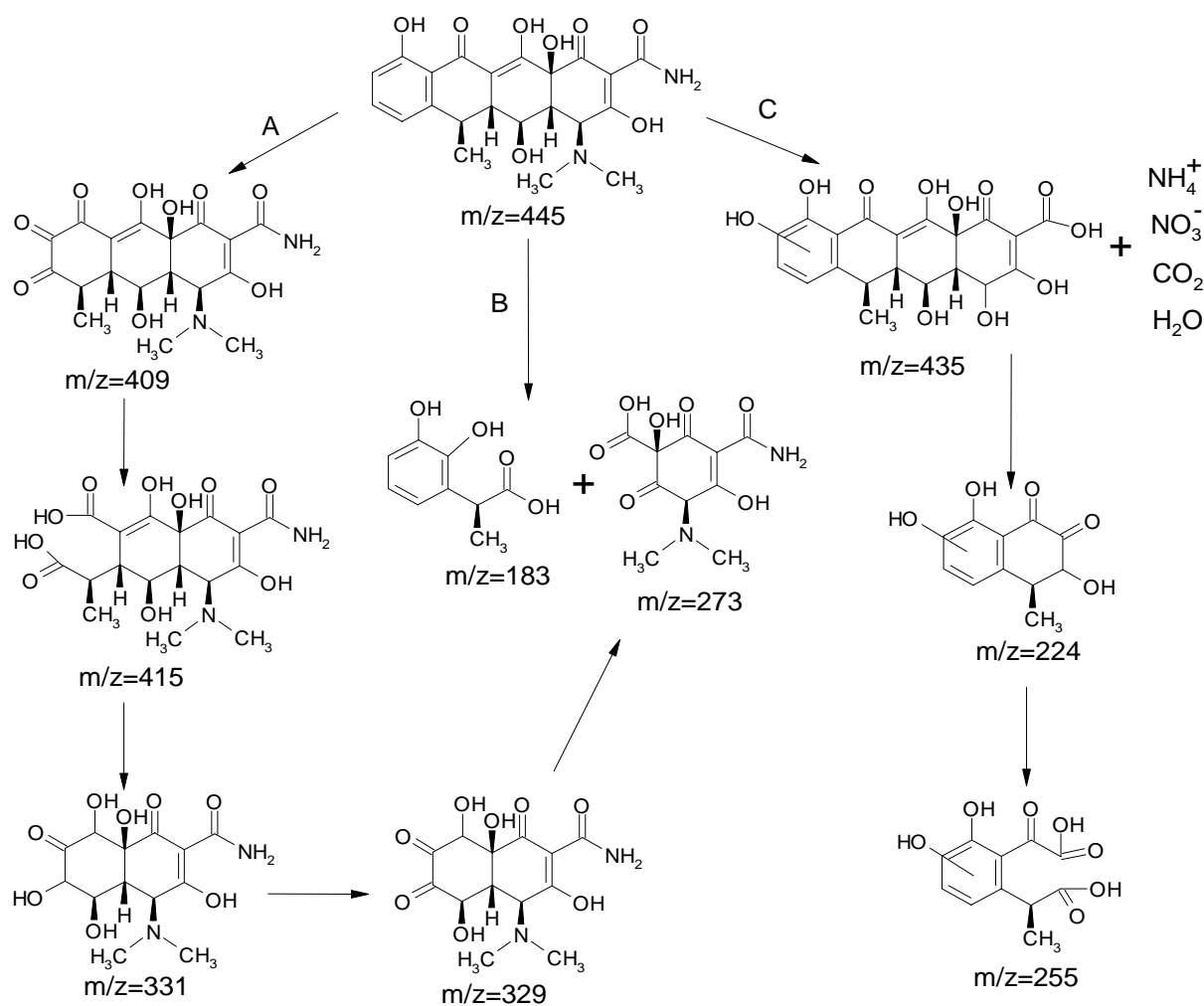


Figure 3. Proposed DC PCO reaction pathways

5. Acknowledgements

The authors thank Dr. Anna Moiseev, TU of Clausthal, for XRD measurements, Mr. Andrew S. Cavanaugh, the University of Colorado, Boulder, for XPS measurements, and Dr. Mai Uibu, Tallinn UT, for surface area measurements. The support of the Estonian Science Foundation (G7541) and the US Civilian Research and Development Foundation (US16062) is greatly appreciated.

6. References

- [1] A. Al-Ahmad, F.D. Daschner, K. Kümmerer, Arch. Environ. Contam. Toxicol., 37 (1999) 158-163
- [2] K. Kümmerer, A. Al-Ahmad, V. Mersch-Sundermann V., Chemosphere, 40 (2000) 701-710
- [3] R. Alexy, T. Kümpel, K. Kümmerer, Chemosphere 57 (2004) 505-512
- [4] T. Herberer, Toxicol. Lett., 131 (2002) 5-17
- [5] M.N. Abellan, B. Bayarri, G. Gimenez, J. Costa, Appl. Catal., B 74 (2007) 233-241
- [6] B. Halling-Sørensen, S. Nors Nielsen, P.F. Lanzky, F. Ingerslev, H.C. Holten Lützhof, S.E. Jørgensen, Chemosphere 36 (1998) 357-393

- [7] C. Hartig, T. Storm, M. Jekel, *J. Chromatogr.*, A 845 (1999) 163-173
- [8] S. Kim, P. Eichhorn, J.N. Jensen, A.S. Weber, D.S. Aga, *Environ. Sci. Technol.* 39 (2005) 5816-5823
- [9] W. Baran, J. Sochacka, W. Wardas, *Chemosphere*, 65 (2006) 1295-1299
- [10] H. Sørum, in: F.M. Aarestrup, *Antimicrobial Resistance in Bacteria of Animal Origin*, American Society for Microbiology Press, Washington, DC, 2006
- [11] A. Chatzikakis, C. Berberidou, I. Paspaltsis, G. Kyriakou, T. Sklaviadis, I. Poullos, *Water Res.*, 42 (2008) 386-394
- [12] R.A. Greenfield, M.S. Bronze, *Drug Discov. Today*, 8 (2003) 881-888
- [13] I. Brook, *Int. J. Antimicrob. Ag.*, 20 (2002) 320-325
- [14] B. Sun, M. Sato, J.S. Clements, *J. Electrostat.*, 39 (1997) 189-202
- [15] D. Bahnemann, *Sol. Energy*, 77 (2004) 445-459
- [16] R.W. Matthews, *Water Res.*, 20 (1986) 569-578
- [17] V. Brezova, Š. Vodny, M. Vesely, M. Ceppan, L. Lapcik, *J. Photochem. Photobiol. A*, 56 (1991) 125-134
- [18] J. Chen, D.F. Ollis, W.H. Rulkens, H. Bruning, *Water Res.*, 33 (1999) 669-676
- [19] Y. Zhang, J.C. Crittenden, D.W. Hand, D.L. Perram, *Environ. Sci. Technol.*, 28 (1994) 435-442
- [20] C. Lettmann, K. Hildenbrand, H. Kisch, W. Macyk, W.H. Maier, *Appl. Catal.*, B 32 (2001) 215-227
- [21] E. Arpac, F. Sayilkan, M. Asiltürk, P. Tatar, N. Kiraz, H. Sayilkan, *J. Hazard. Mater.*, 140 (2007) 69-74
- [22] T. Ihara, M. Miyoshi, Y. Iriyama, O. Matsumoto, S. Sugihara, *Appl. Catal.*, B 42 (2003) 403-409
- [23] S.D. Sharma, D. Singh, K.K. Saini, C. Kant, V. Sharma, S.C. Jain, C.P. Sharma, *Appl. Catal.*, A 314 (2006) 40-46
- [24] D. Li, H. Haneda, S. Hishita, N. Ohashi, *Mater. Sci. Eng.*, B 117 (2005) 67-75
- [25] Z. Wang, W. Cai, X. Hong, X. Zhao, F. Xu, C. Cai, *Appl. Catal.*, B 57 (2005) 223-231
- [26] T. Ohno, M. Akiyoshi, T. Umabayashi, K. Asai, T. Mitsu, M. Matsumura, *Appl. Catal.*, A 265 (2004) 115-121
- [27] D. Klauson, E. Portjanskaja, S. Preis, *Environ. Chem. Lett.*, 6 (2008) 35-39
- [28] D. Klauson, E. Portjanskaja, O. Budarnaja, M. Krichevskaya, S. Preis, *Catal. Comm.*, 11 (2010) 715-720
- [29] D. Klauson, J. Babkina, K. Stepanova, M. Krichevskaya, S. Preis, *Catal. Today*, (2010) in press, doi:10.1016/j.cattod.2010.01.015
- [30] D. Klauson, M. Krichevskaya, M. Borissova, S. Preis, *Environ. Technol.*, (2010) in press
- [31] Z. Liu, D.D. Sun, P. Guo, J.O. Leckie, *Chem.—Eur. J.*, 13 (2007) 1851-1855
- [32] M. Addamo, V. Augigliaro, A. di Paola, E. Garcia-Lopez, V. Loddo, G. Marci, L. Palmisano, *J. Appl. Electrochem.*, 35 (2005) 765-774
- [33] C. Reyes, J. Fernandez, J. Freer, M.A. Mondaca, C. Zaror, S. Malato, H.D. Mansilla, *J. Photochem. Photobiol. A*, 184 (2006) 141-146
- [34] R.A. Palominos, M.A. Mondaca, A. Giraldo, G. Penuela, M. Perez-Moya, H.D. Mansilla, *Catal. Today*, 144 (2009) 100-105
- [35] S.J. Kirkpatrick, *Dent. Mater.*, 21 (2005) 21-26
- [36] L.S. Clesceri, A.E. Greenberg, R.R. Trussel, *Standard methods for the examination of water and wastewater*, 17th ed. APHA, AWWA, WPCF Washington, DC, 1989
- [37] S. Preis, M. Krichevskaya, Y. Terentyeva, A. Moiseev, J. Kallas, *J. Adv. Oxid. Technol.*, 5 (2002) 77-84

Article IX:

Klauson D., Budarnaja O., Stepanova K., Krichevskaya M., Preis S., Aqueous photocatalytic oxidation of selected organic pollutants using carbon-containing titania, submitted to Environmental Technology (as of 14.04.2010)

Aqueous photocatalytic oxidation of selected organic pollutants using carbon-containing titania

D. Klauson^{1*}, Olga Budarnaja¹, Kristina Stepanova¹, M. Krichevskaya¹, S. Preis²

¹ Department of Chemical Engineering, Tallinn University of Technology, Ehitajate tee 5, Tallinn 19086, Estonia

² LUT Chemistry, Lappeenranta University of Technology, P. O. Box 20, Lappeenranta 53851, Finland

Tel.: +372 620 2857, fax: +372 620 2856, e-mail: deniss.klauson@ttu.ee

(Received xxx 2010; final version received xxx 2010)

Aqueous photocatalytic oxidation of methyl-*tert*-butyl ether, *p*-toluidine and phenol was studied using carbon-containing titania as the photocatalyst active in visible light. The selective character of the C-TiO₂ catalysts was observed: with MTBE and *p*-toluidine under visible light the activity of C-TiO₂ catalysts calcined at different temperatures was similar to or even surpassing that of Degussa P25 under UV, although phenol was oxidized poorly.

Keywords: photocatalytic oxidation (PCO), carbon-containing titania, methyl-*tert*-butyl ether (MTBE), *p*-toluidine, phenol

Introduction

Photocatalytic oxidation (PCO) of organic pollutants is based on the action of positively charged holes formed at the semiconductor surface by the displacement of electrons with irradiation, oxidising organic pollutant molecules adsorbed on the photocatalyst surface or water molecules to hydroxyl radicals that subsequently react with the pollutant. Commercially available titanium dioxide photocatalysts with the band-gap energy of 3.2 eV can utilize only ultraviolet radiation photons, i.e. only 4% of the solar radiation reaching the Earth surface. The band-gap can be reduced by introducing additive atoms into titanium dioxide, thus creating a crystalline structure with a misbalance in charge carriers creating a new energetic level inside the band-gap, from which electrons can be displaced with greater wavelength radiation. Various non-metal dopants are used in photocatalyst synthesis widening the active light spectrum, although the results of anion doping are often contradictory: widening the absorption spectrum, the doping makes the photocatalytic activity weak [1, 2]. The authors observed the selective character of the PCO with N-, S- and B-doped catalysts showing dramatically different efficiencies with different substances [3, 4].

The synthesis of doped photocatalysts using hydrolysis of titanium organic substances in presence of doping element admixtures does not produce titania free from admixtures of carbon [3-5]. This requires clarification of its dopant role, undertaken in the present research: the aqueous PCO of methyl *tert*-butyl ether (MTBE), *p*-toluidine, and phenol, using carbon-containing titanium dioxide under visible light was studied.

Methyl *tert*-butyl ether, banned in the USA, is still widely used as an oxygenated component of motor fuels by the rest of the world. This substance is of particular concern because of its accumulation in groundwater due to its low biodegradability [6]. Physical removal and chemical oxidation methods, such as air stripping, activated carbon adsorption, ozonation and treatment with Fenton's reagent have been proven to be ineffective against MTBE [7-9].

p-Toluidine is a widely used chemical with its use ranging from a component of jet and rocket fuels to applications in paint and pharmaceutical industries [10, 11]. Also, at former munitions sites *p*-toluidine is a degradation intermediate of *p*-nitrotoluene. Thus, the pollution of soil and subsequently groundwater with this substance can occur on the site of acting and abandoned military installations. Being non-biodegradable, *p*-toluidine may accumulate in groundwater aquifers.

Phenol has a reputation of a standard contaminant that is used to test the efficiency of various oxidation methods, or the activity of different catalysts [12]. Phenol can also be an environment pollutant, as it is in North-Eastern Estonia, where it gets into aquifers with a leachate from oil shale ash dumps [13].

In the present research, the authors tested eleven carbon-containing titania photocatalysts sensitive to visible light in PCO of the abovementioned pollutants aiming the analysis of the catalyst composition and calcinations temperature impacts on the PCO efficiency. The results were compared to the ones obtained with Degussa P25 titanium dioxide.

Materials and methods

Two thermostatted at $20\pm 1^\circ\text{C}$ mechanically agitated with magnetic stirrers 200-mL simple batch reactors with inner diameter 100 mm (evaporation dishes), irradiated contact surface $40\text{ m}^2\text{ m}^{-3}$, were used in PCO experiments: the one used for the PCO was called “active” and the other, called “reference”, contained no photocatalyst and was not exposed to the UV-light. The samples from the active reactor were compared to the reference samples to avoid complications caused by water evaporation. A UV-light source, Phillips 365-nm low pressure luminescent mercury UV-lamp (Sylvania Blacklight F15 W 350 BL-T8), was positioned horizontally over the active reactor, providing the irradiance of about 0.7 mW cm^{-2} measured at a distance corresponding to the level of the free surface of the reactor by the optical radiometer Micropulse MP100 (Micropulse Technology, UK). With daylight fluorescent lamp (Philps TL-D 15W/33-640), the irradiance was measured indirectly, being calculated from the illuminance, measured by TES luxmeter (TES, Taiwan), using lumen to watt ratio of 684, as the response of human eye to light with the illuminance of 684 lm equals to that to the irradiance of 1 W [14]. With Phillips TLD lamp, the amount of UV-irradiation was also specifically measured using the abovementioned Micropulse radiometer for 254 and 365 nm, as well as the total amount of UV by using Ocean Optics USB2000+UV-VIS spectrometer. Only negligibly small fraction of UV around 365-400 nm was registered, which is in agreement with the data from the lamp manufacturer [15]. Thus, any noticeable action of the photocatalyst when using Phillips TLD lamp as the irradiation source may not be attributed to the UV fraction emitted by the lamp but is clearly due to the activity of the catalysts in visible light.

The experiments were carried out using aqueous solutions of the chemicals supplied by Aldrich. With MTBE, the experiments were conducted with synthetic solutions at 100 mg L^{-1} at naturally set pH 6.5. The maximum treatment time was 1 h. Similarly, with *p*-toluidine 100 mg L^{-1} solution was used, while maximum treatment time was 24 h. The experiments were carried out at pH 3, 6.5 (naturally set) and 11. Phenol 100 mg L^{-1} solutions at the treatment time of 24 h were treated at natural pH 6.5. The pollutant concentrations were chosen with reference to those found in real contaminated aquifers used in previous experiments [13, 16]. The treatment time was chosen to provide the concentration of pollutants reduced to about 50%; this was also used in calculations of the process efficiency E (see Eq. 1). All the experiments were carried out for at least three times under identical experimental conditions to derive the average value of the process efficiency. The average deviation of data in parallel experiments did not exceed 5%. In order to evaluate the stability

of the photocatalysts, the repeated experiments were carried out using the same portion of the photocatalyst. The difference fitted well to the 5% error with no tendencies observed. This corresponds to the carbon incorporated into titanium dioxide crystal lattice in sol-gel synthesis [5].

The experiments were performed using photocatalyst suspension with the concentration of 1 g L^{-1} . Titanium dioxide Degussa P25 and carbon-containing catalysts synthesised on course of the research were used. Carbon-containing photocatalysts were prepared by the hydrolysis of titanium tetrabutoxide, followed by calcination at different temperatures, ranging from 200 to 1000°C , for 4 hours.

The crystallinity of carbon-containing titania was analysed using D 5000 Kristalloflex, Siemens (Cu-K α irradiation source) X-ray diffraction spectroscopy (XRD). Carbon content was measured with PHI 5600 X-ray photoelectron spectroscopy. The specific area (BET and Langmuir adsorption) and the pore volume of the catalysts were measured by the adsorption of nitrogen using KELVIN 1042 sorptometer.

The decrease in the MTBE concentration was determined by gas chromatography using Finnigan Focus GC chromatograph; MTBE was extracted from pre-salinated aqueous samples by benzyl alcohol using IKA Vortex Genius 3 extractor. Oxidation rate was measured by a standard method from the decrease in chemical oxygen demand (COD). This parameter, unlike TOC, was proven to be decreasing with the increasing conversion degree in oxidation reactions.

Concentrations of *p*-toluidine were measured photometrically after diazotation and reaction with phenol at 490 nm, and those of phenol were determined photometrically after reaction with *p*-nitroaniline at 570 nm using Helios β spectrophotometer. The decrease in COD was also followed. The evolution of nitrite and nitrate ions was also monitored using Metrohm 761 Compact IC ion chromatograph.

The performance of PCO with artificial radiation sources was characterised by the process efficiency E . The efficiency E is defined as the decrease in the amount of pollutants divided by the amount of energy reaching the surface of the treated sample (Eq. 1). The values of the efficiency were calculated after a period of time equal to the treatment time.

$$E = \frac{\Delta c \cdot V \cdot 1000}{I \cdot s \cdot t}, \quad (1)$$

where E – PCO efficiency, $\text{mg W}^{-1} \text{ h}^{-1}$; Δc – the decrease in the pollutant's concentration mg L^{-1} or mg O L^{-1} measured as COD; V – the volume of the sample to be treated, L; I – irradiance, mW cm^{-2} ; s – irradiated area, cm^2 ; t – treatment time, h.

Results and discussion

Photocatalyst characterisation

Table 1 shows the data obtained on the structure and composition of carbon-containing photocatalysts. Judging from the XRD analysis, at lower calcinations temperatures (up to 600°C) the catalysts have clearly observable anatase and brookite phases, rutile is also occasionally present, and at higher temperatures rutile is the main fraction. With the growth of calcination temperature from 200°C to 1000°C , carbon content of the catalysts declined from 37.0 to 25.7 at. %, remaining, however, in the composition at rather high level indicating incorporation of carbon into the TiO_2 lattice: none of free carbon or carbonate could remain under the temperature applied. As one can see, the specific surface area of the catalysts decreases with the increasing calcination temperature, whereas micropore volume and area

increased with temperature growing from 200 to 500 °C, approximating zero at higher temperatures within accuracy of measurements.

T(calcination), °C	Crystallographic composition, %			Composition, at. %			S(BET), m ² g ⁻¹	S(Langmuir), m ² g ⁻¹	Micropore area, m ² g ⁻¹	Micropore volume, mm ³ g ⁻¹
	Anatase	Brookite	Rutile	Ti	O	C				
200	71.9	28.1	-	17.2	45.8	37.0	202.3	278.9	0	0
300	67.5	10.1	22.4	17.9	45.6	36.5	157.2	215.8	0.42	0.15
400	78.1	21.9	-	18.1	46.6	35.3	105.7	144.7	4.12	1.54
500	76.9	18.2	5.0	18.5	46.6	34.9	39.45	53.85	3.95	1.39
600	74.4	25.6	-	20.0	49.6	30.4	8.81	12.08	0	0
700	-	-	100	18.0	47.3	34.7	3.52	4.81	0.20	0.07
800	0.8	-	99.2	19.3	52.3	28.4	3.75	5.14	0.13	0.05
850	-	-	100	20.1	53.7	26.2	2.92	4.03	0	0
900	-	-	100	19.3	57.1	27.6	2.94	4.02	0.05	0.02
950	-	-	100	19.3	57.6	27.1	2.62	3.61	0	0
1000	-	-	100	19.5	54.8	25.7	1.92	2.59	0.35	0.12

Table 1. Composition and surface properties of carbon-containing photocatalysts dependent on calcinations temperature

Oxidation of MTBE

Under visible light MTBE was totally degraded within 1 h with all C-TiO₂ catalysts. Evaluated by the decrease in COD, the PCO efficiency somewhat oscillated showing, however, no reasonable trend (Fig. 1). The values of PCO efficiency observed with C-TiO₂ irradiated with visual light were higher than that with UV-irradiated Degussa P25 under similar experimental conditions (170 mg O W⁻¹ h⁻¹, see [16]). The important notice to be made here is the efficiency of rutile C-TiO₂ catalysts equal to or exceeding the one of P25.

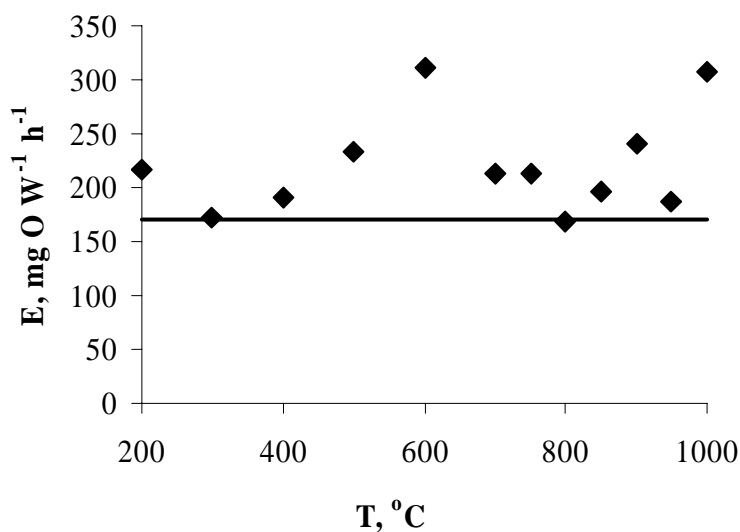


Figure 1. The PCO efficiency of MTBE vs. the temperature of C-TiO₂ calcination compared to Degussa P25 under UV (bold solid line): pH 6.5, 2 h

p-Toluidine

Similarly to Degussa P25 showing the maximum PCO efficiency in acidic media [17], the best performance of C-TiO₂ catalysts with *p*-toluidine was achieved at unregulated natural pH 6.5 shifted on course of PCO to acidic range, at which most of the experiments were consequently carried out. The PCO efficiency observed with C-TiO₂ under artificial daylight was close to that of Degussa P25 under UV. At Figure 2 one can see the PCO efficiency of *p*-toluidine steadily declining with the growth of catalyst calcinations temperature, i.e. with the decrease in carbon content and contact surface area.

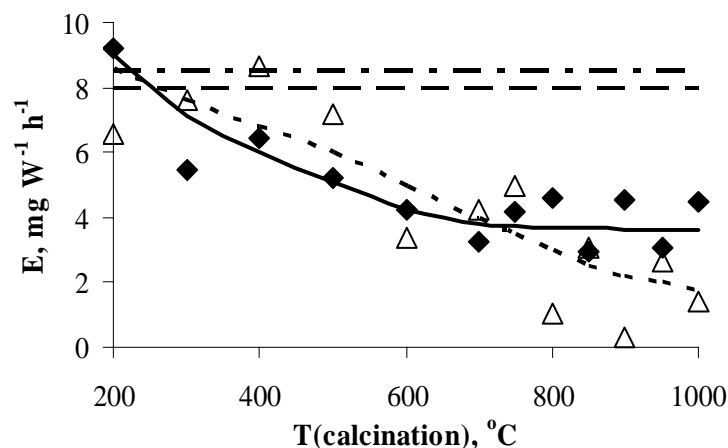


Figure 2. The dependence of *p*-toluidine PCO efficiency on the photocatalysts calcination temperature compared to Degussa P25: *p*-toluidine - diamonds and bold solid line, COD – triangles, dotted line, compared to Degussa P25 under UV (*p*-toluidine - bold dashed line, COD – bold dashed and dotted line); pH 6.5, 24 h

Phenol

With phenol, the PCO efficiency also decreased with the growth of the catalyst calcinations temperature (Figure 3). In comparison, Degussa P25 can degrade phenol with the same initial concentration under UV-irradiation with the PCO efficiency at pH from 7 to 3 from 5 to 10 mg W⁻¹ h⁻¹ [13]. Thus, the results achieved with C-TiO₂ are somewhat lower than the ones achieved with commercial photocatalyst.

Discussion

The differences observed between the behaviour of MTBE, on one hand, and aromatic substances, phenol and *p*-toluidine, on the other, may be explained by the different interactions of these substances with the titania catalysts. No adsorption of the substances was detected beyond the limits of analytical precision, which leaves radical reactions in the vicinity of the catalyst surface the only PCO mechanism responsible for the pollutants' degradation. Under the applied experimental conditions, i.e. slightly acidic pH, both titania and the aromatic substances, are partially protonated and, thus, positively charged. In such case, the aromatic substances are partially repelled by the electrostatic forces, and their PCO efficiency suffers from this. In case of MTBE, however, the pollutant molecule, being electrically neutral, can get closer to the catalyst surface with a larger supply of hydroxyl radicals and, thus, a higher probability of the radical and pollutant molecule impact, resulting in two orders of magnitude higher PCO efficiency. With aromatic substances, increased hydroxyl radical production can lead to the increase in their PCO efficiency, which seems to explain the increase of the substances' PCO efficiency with the decrease of the catalysts' calcinations temperature, i.e. the contact surface and possibly band-gap energy.

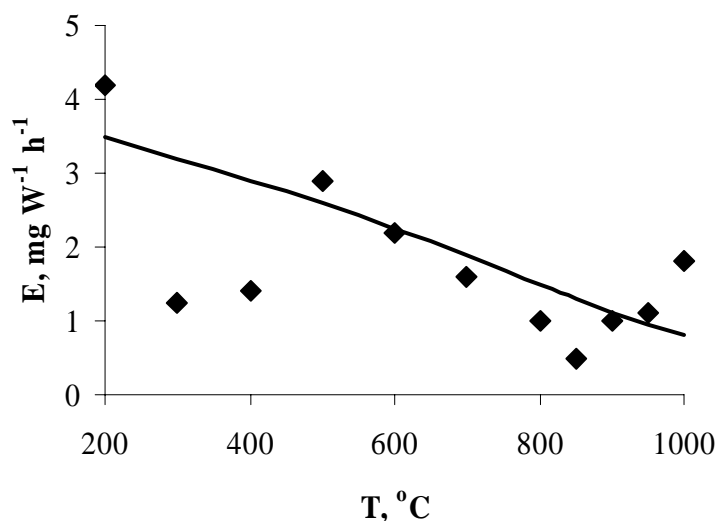


Figure 3. The dependence of phenol PCO efficiency on the photocatalysts calcination temperature: pH 6.5, 24 h

The oxidation potential of positively charged holes formed at the new energetic levels in the semiconductor may be decreased but still sufficient for hydroxyl radicals production thus improving the oxidation efficiency with increased visible light flux or irradiated surface. Similar observations were made by the authors with relatively well-adsorbed amoxicillin most likely hole-oxidized at C- and Fe-TiO₂ catalysts [18]. With the growth of the catalysts' calcinations temperature, more carbon is burned out from the catalyst surface thus increasing the band gap, and also the contact surface decreases. This way the amount of hydroxyl radicals produced decreases with the increase of the catalysts' calcinations temperature thus having the efficiency of aromatic compounds PCO decreasing.

Conclusions

In this research, aqueous photocatalytic oxidation (PCO) of methyl-*tert*-butyl ether (MTBE), *p*-toluidine and phenol was undertaken using visible light-sensitive carbon-containing titania. Those photocatalyst have proven to be an effective means against MTBE: with the majority of the carbon-containing catalysts the PCO efficiency under visible light was higher than that obtained with Degussa P25 under UV. In all cases, the degradation of MTBE was two orders of magnitude faster than the one of phenol and *p*-toluidine. The performance of C-TiO₂ with *p*-toluidine was also better than that with Degussa P25. In case of phenol, the performance of carbon-containing catalysts was comparable to, although somewhat lower than that of Degussa P25.

The widespread opinion concerning phenol used as a single etalon substance in comparison of catalysts is thus compromised by the dramatically different behaviour of different compounds in PCO.

Acknowledgements

The authors would like to thank the team of Prof. Dr.-Ing. Joachim Deubener, Division of Glass and Glass Technology Institute of Nonmetallic Materials of the Technical University of Clausthal and especially Mrs. Anna Moiseev, PhD, for providing XRD measurements, Mr. Andrew S. Cavanaugh, Doctoral Candidate in Physics of the University of Colorado at Boulder, for providing XPS measurements, and Ms. Mai Uibu, PhD, of the Laboratory of Inorganic Materials of Tallinn University of Technology, for providing specific surface area measurements of the catalysts. The authors would also like to thank Estonian Science Foundation (grant G7541) and United States Civilian Research and Development Foundation (grant GUS16062) for the financial support of the research.

D. Klauson (born 1983) is a final year doctoral student at Tallinn University of Technology (TUT), Estonia, Department of Chemical Engineering. His academic grades are Bachelor of Science (2005) and Master of Science (2006). Currently, he is employed at TUT at the position of Engineer.

O. Budarnaja (born 1986) is a final year master at Tallinn University of Technology (TUT), Estonia, Department of Chemical Engineering.

K. Stepanova (born 1986) is a final year master at Tallinn University of Technology (TUT), Estonia, Department of Chemical Engineering.

M. Krichevskaya (born 1974) is a Senior Researcher at the department of Chemical Engineering, TUT. She received her PhD degree in 2003.

S. Preis (born 1959) is an Associate Professor at Lappeenranta University of Technology (LUT), Finland. His academic degrees are Doctor in Environmental Engineering (TUT, 1988) and Doctor in Chemical Engineering (LUT, 2002).

References

[1] A. Fujishima, X.T. Zhang, and D.A. Tryk, *TiO₂ photocatalysis and related surface phenomena*, Surf Sci Reports 63 (2008), pp. 515-582

[2] Z. Liu, D.D. Sun, P. Guo, and J.O. Leckie, *One-step fabrication and high photocatalytic activity of porous TiO₂ hollow aggregates by using a low-temperature hydrothermal method without templates*, Chem. Eur. J. 13 (2007), pp. 1851-1855

[3] D. Klauson, E. Portjanskaja, and S. Preis, *Visible light-assisted photocatalytic oxidation of organic pollutants using nitrogen-doped titania*, Environ. Chem. Lett. 6 (2008), pp.35-39

[4] D. Klauson, E. Portjanskaja, O. Budarnaja, M. Krichevskaya, and S. Preis, *The synthesis of sulphur- and boron-containing titania photocatalysts and the evaluation of their photocatalytic activity*, Cat. Comm. 11 (2010), pp. 715-720

[5] Y. Park, W. Kim, H. Park, T. Tachikawa, T. Majima, and W. Choi, *Carbon-doped TiO₂ photocatalyst synthesized without using an external carbon precursor and the visible light activity*, Appl. Cat. B 91 (2009), pp. 355-361

[6] C.K. Yeh, and J.T. Novak, *Anaerobic biodegradation of gasoline oxygenates in soils*, Wat. Environ. Res. 66 (1994), pp. 744-752

[7] P. Johnson, *Assesment of the Contribution of Volatilization and Biodegradation to In Situ Air Sparging Performance*, Environ. Sci. Technol. 32 (1998), pp. 276-281

[8] A. Safarzadeh-Amiri, *O₃/H₂O₂ treatment of methyl-tert-butyl ether (MTBE) in contaminated waters*, Wat. Res. 35 (2001), pp. 3706-3714

[9] X.R. Xu, Z.X. Zhao, X.Y. Li, and J.P. Gu, *Chemical oxidative degradation of methyl-tert-butyl ether in aqueous solution by Fenton's reagent*, Chemosphere 55 (2004), pp. 73-79

[10] K.K.Papok, and E.G. Semenido *Motor, jet and rocket fuels* (Motornye, reaktivnye i raketnye topliva), (1962), Gostoptehizdat, Moscow, (in Russian)

[11] R. Srour, *Mononitrotoluenes and Derivatives: A.VII. p-Toluidine* (2002), Paris

[12] G. Busca S. Berardinelli, C. Resini, and L. Arrighi, *Technologies for the removal of phenol from fluid streams: a short review of recent developments*, J. Hazard. Mater. 160 (2008), pp. 265-288

[13] S. Preis, M. Krichevskaya, Y. Terentyeva, A. Moiseev, and J. Kallas, *Treatment of phenolic and aromatic amino compounds in polluted waters by photocatalytic oxidation*, J. Adv. Oxid. Technol. 5 (2002), pp. 77-84

[14] S.J. Kirkpatrick, *A primer on radiometry*, Dent. Mater. 21 (2005), pp. 21-26

[15] Royal Philips. Available from: <http://www.prismaecat.lighting.philips.com/FredhopperPDFWebServiceInter/docts/f38f1cfb-c971-4d99-87eb-c718c1020c4b/product.pdf>

[16] M. Krichevskaya, A. Kachina, T. Malygina, S. Preis, and J. Kallas, *Photocatalytic degradation of fuel oxygenated additives in aqueous solutions*, Int. J. Photoenergy 5 (2003), pp. 81-86

[17] S. Preis, M. Krichevskaya, and A. Kharchenko, *Photocatalytic oxidation of aromatic aminocompounds in aqueous solutions and groundwater from abandoned military bases*, Wat. Sci. Technol. 35 (1997), pp. 265-272

[18] D. Klauson, J. Babkina, K. Stepanova, M. Krichevskaya, and S. Preis, *Aqueous photocatalytic oxidation of amoxicillin*, Cat. Today, in press (2010), doi:10.1016/j.cattod.2010.01.015

APPENDIX III
CURRICULUM VITAE

ELULOOKIRJELDUS

1. Isikuandmed

Ees- ja perekonnanimi: Deniss Klauson
Sünniaeg ja -koht: 24. märts 1983. a., Tallinn
Kodakondsus: Eesti

2. Kontaktandmed

Address: TTÜ, Keemiatehnika instituut, Ehitajate tee 5, 19086 Tallinn,
Eesti

Telefon: +372 620 2857

E-posti address: deniss.klauson@ttu.ee

3. Hariduskäik

Õppeasutus (nimetus lõpetamise ajal)	Lõpetamise aeg	Haridus (eriala/kraad)
Tallinna Tehnikaülikool	2006	Tehnikateaduste magistrikraad
Tallinna Tehnikaülikool	2005	Tehnikateaduste bakalaureusekraad
Tallinna Tõnismäe reaalkool	2001	Keskharidus

4. Keelteoskus (alg-, kesk- või kõrgtase)

Keel	Tase
Eesti	Kõrgtase
Vene	Kõrgtase
Inglise	Kõrgtase
Saksa	Algtase
Prantsuse	Algtase

5. Täiendusõpe

Õppimise aeg	Täiendusõppe läbiviija
Märts 2010–k.a.	AS Tallinna Vesi, Fontes PMP OÜ
Jaauar–aprill 2010	Informaatika ja Arvutustehnika kool
September–detsember 2009	Informaatika ja Arvutustehnika kool
Jaauar–veebuar 2009	AS Tallinna Vesi

19.–20. veebruar 2009	Tallinna Tehnikaülikool, Tallinna Ülikool
November 2006–veebruar 2007	Tallinna Tehnikaülikool, Tallinna Ülikool
Juuni–august 2004	Lappeenranta Tehnikaülikool

6. Teenistuskäik

Töötamise aeg	Tööandja nimetus	Ametikoht
2009–k.a.	AS Tallinna Vesi	Projektijuht
2008–k.a.	TTÜ	Insener
2005–k.a.	AS Tallinna Vesi	Noorempetsialist
2007–2008	TTÜ	Erakorraline teadur
2008–2008	UTTP doktorikool	Erakorraline teadur
2004–2005	AS Tallinna Vesi	Laborant
2002–2007	Tallinna Tehnikaülikool	

7. Teadustegevus

Mootorkütuste hapnikurikaste lisandite oksüdatsioon vees (2002–2005). Grandi allikas – Eesti Teadusfond.

Orgaaniliste ainete vesifaasiline fotokatalüütiline oksüdatsioon (2005–2006). Grandi allikas – Eesti Teadusfond.

Uus märgosoonimisega veetöötlemise tehnika ja tehnoloogia (2006–2008). Finantseerimise allikas – Euroopa Liit ja Ettevõtluse Arendamise Sihtasutus.

Nähtavas valguses aktiivse fotokatalüsaatori väljatöötamine (2008–2010). Grandi allikas – Eesti Teadusfond ja USA Tsiviilteaduse ja arenduse fond (US Civilian Research and Development Foundation).

Nähtavas valguses aktiivsete fotokatalüsaatorite süntees ja nende kinnitamine pindadele saasteainete mineraliseerimiseks (2008–2011). Grandi allikas – Eesti Teadusfond.

8. Kaitsstud lõputööd

Tehnikateaduste magistrikraad (2006): Kütuselisandite fotokatalüütilisele oksüdatsioonile mõjuvate faktorite uurimine. Juhendaja Keemiatehnika instituudi vanemteadur Sergei Preis

Tehnikateaduste bakalaureuse kraad (2005): Rauaioonide mõju 2-etoksüetanooli fotokatalüütilisele oksüdatsioonile vesifaasis. Juhendajad Keemiatehnika instituudi vanemteadur Sergei Preis ja vanemteadur Marina Kritševskaya

9. Teadustöö põhisuunad

Bioloogiliselt lagunematute saasteainete fotokatalüütiline oksüdatsioon vesifaasis, nähtavas valguses aktiivsete fotokatalüsaatorite süntees, omaduste ja töö uurimine. Reaktsioonimehhanismide uurimine. Lisandite mõju fotokatalüüsile. Katalüsaatorite rakendusviiside uurimine.

10. Teised uurimisprojektid

Projekt SF0142719s06 (2006–k.a): Tehnoloogiliste protsesside intensiivistamine aktuaalsete keskkonnaprobleemide lahendamiseks

Projekt 673F (2006–2008): Uus märgosoonimisega veetöötlemise tehnika ja tehnoloogia.

CURRICULUM VITAE

1. Personal data

Name: Deniss Klauson

Date and place of birth: 24th March 1983, Tallinn

2. Contact information

Address: TUT, Department of Chemical Engineering, Ehitajate tee 5, 19086 Tallinn, Estonia

Phone: +372 620 2857

E-mail: deniss.klauson@ttu.ee

3. Education

Educational institution	Graduation year	Education (field of study/degree)
Tallinn University of Technology	2006	Master of Science
Tallinn University of Technology	2005	Bachelor of Science
Tallinna Tõnismäe reaalkool	2001	High school education

4. Language competence/skills (fluent; average, basic skills)

Language	Level
Estonian	Fluent
Russian	Fluent
English	Fluent
German	Basic skills
French	Basic skills

5. Special Courses

Period	Educational or other organisation
March 2010–onwards	AS Tallinna Vesi, Fontes PMOP OÜ
January–April 2010	School of Informatics and Computing Technology
September–December 2009	School of Informatics and Computing

	Technology
January–February 2009	AS Tallinna Vesi
February 19–20 2009	Tallinn University of Technology, Tallinn University
November 2006–February 2007	Tallinn University of Technology, University of Tartu
June–August 2004	Lappeenranta University of Technology

6. Professional Employment

Period	Organisation	Position
2009–onwards	AS Tallinna Vesi	Project Manager
2008–onwards	TUT	Engineer
2005–onwards	AS Tallinna Vesi	Junior Specialist
2007–2008	TUT	Extraordinary Researcher
2008	UTTP Doctoral School	Extraordinary Researcher
2004–2005	AS Tallinna Vesi	Laboratory Technician
2002–2007	TUT	Research Associate

7. Scientific work

Photocatalytical oxidation of oxygenated motor fuel additives in aqueous phase (2002–2005). Grant source – Estonian Science Foundation

Photocatalytical oxidation of organic compounds in aqueous phase (2005–2006). Grant source – Estonian Science Foundation

Novel wet ozonation engineering and technology in water treatment (2006–2008). Finance source – European Union and Enterprise Estonia.

The development of photocatalyst for visible light (2008–2010). Grant source – Estonian Science Foundation and United States Civilian Research and Development Foundation

Synthesis of photocatalysts active under visible light and their immobilization on surfaces for mineralisation of environmental pollutants (2008–2011). Grant source – Estonian Science Foundation.

8. Defended theses

Master of Science (2006): The examination of factors influencing the aqueous photocatalytic oxidation of fuel additives. Supervisor – Senior Researcher Sergei Preis, Department of Chemical Engineering, TUT

Bachelor of Science (2005): The influence of iron ions on the aqueous photocatalytic oxidation of 2-ethoxy ethanol. Supervisors: Senior Researcher Sergei Preis and Senior Researcher Marina Krichevskaya, Department of Chemical Engineering, TUT

9. Main areas of scientific work/Current research topics

Aqueous photocatalytic oxidation of non-biodegradable pollutants. The synthesis of visible light-sensitive titania-based photocatalysts and the evaluation of their properties and performance. The research of reaction mechanisms. The influence of additives on the photocatalytic oxidation performance. Engineering solutions for photocatalysts applications.

10. Other research projects

Project SF0142719s06 (2006–onwards): Intensification of technological processes for the solution of actual environmental problems

Project 673 F (2006 – 2008): Novel wet ozonation engineering and technology in water treatment

**DISSERTATIONS DEFENDED AT
TALLINN UNIVERSITY OF TECHNOLOGY ON
*CHEMISTRY AND CHEMICAL ENGINEERING***

1. **Endel Piiraja**. Oxidation and destruction of polyethylene. 1993.
2. **Meili Rei**. Lihatehnoloogia teaduslikud alused. Fundamentals of Food Technology. 1995.
3. **Meeme Põldme**. Phase transformations in hydrothermal sintering processing of phosphate rock. 1995.
4. **Kaia Tõnsuaadu**. Thermophosphates from Kovdor and Siilinjärvi apatites. 1995.
5. **Anu Hamburg**. The influence of food processing and storage on the N-nitrosamines formation and content in some Estonian foodstuffs. 1995.
6. **Ruth Kuldvee**. Computerized sampling in ion chromatography and in capillary electrophoresis. 1999.
7. **Külliki Varvas**. Enzymatic oxidation of arachidonic acid in the coral *Gersemia fruticosa*. 1999.
8. **Marina Kudrjašova**. Application of factor analysis to thermochromatography and promotion studies. 2000.
9. **Via Lepane**. Characterization of aquatic humic substances by size exclusion chromatography and capillary electrophoresis. 2001.
10. **Andres Triikkel**. Estonian calcareous rocks and oil shale ash as sorbents for SO₂. 2001.
11. **Marina Kritševskaja**. Photocatalytic oxidation of organic pollutants in aqueous and gaseous phases. 2003.
12. **Inna Kamenev**. Aerobic bio-oxidation with ozonation in recalcitrant wastewater treatment. 2003.
13. **Janek Reinik**. Methods for purification of xyloidine-polluted water. 2003.
14. **Andres Krumme**. Crystallisation behaviour of high density polyethylene blends with bimodal molar mass distribution. 2003.
15. **Anna Goi**. Advanced oxidation processes for water purification and soil remediation. 2005.
16. **Pille Meier**. Influence of aqueous solutions of organic substances on structure and properties of pinewood (*Pinus sylvestris*). 2007.

17. **Kristjan Kruusement.** Water conversion of oil shales and biomass. 2007.
18. **Niina Kulik.** The application of Fenton-based processes for wastewater and soil treatment. 2008.
19. **Raul Järviste.** The study of the changes of diesel fuel properties a its long term storage. 2008.
20. **Mai Uibu.** Abatement of CO₂ emissions in Estonian oil shale-based power production. 2008.
21. **Valeri Gorkunov.** Calcium-aluminothermal production of niobium and utilization of wastes. 2008.
22. **Elina Portjanskaja.** Photocatalytic oxidation of natural polymers in aqueous solutions. 2009.
23. **Karin Reinhold.** Workplace assessment: determination of hazards profile using a flexible risk assessment method. 2009.
24. **Natalja Savest.** Solvent swelling of Estonian oil shales: low temperature thermochemical conversion caused changes in swelling. 2010.
25. **Triin Märtson.** Methodology and equipment for optical studies of fast crystallizing polymers. 2010.